Title
Evaluating Climate Change Impacts on Water Resources and Food Systems – A Global Perspective with Insights from Africa and California.

Author
Beltran-Pena, Areidy Aracely

Publication Date
2023

Peer reviewed|Thesis/dissertation

Evaluating Climate Change Impacts on Water Resources and Food Systems – A Global Perspective with Insights from Africa and California.

by

Areidy Aracely Beltran-Peña

A dissertation submitted in partial satisfaction of the

requirements for the degree of

Doctor of Philosophy

in

Environmental Science, Policy, and Management

and the Designated Emphasis

in

Development Engineering

in the

Graduate Division

of the

University of California, Berkeley

Committee in charge:

Professor Paolo D'Odorico, Chair

Professor Dennis Baldocchi

Professor Manuela Girotto

Professor Alice Agogino

Summer 2023

Evaluating Climate Change Impacts on Water Resources and Food Systems – A Global Perspective with Insights from Africa and California.

by

Areidy Aracely Beltran-Peña

Abstract

Evaluating Climate Change Impacts on Water Resources and Food Systems – A Global Perspective with Insights from Africa and California.

by

Areidy Aracely Beltran-Peña

Doctor of Philosophy in Environmental Science, Policy and Management

Designated Emphasis in Development Engineering

University of California, Berkeley

Professor Paolo D'Odorico, Chair

This dissertation focuses on evaluating the hydrological impacts of climate change on water and food systems through integrated assessment models at various scales (global, country, and regional). The first chapter explores the future of global food self-sufficiency analysis in the 21st century under sustainable intensification of agriculture. By integrating biophysical, hydrological, climate, and societal models, the study considers factors such as sustainability, diet changes, population growth, agricultural intensification, and climate to project future scenarios. The findings reveal a concerning trend, indicating a probable decline in global food self-sufficiency within the middle-of-the-road and business-as-usual trajectories. In the second chapter, the focus shifts to Africa, a region experiencing high levels of food insecurity due to climate change and population growth. By assessing the impact of irrigation expansion on agricultural productivity and climate adaptation, the study highlights the limitations of irrigation alone in achieving food self-sufficiency. Under a 3°C warmer climate, Africa's total food production would only be sufficient to feed 1.35 billion people, while the population is projected to reach 3.5 billion. This underscores the need for additional strategies beyond irrigation alone to achieve food self-sufficiency, such as cropland expansion or increased reliance on imports. At a regional level, the third chapter employs Earth system models to assess the vulnerability of California's water-food nexus to changing snow regimes due to climate change. With a majority of snow monitoring sites showing declines in snowpack depths and earlier snowmelt onset, the study highlights the potential consequences of declining snowmelt on water availability for crop production, raising concerns about food security in a region already grappling with increased demand. This dissertation provides a comprehensive understanding of the complex dynamics influencing global food security. The findings emphasize the importance of sustainable practices, the limitations of irrigation expansion in addressing food deficits in Africa, and the vulnerability of water resources to declining snowpack in California. These insights contribute valuable knowledge for policymakers and stakeholders in formulating effective strategies to ensure a sustainable and secure food future for the global population.

Dedication

Dedico este doctorado a mis queridos padres, María Lourdes Beltrán-Peña y Javier Cirilo Beltrán, quienes han sido mi apoyo constante e inspiración a lo largo de mi trayectoria académica. Como estudiante de primera generación, hemos recorrido juntos un camino desconocido, enfrentando desafíos con determinación y resiliencia. Agradezco su fe inquebrantable en mí y por impulsarme a superar obstáculos. Estoy eternamente agradecida por los sacrificios que han realizado y las noches incansables que han trabajado para brindarnos a nuestra familia, siempre animándome a soñar en grande y alcanzar mis metas más altas. Este logro es también suyo, y dedico este doctorado con gratitud y en reconocimiento a su apoyo incondicional. Sin su amor y apoyo incondicional, no habría logrado convertirme en la Doctora Areidy Beltrán-Peña.

This dissertation is dedicated to the individuals who have supported me unwaveringly throughout my journey, as I strive to become the first Doctor in my family's history. To my parents, academic mentors, family, and friends, I am profoundly grateful for your constant support and belief in me. A special thanks goes to my research mentors, starting with my graduate advisor, Paolo D'Odorico. From day one, you believed in me and served as my advocate and guide throughout my Ph.D. studies. To my dissertation committee, qualification exam committee, and co-authors (Manuela Girotto, Dennis Baldocchi, Alice Agogino, Alan Rhoades, Inez Fung, Anna Michalak, Lorenzo Rosa, and Van Butsic), I am indebted to you for your unyielding support, valuable feedback, encouragement, and for consistently challenging me to reach new heights. Through your guidance, I have grown as an academic and scientist. I express my sincere gratitude to the Carnegie Institution for Science at Stanford and the Lawrence Berkeley National Laboratory for warmly welcoming me as a visiting student and fostering a supportive community environment. Your open arms and inclusive atmosphere have provided me with a nurturing space to conduct my research and engage in fruitful collaborations. I would also like to acknowledge the invaluable support of my ESPM GSAO, Ryann Madden, who advocated for me during challenging situations and helped me navigate bureaucratic obstacles. Thank you to Annamaria Bellezza for teaching me to speak Italian fluently during my Ph.D. studies. Additionally, I extend my heartfelt gratitude to all the mentors I have encountered at UC Berkeley since my undergraduate years. You not only taught me how to navigate the university system as a first-generation, low-income student but also provided care and guidance during my most challenging times.

To my beloved family and friends, your unwavering support throughout this demanding journey has been a source of strength. Your words of encouragement, moments of laughter, and our phone conversations have brought joy to my life and provided solace during moments of stress. Despite the distance, your friendship has enriched this remarkable journey. I am deeply grateful for each and every one of you, whether mentioned by name or not. Thank you for believing in me, encouraging me, and contributing to my personal and academic growth. Your impact on my development is immeasurable. This dissertation is a testament to the support I have received, and I dedicate it to all of you.

Acknowledgements

Acknowledgments Chapter 1: Areidy Beltran-Peña was funded by the NSF InFEWS Fellowship grant number DGE-1633740. L.R. was supported by The Ermenegildo Zegna Founder's Scholarship and by the AGU Horton Hydrology Research grant. P D was funded by the USDA Hatch Multistate project #W4190 capacity fund. We thank all those who made the data used in this study freely available, Dr. Sebastian Ostberg of the Potsdam-Institute for Climate Impact Research for sharing crop-specific yield data under the RCP scenarios considered in this study, and Nick Dekutoski from the University of California Berkeley for his advice on constructing the code for data analysis.

Acknowledgments Chapter 2: Areidy Beltran-Peña was funded by National Academies of Science, Engineering, and Medicine through the Ford Foundation Dissertation Fellowship. We thank all those who made the data used in this study freely available.

Acknowledgments Chapter 3: This material is based upon work supported by the U.S. Department of Energy, Office of Science, Office of Workforce Development for Teachers and Scientists, Office of Science Graduate Student Research (SCGSR) program. The SCGSR program is administered by the Oak Ridge Institute for Science and Education (ORISE) for the DOE. ORISE is managed by ORAU under contract number DE-SC0014664. All opinions expressed in this paper are the author’s and do not necessarily reflect the policies and views of DOE, ORAU, or ORISE.

Table of Contents

List of Figures

List of Tables

INTRODUCTION TO DISSERTATION

The increasing demand for agricultural products as a result of demographic growth and dietary transitions is raising new concerns on the extent to which humanity will be able to continue to feed itself with the limited resources of the planet (Godfray et al., 2010; Foley et al., 2011; Kummu et al., 2017). According to some predictions global crop production will need to at least double by 2050 to meet projected food demand resulting from population growth and the ongoing shift to richer diets (Godfray et al., 2010; Tilman et al., 2011; Alexandratos and Bruinsma 2012). At the same time, it is necessary to ensure food security for the 821 million people now chronically undernourished (United Nations 2018). However, current crop yield trends do not put us on track to double food production by 2050 (Ray et al., 2013). The combination of current levels of chronic malnutrition, rapid population growth, changes in diets and predicted stagnation or even decreases in crop yields is alarming.

Water and nutrients are important factors limiting crop production (Mueller et al., 2012). While advances in technologies have allowed humanity to economically produce fertilizers (Erisman 2008), water still remains a major limiting factor constraining crop production (e.g., Falkenmark and Rockstrom 2004; D'Odorico et al., 2018). Sustainable irrigation expansion to enhance crop yields on current water-limited rain-fed croplands has recently received particular attention as a viable strategy to meet the increasing demand for food (Rosa et al., 2018; Rosa et al., 2020). Sustainable irrigation expansion ensures that freshwater stocks are not depleted and environmental flows are maintained, while preventing agricultural expansion into biodiversity-rich ecosystems (Rosa et al., 2019). Hence, by sustainably expanding irrigation onto rain-fed croplands in locations where sustainable irrigation is deemed feasible (Rosa et al., 2018; Rosa et al., 2020), crop production and food availability can be increased without incurring in the environmental impacts arising from the expansion of the land footprint of agriculture into pristine ecosystems.

Many studies suggest that under a changing climate, snowmelt dynamics will be perturbed, the fraction of precipitation falling as snow will decrease and the timing of snowmelt will be altered (Hammond et al., 2018; Bormann et al., 2018; Sarangi et al., 2018; Painter et al., 2007; Lutz et al., 2014; Qin et al., 2020; Qin et al., 2022). According to Qin et al., 2020, in all snow-dependent basins, the fraction of irrigation water supplied by snowmelt runoff will decrease and food production may be impacted in areas where changes in rainfall cannot compensate for snowmelt loss (Biemans et al., 2019; Qin et al., 2020). In addition, due to international trade, the number of countries exposed to snowmelt risks will grow due to their imports of agricultural goods reliant on snowmelt (Qin et al., 2022). In the western United States, where nearly 75% of freshwater originates as snow in the Sierra Nevada, Rocky and Cascade mountain ranges (Livneh and Badger 2020; Viviroli et al., 2007; Simkins 2018), over 90% of snow monitoring sites show declines in snowpack and earlier melting times (Mote et al., 2018; Stewart et al., 2005). California is the largest agricultural producer in the United States and the country's largest agricultural exporter with an output valued at US $59.4 billion, one-third of which is derived from perennial crops (i.e. almonds, grapes, and strawberries) (Cooley et al., 2015; USDA-NASS 2018; Hong et al., 2020). The state produces a third of the vegetables and two-thirds of the fruits consumed in the U.S. and exports approximately 28% of its agricultural production (CDFA 2018a, CDFA 2018b, Hong et al., 2020). California's mountain ranges are important assets for its water supply (Immerzeel et al., 2020). At the same time, California's snow-dependent basins are actively threatened by anthropogenic climate change which will reduce freshwater availability from snow and in turn could significantly affect crop yields and crop mixes (Qin et al., 2020).

My dissertation addresses the following questions at the confluence between climate change and food security:

1) How many people can the planet sustainably feed with the limited water resources of the planet? How are changes in food demand and production going to affect global patterns of self-sufficiency?

2) To what extent can climate adaptation strategies improve food self-sufficiency in African counties- a global hotspot for food insecurity?

3) What are the climate risks faced by snowmelt-dependent agricultural systems? With California as a case-study, how will the timing and availability of snowmelt runoff from the Sierra Nevada Mountain range change throughout the 21st century? How much water will be available for irrigation in the Central Valley?

Chapter 1: Global food self-sufficiency in the 21st century under sustainable intensification of agriculture.

Reference: Beltran-Peña, A., Rosa, L. and D'Odorico, P., 2020. Global food self-sufficiency in the 21st century under sustainable intensification of agriculture. Environmental Research Letters, 15(9), p.095004.

Here, we assessed food production and demand throughout the 21st century. We first evaluated future food production assuming that current yields will be boosted, through sustainable irrigation (Rosa et al., 2018), to 80% of yield potential in years 2030, 2050, 2080, and 2100. We then accounted for the effects of climate change on crop yields under four Representative Concentration Pathway (RCP) scenarios using five different global gridded crop models forced by the bias-corrected HadGEM2-ES global climate model (Warszawski et al., 2014; Osteberg et al., 2018). To assess food production available for direct human consumption, we also accounted for food waste and first-generation biofuel production (FAO 2018). Using the agricultural demand indicators of three Shared Socio-economic Pathways (SSP) Integrative Assessment Model scenarios (Riahi et al., 2017; O'Neill et al., 2014; Popp et al., 2017), we assessed changes in plant- and animal-based consumption in diets, while also accounting for different population growth forecasts from the 2019 United Nations Population Prospects. Finally, by combining projected food demand and production, we assessed self-sufficiency ratios for 165 countries, considering different scenarios of population growth, climate change, and dietary changes under sustainable irrigation intensification in a world where biofuel consumption and food waste are assumed to continue. Self-sufficiency is defined as the ability of a country to meet the caloric demand of its population through domestic food production each year. The results of this study present different scenarios of self-sufficiency ratios in the 21st century that could be used to determine future hotspots of food insecurity, the reliance of countries on food imports (Macdonald 2013), and vulnerability to food supply shocks (Puma et al., 2015).

Chapter 2: Food security in Africa under climate change.
Reference: Beltran-Peña, A. and D'Odorico, P., 2022. Future food security in Africa under climate change. Earth's Future, 10(9), p.e2022EF002651.

We conducted an assessment using agrohydrological, climate, and socioeconomic models to analyze food self-sufficiency and climate vulnerability for 49 African countries under a global temperature 3°C above preindustrial levels. The results indicate a severe disparity between population size and food autonomy in Africa under a 3°C warmer climate. By 2075, food production in Africa will only be able to feed 1.35 billion people out of an estimated 3.5 billion—even with increased agricultural productivity through improved irrigation and sustainable practices. Narrowing yield gaps through sustainable irrigation expansion on currently rainfed croplands alone will not suffice to meet food demand. Therefore, African nations will need to expand cropland and rely more heavily on food imports. However, both approaches come with significant drawbacks. Expanding cropland poses potentially disastrous ecological ramifications, while dependence on imports would make Africa more susceptible to volatility in global food prices. This analysis reveals that eastern and western Africa will face the highest import needs requirements. The research also proposes measures to address the concerning projections. Increasing the consumption of plant-based foods and enhancing water storage—particularly in arid regions—can help mitigate growing food insecurity. Additionally, halving current food loss and waste rates could boost domestic food availability and feed an additional 130 million people. However, even with these solutions, projected food deficits on the continent will not be entirely eliminated. It is important to note that these findings challenge the feasibility of achieving the second of the United Nations' Sustainable Development Goal of ending hunger and malnutrition in Africa under the current emissions and warming trajectory.

Chapter 3: Assessing the impacts of climate change on water resources using Earth system models to project hydroclimate variability and snowpack changes in the California Sierra Nevada.

Although previous studies have assessed the impacts of changes in precipitation on agriculture (Elliot et al., 2014; Howitt et al., 2015), few have focused specifically on quantifying the risks from declining snowmelt on agriculture (Qin et al., 2020; Qin et al., 2022). Still, these studies are global analyses which highlight major patterns in significant agricultural regions. We develop a framework that combines variable resolution Earth System Models and crop-water models to assess water supply and demand vulnerability of California's water-food nexus to changing snow regimes in the Sierra Nevada under climate change. We highlight changing precipitation patterns in the Sierra Nevada as the climate warms with significant decreases in snowfall and consequently snowpack, and an increase in rainfall. The projected shift from a snow to rain dominated region due to significant losses in snowpack, will lead to earlier water availability and substantial declines in runoff during the warm summer months when irrigation demand is highest. Despite the increased water availability from rainfall runoff, without adequate reservoir storage (both surface and subsurface), the excess water will be lost and will not compensate for the loss of snowmelt runoff to meet water demand from the agricultural sector.

Introduction References

Alexandratos N and Bruinsma J 2012 *World Agriculture towards 2030/2050: the 2012 revision* (Rome) Online: www.fao.org/economic/esa

Biemans, H., Siderius, C., Lutz, A.F., Nepal, S., Ahmad, B., Hassan, T., von Bloh, W., Wijngaard, R.R., Wester, P., Shrestha, A.B. and Immerzeel, W.W., 2019. Importance of snow and glacier meltwater for agriculture on the Indo-Gangetic Plain. Nature Sustainability, 2(7), pp.594-601.

Bormann, K. J., Brown, R. D., Derksen, C. & Painter, T. H. Estimating snow-cover trends from space. *Nat. Clim. Chang*. 8, 924–928 (2018).

California Agricultural Production Statistics (California Department of Food and Agriculture, 2018a); https://www.cdfa.ca.gov/Statistics

California Agricultural Statistics Review (California Department of Food and Agriculture, 2018b); https://www.cdfa.ca.gov/statistics/PDFs/2017-18AgReport.pdf

California County Agricultural Commissioners' reports (USDA-NASS, 2018); https://www.nass.usda.gov/Statistics_by_State/California/Publications/AgComm/index.php

Cooley, H., Donnelly, K., Phurisamban, R. and Subramanian, M., 2015. Impacts of California's ongoing drought: agriculture. Pacific Institute, Oakland, 24.

D'Odorico P, Davis K F, Rosa L, Carr J A, Chiarelli D, Dell'Angelo J, Gephart J, MacDonald G K, Seekell D A, Suweis S and Rulli M C 2018 The Global Food-Energy-Water Nexus *Rev. Geophys.* 56 456–531

Elliott, J. et al. Constraints and potentials of future irrigation water availability on agricultural production under climate change. Proc. Natl Acad. Sci. USA 111, 3239–3244 (2014).

Erisman, J.W., Sutton, M.A., Galloway, J., Klimont, Z. and Winiwarter, W., 2008. How a 533 century of ammonia synthesis changed the world. *Nature Geoscience*, *1*(10), p.636.

Falkenmark M, and Rockström J 2004 Balancing water for humans and nature: The new approach in ecohydrology. London & Sterling, VA: *Earthscan*.

FAO. The State of Food Insecurity in the World 2018. Building Climate Resilience for Food Security and Nutrition. www.fao.org/publications (2018).

Godfray H C J, Beddington J R, Crute I R, Haddad L, Lawrence D, Muir J F, Pretty J, Robinson S, Thomas S M and Toulmin C 2010 Food security: The challenge of feeding 9 billion people *Science (80-.).* 327 812–8

Hammond, J. C., Saavedra, F. A. & Kampf, S. K. Global snow zone maps and trends in snow persistence 2001–2016. *Int. J. Climatol*. 38, 4369–4383 (2018).

Hong, C., Mueller, N.D., Burney, J.A., Zhang, Y., AghaKouchak, A., Moore, F.C., Qin, Y., Tong, D. and Davis, S.J., 2020. Impacts of ozone and climate change on yields of perennial crops in California. Nature Food, 1(3), pp.166-172.)

Howitt, R., MacEwan, D., Medellín-Azuara, J., Lund, J.R. and Sumner, D., 2015. Economic analysis of the 2015 drought for California agriculture. University of California, Davis, CA:

Center for Watershed Sciences.

Immerzeel, W.W., Lutz, A.F., Andrade, M., Bahl, A., Biemans, H., Bolch, T., Hyde, S., Brumby, S., Davies, B.J., El more, A.C. and Emmer, A., 2020. Importance and vulnerability of the world's water towers. Nature, 577(7790), pp.364-369.

Kummu M, Fader M, Gerten D, Guillaume J H, Jalava M, Jägermeyr J, Pfister S, Porkka M, Siebert S and Varis O, 2017. Bringing it all together: Linking measures to secure nations' food supply. *Current opinion in environmental sustainability*, *29*, pp.98-117.

Livneh, B. and Badger, A.M., 2020. Drought less predictable under declining future snowpack. Nature Climate Change, 10(5), pp.452-458.

Lutz, A. F., Immerzeel, W. W., Shrestha, A. B. & Bierkens, M. F. P. Consistent increase in High Asia's runoff due to increasing glacier melt and precipitation. *Nat. Clim. Chang*. 4, 587–592 (2014).

Macdonald, G. K. Eating on an interconnected planet. Environmental Research Letters vol. 8 (2013).

Mote, P.W., Li, S., Lettenmaier, D.P., Xiao, M. and Engel, R., 2018. Dramatic declines in snowpack in the western US. Npj Climate and Atmospheric Science, 1(1), pp.1-6.

Mueller N D, Gerber J S, Johnston M, Ray D K, Ramankutty N and Foley J A 2012 Closing yield gaps through nutrient and water management *Nature* 490 254–7

O'Neill, B. C. et al. A new scenario framework for climate change research: The concept of shared socioeconomic pathways. Clim. Change 122, 387–400 (2014).

Ostberg, S., Schewe, J., Childers, K. & Frieler, K. Changes in crop yields and their variability at different levels of global warming. Earth Syst. Dyn. 9, 479–496 (2018).

Painter, T. H. et al. Impact of disturbed desert soils on duration of mountain snow cover. *Geophys. Res. Lett*. 34, L12502 (2007).

Popp A, Calvin K, Fujimori S, Havlik P, Humpenöder F, Stehfest E, Bodirsky B L, Dietrich J P, Doelmann J C, Gusti M and Hasegawa T 2017 Land-use futures in the shared socio-economic pathways. Global Environmental Change, 42, pp.331-345.

Puma, M. J., Bose, S., Chon, S. Y. & Cook, B. I. Assessing the evolving fragility of the global food system. Environ. Res. Lett. 10, (2015).

Qin, Y., Hong, C., Zhao, H., Siebert, S., Abatzoglou, J.T., Huning, L.S., Sloat, L.L., Park, S., Li, S., Munroe, D.K. and Zhu, T., 2022. Snowmelt risk telecouplings for irrigated agriculture. *Nature Climate Change*, *12*(11), pp.1007-1015.

Qin, Y., Abatzoglou, J.T., Siebert, S., Huning, L.S., AghaKouchak, A., Mankin, J.S., Hong, C., Tong, D., Davis, S.J. and Mueller, N.D., 2020. Agricultural risks from changing snowmelt. Nature Climate Change, 10(5), pp.459-465.

Ray D K, Mueller N D, West P C and Foley J A 2013 Yield Trends Are Insufficient to Double Global Crop Production by 2050 ed J P Hart *PLoS One* 8 e66428

Riahi, K. et al. The Shared Socioeconomic Pathways and their energy, land use, and greenhouse gas emissions implications: An overview. Glob. Environ. Chang. 42, 153–168 (2017).

Rosa L, Chiarelli D D, Tu C, Rulli M C and D'Odorico P 2019 Global unsustainable virtual water flows in agricultural trade *Environ. Res. Lett.*

Rosa L, Rulli M C, Davis K F, Chiarelli D D, Passera C and D'Odorico P 2018 Closing the yield gap while ensuring water sustainability *Environ. Res. Lett.* 13

Rosa, L., Chiarelli, D.D., Rulli, M.C., Dell'Angelo, J. and D'Odorico, P., 2020. Global agricultural economic water scarcity. *Science Advances*, *6*(18), p.eaaz6031.

Sarangi, C. et al. Impact of light-absorbing particles on snow albedo darkening and associated radiative forcing over High Mountain Asia: high resolution WRF-Chem modeling and new satellite observations. *Atmos. Chem. Phys. Discuss*. https://doi.org/10.5194/acp-2018-979 (2018).

Simpkins, G. Snow-related water woes. Nat. Clim. Change 8, 945 (2018).

Stewart, I.T., Cayan, D.R. and Dettinger, M.D., 2005. Changes toward earlier streamflow timing across western North America. Journal of climate, 18(8), pp.1136-1155.

Tilman D, Balzer C, Hill J and Befort B L 2011 Global food demand and the sustainable intensification of agriculture *Proc. Natl. Acad. Sci. U. S. A.* 108 20260–4

United Nations 2018 *The Sustainable Development Goals Report 2018*

Viviroli, D., Dürr, H. H., Messerli, B., Meybeck, M. & Weingartner, R. Mountains of the world, water towers for humanity: typology, mapping, and global significance. Water Resour. Res. 43, W07447 (2007).

Warszawski, L. et al. The Inter-Sectoral Impact Model Intercomparison Project (ISI–MIP): Project framework. Proc. Natl. Acad. Sci. 111, 3228–3232 (2014).

CHAPTER 1

Global food self-sufficiency in the 21st century under sustainable intensification of agriculture

Reference: Beltran-Peña, A., Rosa, L. and D'Odorico, P., 2020. Global food self-sufficiency in the 21st century under sustainable intensification of agriculture. Environmental Research Letters, 15(9), p.095004. https://doi.org/10.1088/1748-9326/ab9388

1.1 Abstract

Meeting the increasing global demand for agricultural products without depleting the limited resources of the planet is a major challenge that humanity is facing. Most studies on global food security do not make projections past the year 2050, just as climate change and increasing demand for food are expected to intensify. Moreover, past studies do not account for the water sustainability limits of irrigation expansion to presently rainfed areas. Here we perform an integrated assessment that considers a range of factors affecting future food production and demand throughout the 21st century. We evaluate the self-sufficiency of 165 countries under sustainability, middle-of-the-road, and business-as-usual scenarios considering changes in diet, population, agricultural intensification, and climate. We find that under both the middle-of-the-road and business-as-usual trajectories global food self-sufficiency is likely to decline despite increased food production through sustainable agricultural intensification since projected food demand exceeds potential production. Contrarily, under a sustainability scenario, we estimate that there will be enough food production to feed the global population. However, most countries in Africa and the Middle East will continue to be heavily reliant on imports throughout the 21st century under all scenarios. These results highlight future hotspots of crop production deficits, reliance on food imports, and vulnerability to food supply shocks.

1.2 Introduction

The increasing demand for agricultural products as a result of demographic growth and dietary transitions is raising new concerns on the extent to which humanity will be able to continue to feed itself with the limited resources of the planet (Godfray *et al* 2010, Foley *et al* 2011, Kummu *et al.* 2017). According to some predictions global crop production will need to at least double by 2050 to meet projected food demand resulting from population growth and the ongoing shift to richer diets (Godfray *et al* 2010, Tilman *et al* 2011, Alexandratos and Bruinsma 2012). At the same time, it is necessary to ensure food security for the 821 million people now chronically undernourished (United Nations 2018). However, current crop yield trends do not put us on track to double food production by 2050 (Ray *et al* 2013). The combination of current levels of chronic malnutrition, rapid population growth, changes in diets and predicted stagnation or even decreases in crop yields is alarming (e.g., Brown 2012).

Previous studies have assessed the avenues by which humanity can meet future food needs by reducing demand and/or increasing production (e.g., Foley *et al* 2011). For instance, there are ways to moderate food demand by decreasing meat consumption and shifting to plant-based diets (Cassidy *et al* 2013, Jalava *et al* 2014, Davis *et al* 2014), reducing food waste (Kummu *et al* 2012), minimizing inefficiencies in resource use through improved technology and management

(Springmann *et al* 2018), optimization in the spatial distribution of crops (Davis *et al* 2017), or more efficient fertilization and watering techniques (e.g., Jägermeyr *et al* 2016). Other studies have estimated ways to increase food production by sustainably increasing crop yields on existing croplands, while preventing agricultural expansion into biodiversity-rich ecosystems (Pretty 2018, Phalan *et al* 2011, Garnett *et al* 2013). In fact, it has been estimated that much of the world's croplands can still attain higher crop yields potentially increasing crop production by 45% to 70% (Mueller *et al* 2012). Importantly, narrowing yields gaps – the difference between biophysical potential yield and current yield (Lobell *et al* 2009, Van Ittersum *et al* 2013) – in underperforming croplands will enhance food self-sufficiency in developing countries where almost all the increase in food demand will come from (Alexandratos and Bruinsma 2012).

Water and nutrients are important factors limiting crop production (Mueller *et al* 2012). While advances in technologies have allowed humanity to economically produce fertilizers (Erisman 2008), water still remains a major limiting factor constraining crop production (e.g., Falkenmark and Rockstrom 2004, D'Odorico *et al* 2018). Sustainable irrigation expansion to enhance crop yields on current water-limited rain-fed croplands has recently received particular attention as a viable strategy to meet the increasing demand for food (Rosa *et al* 2018, Rosa *et al* 2020). Sustainable irrigation expansion ensures that freshwater stocks are not depleted and environmental flows are maintained, while preventing agricultural expansion into biodiversity-rich ecosystems (Rosa *et al* 2019). Currently, 500 million small farms world-wide (most of which are rain-fed croplands), provide approximately 80 percent of food consumed in the developing world (United Nations 2018). Hence, by sustainably expanding irrigation onto rain-fed croplands in locations where sustainable irrigation is deemed feasible (Rosa *et al* 2018; Rosa *et al* 2020), crop production and food availability can be increased without incurring in the environmental impacts arising from the expansion of the land footprint of agriculture into pristine ecosystems. The focus here is on water resources as the limiting factor to yield gap closure because nutrient limitations can be overcome through fertilizer applications. Conversely, irrigation water scarcity can seldom be addressed with physical water transfers, as irrigation water volumes are too cumbersome and heavy to be transported over long distances.

The extent to which yield gaps will be narrowed will also depend on climate change, which is expected to decrease crop productivity in major global breadbaskets (Aggarwal *et al* 2019, Schleussner *et al* 2018, Vogel *et al* 2019). Climate change will alter yields through changes in temperature, precipitation, insect pests, and atmospheric concentration of CO_2 (Lobell and Gourdji 2012, Deutsch *et al* 2018, Ostberg *et al* 2018, Warszawski *et al* 2014). Importantly, yields are likely to be reduced in low-input agricultural systems characterized by large yield gaps (Rosenzweig *et al* 2014). For example, rain-fed croplands will be severely exposed to more unpredictable rainfall and precipitation patterns (Rojas *et al* 2019, Fitton *et al* 2019).

Most studies on global food security do not make projections past the year 2050 (e.g., Godfray *et al* 2010, Fader *et al* 2013), just as climate change and increasing demand for food are expected to intensify. Moreover, previous studies have accounted for major drivers of global food production and demand independently, without considering the full-suite of factors that will affect future food security: population growth, dietary changes, climate change, and the extent by which crop yield gaps can be sustainably narrowed with the limited freshwater resources of the planet.

Here we assess food production and demand throughout the 21st century. Food production is evaluated by accounting for changes in crop yields due to climate change for four major crops under three Representative Concentration Pathway (RCP) scenarios (IPCC 2014; Warszawski *et*

al 2014) and assuming that current yields will be boosted through sustainable irrigation expansion (Rosa *et al* 2018), to 80% of yield potential. Using the agricultural demand indicators of three Shared Socio-economic Pathways (SSP) (Riahi *et al* 2017, O'Neill *et al* 2014; Popp *et al* 2017), we assess changes in plant- and animal-based demand in diets, while also accounting for different population growth forecasts. While the SSP scenarios allow for an increase in cropland area, here we use them only to infer future dietary shifts without changing the spatial extent of farmland. Rather, we account for the increase in crop production that would result from the sustainable intensification of agriculture. Indeed, the goal of this study is to evaluate the extent to which it is possible to sustainably meet the increasing food demand without further encroachment of agriculture into natural ecosystems. By combining food demand and production, we assess self-sufficiency ratios for 165 countries, considering different scenarios of population growth, climate change, and dietary changes under sustainable irrigation expansion.

This analysis sheds light on possible pathways of food self-sufficiency in the 21st century in the context of food availability. This study solely considers the food availability pillar of food security and does not consider food access and utilization (Sen, 1981; FAO, 2002). Nevertheless, food security depends on the ability of agricultural lands to produce enough food to meet rising demand. Thus, here we focus on the sustainable intensification of agriculture through irrigation, complementing previous studies on food system resilience and economic access to food (Kinnunen *et al* 2020; Puma *et al* 2015; Suweis *et al* 2015; Seekell *et al* 2017). Self-Sufficiency ratios inform us about which countries may produce enough crops to meet their domestic demand, and which will likely depend on international food trade to feed their population (Puma *et al* 2015; Suweis *et al* 2015; Seekell *et al* 2017). The results of this study could be used to determine future hotspots of crop production deficits or surpluses, the reliance of countries on food imports (Macdonald 2013; Porkka *et al* 2013), and their vulnerability to food supply shocks (Puma *et al* 2015; Marchand *et al* 2016).

1.3 Methods

We define self-sufficiency as the ability of a country to meet the caloric demand of its population through domestic food production in a given year. The country-specific self-sufficiency ratios (SSR) are measured as the total estimated kcal production divided by the total estimated kcal demand of each individual country for the years 2030, 2050, 2080, and 2100. A country is considered self-sufficient (in terms of food availability) if it has an SSR of 1 or greater (>1 indicates a surplus), while a country with an SSR less than 1 is not self-sufficient. For countries that are not self-sufficient, the number of people that cannot be fed is derived by subtracting the self-sufficiency ratio from 1 and multiplying by the projected population of the respective country. Figure 1 shows the conceptual framework used to assess the projected production and demand in the 21st century.

Projected food production is a function of sustainable irrigation expansion, and changes in yield due to climate change (figure 1). We assume that current yields for 22 crop classes will be boosted to 80% of yield potential through sustainable irrigation intensification globally (Rosa *et al* 2018). The percentage of losses and other uses (e.g. biofuels) per crop were calculated as the five-year average of the 2009 - 2013 period (FAO 2017a) and assumed to remain constant. Estimates of percent yield change under climate change were derived for the four major crops (rice, maize, wheat and soy) under three RCP scenarios (RCP 2.6, RCP 6.0, and RCP 8.5) from five global gridded crop models (GGCMs) (GEPIC, LPJ-GUESS, LPJmL, PEGASUS, and pDSSAT) forced by the bias-corrected global climate model HadGEM2-ES from the Inter-Sectoral

Impact Model Intercomparison Project (ISIMIP) (Rosenzweig *et al* 2014, Warszawski *et al* 2014, Taylor *et al* 2012, Ostberg *et al* 2018, van Vuuren *et al* 2011). The multi-model mean of percent yield change (ΔY_{clim}) for the four major crops was calculated for each of the three RCPs for the years 2030 to 2100. The projected production accounting for climate change for maize, rice, wheat and soybean was then added to the current available production data of the remaining 18 crops (without accounting for possible effects of climate change) to find the total available production in kilocalories for food and feed ($P_{available}$) for each country, year, and RCP scenario.

Projected demand is a function of dietary changes and population growth forecasts (Figure 1). Under SSP1, diets with low-animal calorie shares prevail; under SSP2 caloric consumption and animal calorie shares converge towards moderate levels; and under SSP3 diets with higher animal shares prevail (Riahi *et al* 2017, van Vuuren *et al* 2017, Fricko *et al* 2017, Fujimori *et al* 2017, Popp *et al* 2017). The annual fractions of animal-based consumption and vegetal-based consumption of per capita diets were extrapolated from the IIASA agricultural demand data (SSP Database Version 2.0) (Riahi *et al* 2017; Popp *et al* 2017). We assumed that for human well-being, an individual should consume a daily energy requirement, F_{wb}, of 2327 kcal per capita per day (e.g., D'Odorico *et al* 2019a). The diet scenarios considered in this study differ in the fraction of animal and plant products consumed, but not in the caloric intake itself, which is assumed to be constant. In order to calculate the crop calorie demand from animal products (i.e., the feed demand), the plant to animal caloric conversion factors (q) per country and the initial fraction of total animal calories from feed-fed production (r) were taken from Davis *et al* (2014). We estimated the total annual projected caloric demand per country by multiplying the per capita demand by the estimated population of a country under the corresponding population variant (*var*) (Figure 1). Population estimates were taken from the United Nations 2019 World Population Prospects which include low, medium, and high population variants (United Nations 2019). We define three main scenarios in which we group these factors – sustainability, middle-of-the-road, and business-as-usual. Under the sustainability scenario, we pair the low climate change scenario (RCP 2.6), diets with low animal-calorie shares (SSP1), and the low population variant. Under the business-as-usual scenario, we pair the high climate change scenario (RCP 8.5), diets with high animal-calorie shares (SSP3), and the high population variant. The middle-of-the-road scenario pairs RCP 6.0, with moderate diets (SSP2), and the medium population variant (Riahi *et al* 2017, Popp *et al* 2017). A more detailed description of the methods is in the Supplementary Materials.

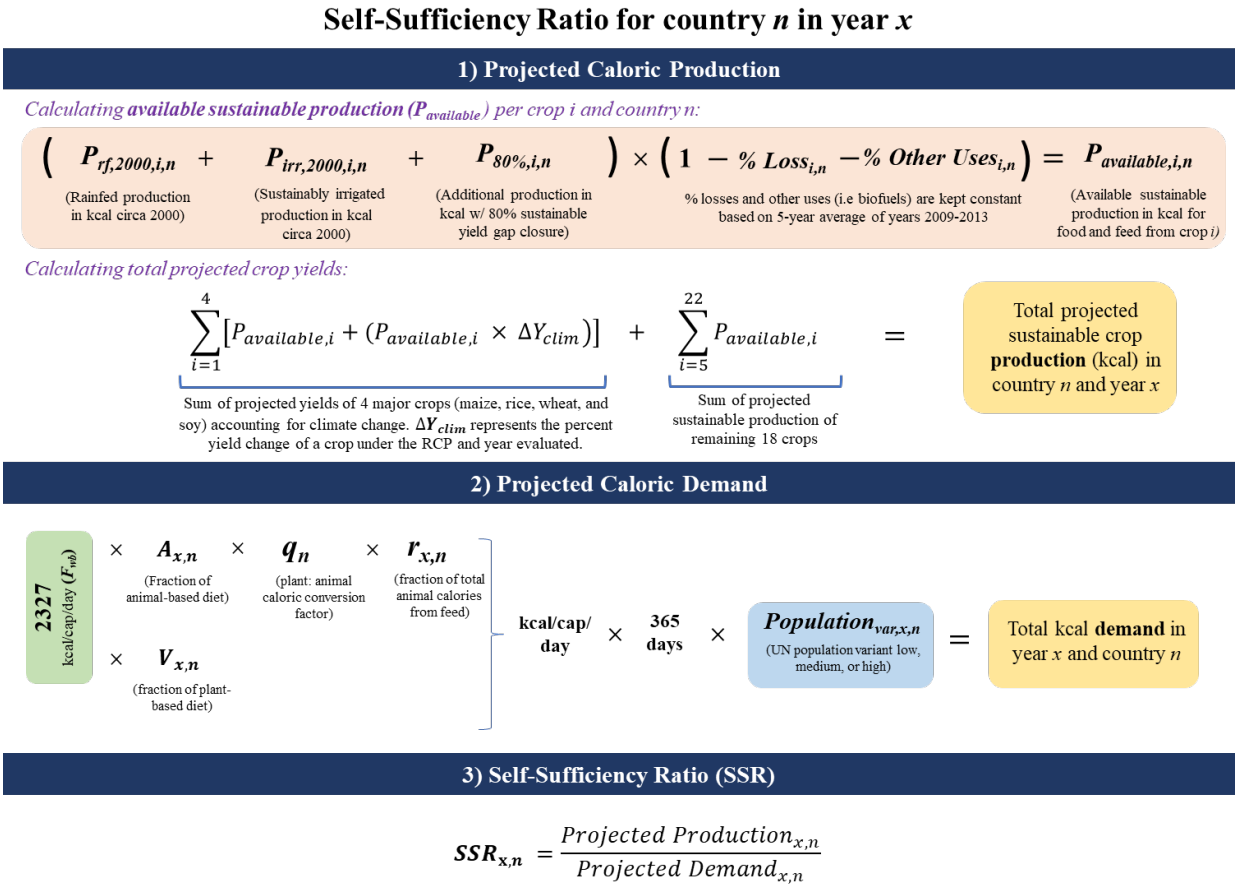

Figure 1. Self-sufficiency ratio framework. This figure shows the methodological framework used to carry-out our analysis. Note that ΔY_{clim} depends on RCP; $A_{x,n}$ and $V_{x,n}$ depend on SSP; and population variant depends on scenario evaluated.

1.4 Results

1.4.1 Future food demand

We find that future food demand will strongly depend on the population estimates and future diets of the scenario pursued. Under the sustainability scenario, food demand for crops and animal products increases gradually until mid-century and then decreases by 12% by 2100 compared to 2019 (Figure 2). Under the middle-of-the-road scenario food demand for crops and animal products increases by approximately 45% by the end of the century. Under the more conservative sustainability and middle-of-the-road scenarios, the share of animal-based products in diets will range from 5% to 12% globally, respectively. Under a business-as-usual scenario, animal-based product consumption may be up to 52% in OECD countries and will increase in every region. We find that current food production will have to triple by 2100 to meet demand under business-as-usual (Figure 2).

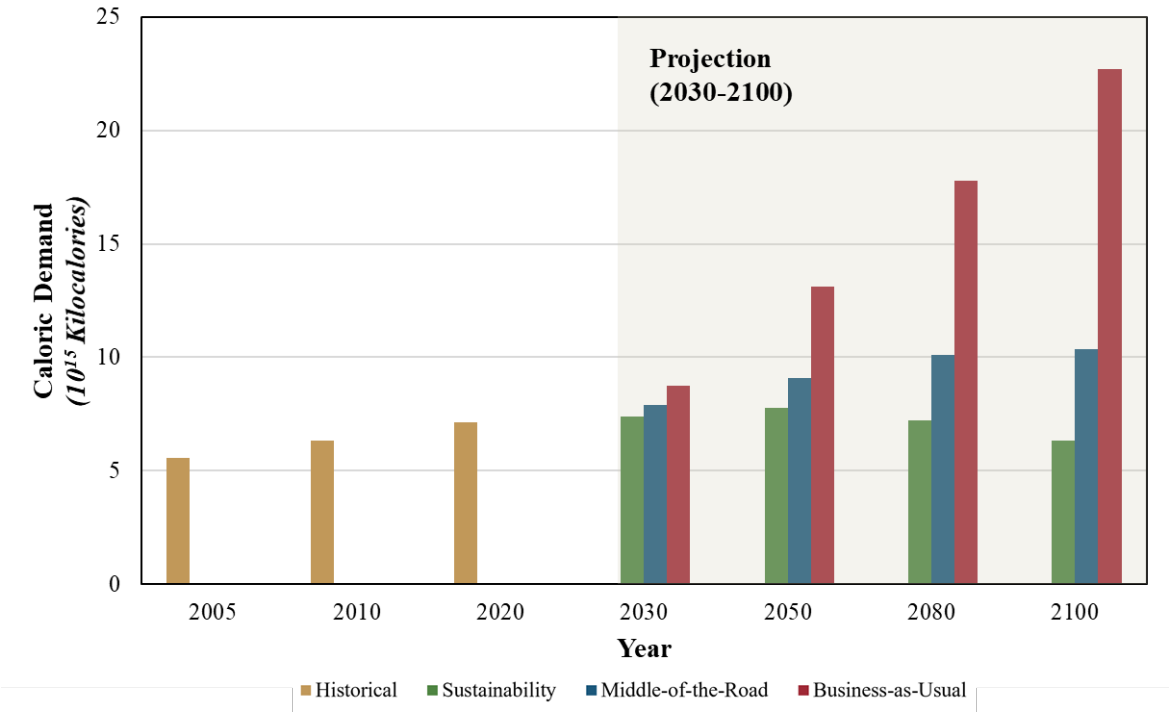

Figure 2. Global caloric demand in the 21st century. This figure shows the historical (gold) and projected global caloric demand from 2005 to 2100 based on the projected dietary trends paired with low, medium, and high population growth estimates for the sustainability (green), middle-of-the-road (blue), and business-as-usual (red) scenarios, respectively.

1.4.2 Self-sufficiency in the 21st century

We currently produce enough food globally to feed today's global population (Holt-Giménez *et al* 2012). In year 2000 most countries were self-sufficient and there was enough excess food production in certain regions to meet demand with trade in countries that were not self-sufficient (Figure 3a).

1.4.2.1 Sustainability Scenario

We deduce that by the end of the century under a sustainability scenario, half of the world's countries will be self-sufficient whilst the other half will be dependent on food imports (Figure 3b). In 2100, Nigeria, Democratic Republic of Congo, Ethiopia, and the United Republic of Tanzania will need to import vast quantities of food to feed an estimated 885 million people (Figure 4b), while China, the United States, Brazil, Russia, Argentina, Ukraine, Canada, and Australia will produce a surplus of food that could be exported and potentially feed 3.65 billion people (Figure 4a). Under this scenario, by 2100 enough food could be produced to feed the forecasted global population of 7.3 billion people (Table 1). Interestingly, China will transition to a state of surplus production and net export as a result of narrowing yield gaps through sustainable irrigation expansion and the expected stagnation in food demand.

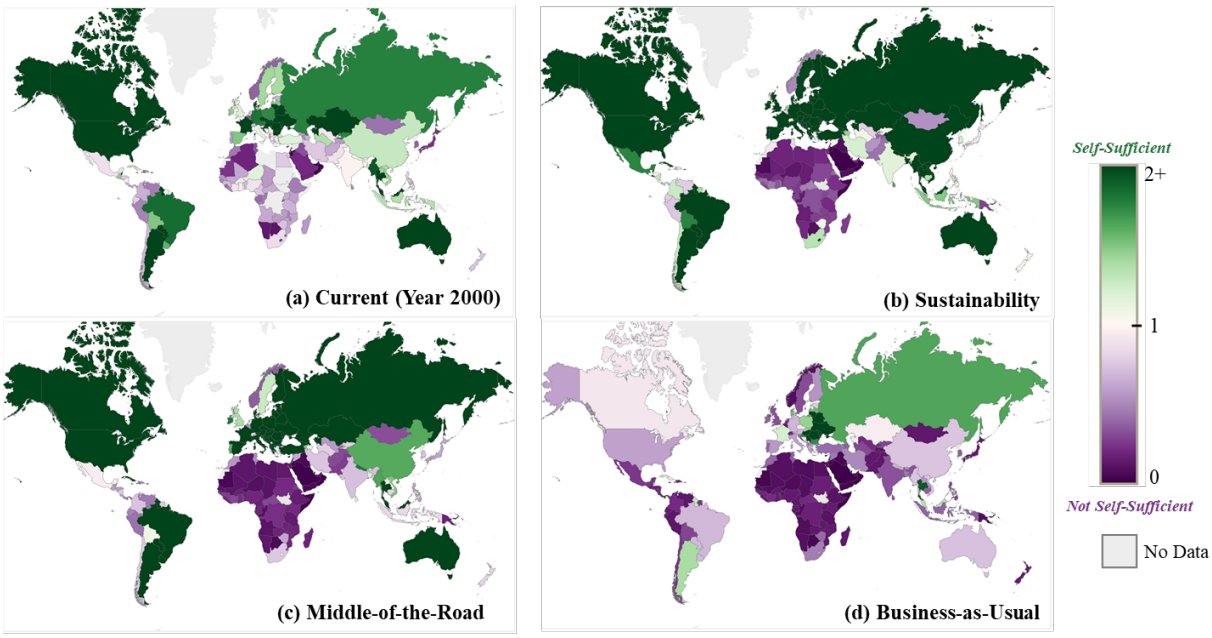

Figure 3. Global self-sufficiency ratios in the 21st century. This figure displays current country-specific self-sufficiency ratios in year 2000 (a) and projected country-specific self-sufficiency ratios in year 2100 under the three scenarios considered in this study – sustainability (b), middle-of-the-road (c), and business-as-usual (d). A country is considered self-sufficient if it has a SSR of 1 or greater (>1 indicates a surplus) shown in green, while a country with an SSR of less than 1 will not be self-sufficient (purple).

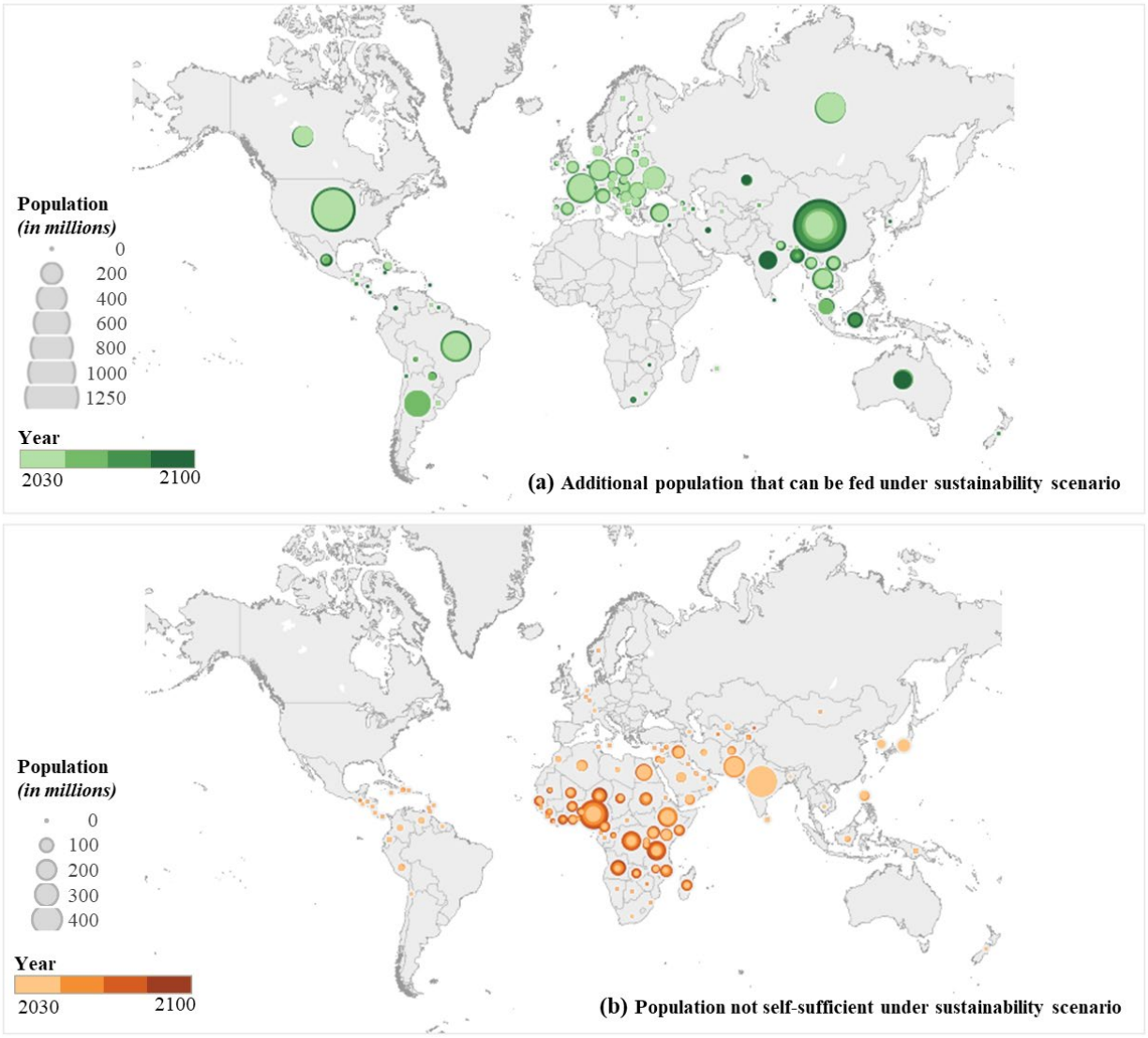

Figure 4. Excess population that can be fed (a) and population for which caloric demand will not be met (b) (in millions of people) from years 2030 to 2100 under sustainability scenario. (a) country-specific additional population that could be fed under sustainable yield gap closure based on excess crop production. (b) population whose food demand will not be met through domestic food production in each country. Population (in millions) is represented by the varying bubble sizes. The years are represented by the respective color scales with the lightest shade for year 2030 and the darkest shade for 2100. If a country has a deficit in one year and excess another, it will appear on both panels. This figure represents the sustainability scenario. A similar figure for the middle-of-the-road scenario can be found in the Supplementary Materials Figure 4.

1.4.2.2 Middle-of-the-Road Scenario

Following a middle-of-the road trajectory and reaching a population of 10.8 billion people by 2100, only 36% of countries worldwide will be self-sufficient, while 64% of countries will not produce enough crops domestically to feed their population (Figure 3c). Under this scenario, Nigeria, India, Pakistan, Ethiopia, and the Democratic Republic of Congo will heavily depend on imports while, while China, the United States, Russia, Brazil, Argentina, Ukraine, Canada, and Australia will produce a surplus of food that could be exported and potentially feed 2.69 billion people (Supplementary Figure 4). However, even accounting for all excess production under the middle-of-the-road scenario, we find that approximately 555 million people would remain food insecure in 2100 (Table 1).

Table 1. Population self-sufficiency per region under three scenarios (in millions of people). The table gives the total number of additional people that can be fed or the number of people that will be food insecure (negative values) under the sustainability, middle-of-the-road, and business-as-usual scenarios for years 2050 and 2100.

Region	**Sustainability** *RCP 2.6, SSP 1, Low Pop Variant*	**Middle-Of-The-Road** *RCP 6.0, SSP 2, Medium Pop Variant*	**Business-As-Usual** *RCP 8.5, SSP 3, High Pop Variant*
		2050	
Asia	98	-674	-1,152
Latin America	556	415	251
Middle East and Africa	-1,684	-1,925	-2,219
OECD	2,374	2,047	-293
Former Soviet Union	669	667	492
WORLD	2,013	529	-2,921
		2100	
Asia	1,856	72	-3,229
Latin America	836	444	-570
Middle East and Africa	-2,332	-3,780	-5,577
OECD	2,669	2,040	-608
Former Soviet Union	677	669	131
WORLD	3,706	-555	-9,852

1.4.2.3 Business-as-Usual Scenario

Under business-as-usual, some countries continue to be self-sufficient with excess production before mid-century (i.e. United States and China) (Figure 5 and Supplementary Figure 3). However, if a business-as-usual pathway is pursued and global population reaches 15.6 billion people, global food demand will dangerously outpace food production by the end of the century. In other words, 141 countries will not be self-sufficient (Figure 3d) and food production will not suffice to meet the caloric demands of approximately 9.8 billion people (~63% of the global population in year 2100) (Figure 5b and Table 1). Only 14% of countries in the world will be self-sufficient and have excess crop production. Our study points to Russia, Eastern Europe, and Thailand as the major bread baskets with export capabilities at the end of the century (Figure 5a).

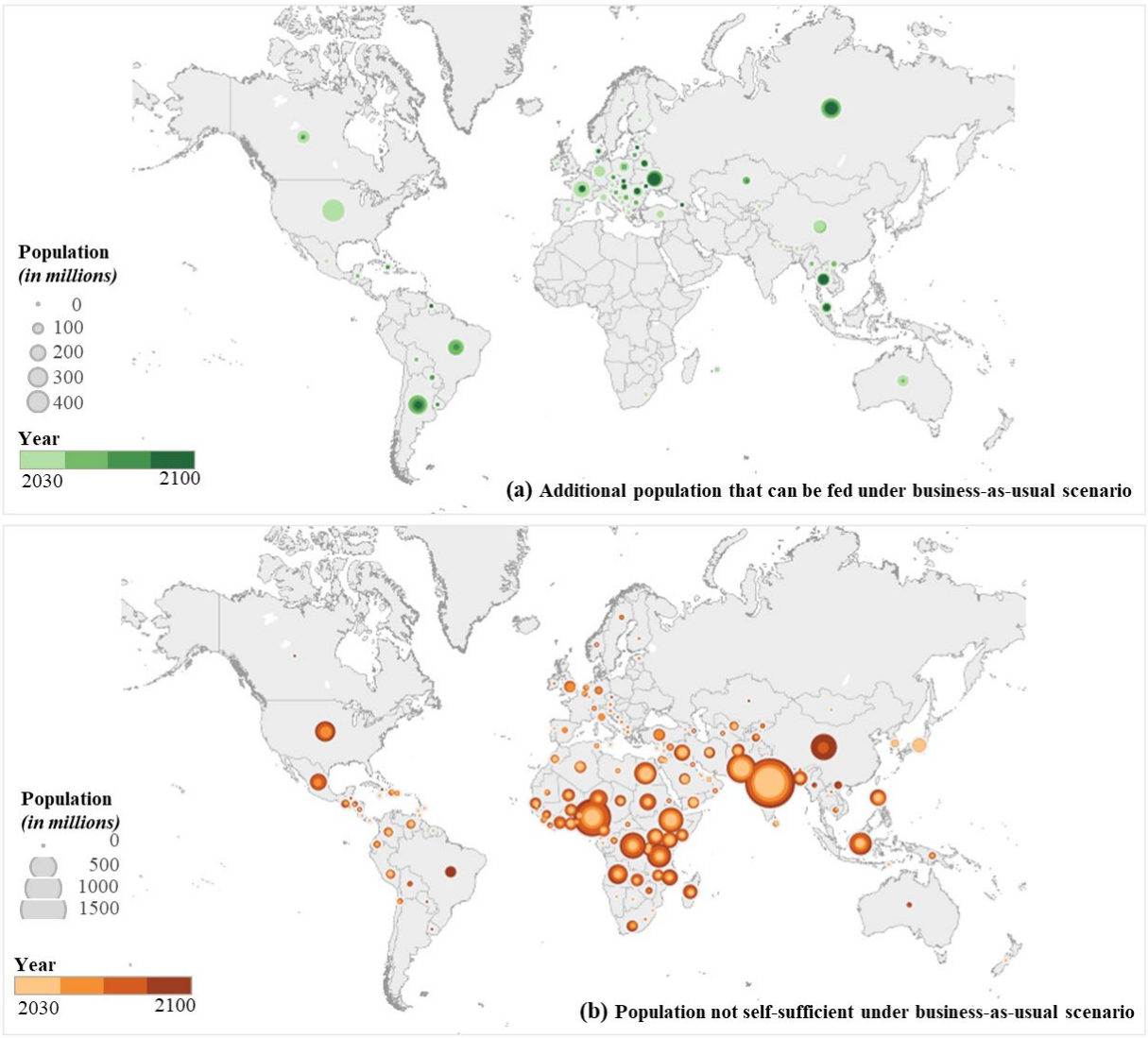

Figure 5: Excess population that can be fed (a) and population for which caloric demand will not be met (b) (in millions of people) from years 2030 to 2100 under business-as-usual scenario. (a) country-specific additional population that could be fed under sustainable yield gap closure based on excess crop production. (b) population whose food demand will not be met through domestic food production in each country. Population (in millions) is represented by the varying bubble sizes. The years are represented by the respective color scales with the lightest shade for year 2030 and the darkest shade for 2100. If a country has a deficit in one year and excess another, it will appear on both panels. This figure represents the business-as-usual scenario.

1.5 Discussion

We show the evolving fragility of the global food system considering different socio-economic pathways in the 21st century. In pairing the crop demand data with the crop production data , we found that under a sustainability scenario with a low population estimate of 7.3 billion people eating diets with lower animal-calorie shares, there will be enough crop production to feed the

global population and an additional 3.4 billion people by 2100 (Table 1). These results agree with recent studies (Gerten *et al* 2020) that found that within the current extent of croplands it is possible to sustainably feed 10.2 billion people (though, without accounting for changes in yields due to climate change). Under a middle-of-the-road pathway with a medium population estimate of 10.8 billion people with moderate diets, there will not be sufficient food production to meet the dietary needs of approximately 555 million people by 2100. Failure to pursue a sustainable trajectory and continuing a business-as-usual trajectory, will result in insufficient food availability to meet the dietary needs of approximately 9.8 billion people (Table 1).

Today, most countries in Middle East and Africa are not self-sufficient. Our results suggest that this region will continue to be heavily reliant on imports throughout the 21st century under all future scenarios. Population in this region is expected to grow significantly under middle-of-the-road and business-as-usual scenarios – increasing the number of people that may be food insecure (in terms of food availability). Contrarily, our study finds that many Former Soviet Union states are going to be major food producers and exporters through the 21st century.
While, some of the deficit may be supplemented by international food trade (D'Odorico *et al* 2019b), if trade fails to meet the needs of regions that are not self-sufficient, then millions of people may become food insecure. Moreover, in the middle-of-the-road and business-as-usual scenarios the global demand for food commodities will not be able to be completely met through trade.

Future projections of global self-sufficiency differ depending on socio-economic pathways pursued and varying degrees of radiative forcing. Our results are more sensitive to the population and diet assumptions of the shared socioeconomic pathways than to climate change (Figure 6). In fact, since we took the multi-model mean of percent-yield change across five GGCMs for three RCPs, our estimates of the effect of climate change on crop production for the four major crops do not show the uncertainties and variability associated with climate projections.

Our sensitivity analysis (Figure 6) demonstrates the sensitivity of our global self-sufficiency projections to different diet, population and climate scenarios. The extent of each bar represents the sensitivity of global self-sufficiency to population growth variants under the diet scenario in each panel. For example, under the sustainability scenario with an SSP1 diet in the year 2100 and a low population scenario there is excess food production. However, under the same diet assumption and year but with a high population, there is not enough food produced to meet demand. Additionally, by maintaining the population scenario and the year constant the differences in projected global self-sufficiency across all three scenario panels reflect the different results based on dietary assumptions (in other words, the sensitivity of global self-sufficiency projections to the different diets). For example, assuming a high population in year 2100, under each SSP diet scenario separately, approximately 4 billion (SSP1), 5.5 billion (SSP2), or 9.8 billion (SSP3) people cannot be fed. Thus, moderating diets (as well as reducing food losses, waste, and biofuel production – which are not explicitly accounted for in our scenario-based analysis) will be crucial strategies to increase food availability and minimize the number of food-insecure people when crop production becomes limited (Foley *et al* 2011; Davis *et al* 2014; Gephart *et al* 2016; Kummu *et al* 2017). As depicted in the figure, the effects of climate change on crop production (black interval bars) are minimal due to the averaging effect (see limitations and uncertainty section). Table 1 displays values of net population the can or cannot be fed in years 2050 and 2100 for the Sustainability, Middle-of-the-Road, and Business-as-usual scenarios as defined in the paper. The results of the various possible combinations of climate (RCP), diet (SSP), and population (UN) scenarios assuming 80% yield gap closure are shown as a sensitivity analysis in Figure 6.

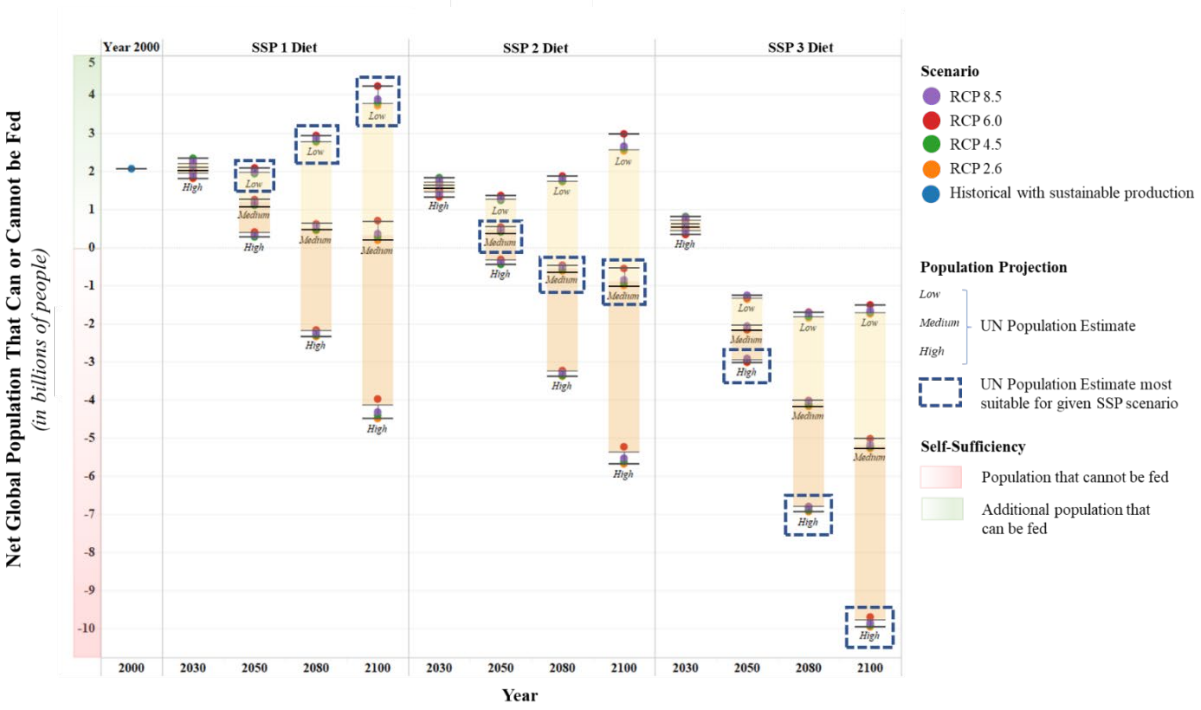

Figure 6. Sensitivity analysis of global net population that can or cannot be fed (in billions of people). Number of people (in billions) that can be fed (in green) – in addition to global population; and the projected number of people for whom there will not be enough crop production available to meet their caloric needs (pink). The first panel (left) represents year 2000 self-sufficiency, which shows the planet's ability to feed additional 2 billion people, while the remaining three panels represent the SSP1, SSP2 and SSP3 scenarios of *per capita food demand*. The blue dashed box denotes the UN population variant that best matches each of the SSP scenarios based on their underlying assumptions. The SSP1 diet with the low population is representative of the Sustainability scenario; the SSP2 diet with the medium population represents the Middle-of-the-Road scenario; and the SSP3 diet with the high population represents the Business-as-Usual scenario.

1.5.1 Limitations, Assumptions, and Uncertainties

The complexity of a global analysis often requires the adoption of suitable assumptions. Our study assumes an 80% yield gap closure globally based on the blue water availability estimates from Rosa *et al* (2018). Without narrowing the yield gap, food insecurity will be much higher than what our study forecasts. Unlike previous studies (e.g., Davis *et al* 2014) that quantified the size of the global population that could be fed at yield gap closure without accounting for the availability of water resources for irrigation, here it is assumed that irrigation is adopted to close the yield gap only in regions where it is water sustainable. In this study we consider potential future changes in food production (for the major 4 crops) from changes in precipitation and temperature regimes that could affect future water availability and crop production based on the HadGEM2-ES earth system model. However, we neither account for the effects of climate related shocks, such as droughts, floods, and other extreme climate events, nor for the impact of climate change

on the sustainable expansion irrigation to rainfed areas. These points will be explored in future studies.

The rates of food loss or waste as well as the biofuel production per crop per country were based on the five-year average from 2009-2013 and were assumed to remain constant until 2100. We expect food loss and waste to continue to persist in the 21st century, but the rate of change is difficult to accurately predict and for this reason we kept them constant. The OECD-FAO Agricultural Outlook projects global biofuel production up to year 2028 (OECD/FAO 2019) with strong uncertainties. Hence, to not add further assumptions in our estimates, we assumed the current rate of biofuel production to remain constant as well.

To assess the effects of climate change on crop yields we considered five global gridded crop models. These models are subjected to substantial uncertainties from both model structure and parametrization as well as from calibration and input data quality (Müller *et al* 2017, Elliott *et al* 2015). There are significant differences among the crop model outcomes for changes in crop yields based on the three RCP scenarios evaluated. In this study we do not show the range of variability associated with GGCMs but took the multi-model mean for changes in crop yields. In taking the multi-model mean, the effects of climate change on crop production are minimal in our results (Figure 6). Additionally, due to data availability, the percent yield change due to climate change was only considered for four major crops (maize, soy, wheat, and rice) which account for 70% of global crop production (D'Odorico *et al* 2014, Warszawski *et al* 2014). Crop yields data for the four major crops under different climate scenarios were aggregated to the current yield data of the remaining 18 crops (not accounting for climate change for these 18 crops) which account for a significant portion of the remaining crop production. Finally, this study solely considers the food availability pillar of food security and does not consider patterns of food access and utilization.

1.6 Conclusion

End of hunger, achievement of food security, and improvement in nutrition are at the heart of the United Nations' Sustainable Development Goals. This study evaluates the impact of sustainable irrigation expansion, climate change, population growth, and dietary changes on global self-sufficiency ratios through an integrative assessment approach for the remainder of the 21st century. Our results assume achievement of 80% yield gap closure globally through sustainable irrigation expansion onto currently rainfed croplands. This is a significant assumption, yet even with the increased production, our results show that global food availability will only meet the global food demand under the sustainability scenario. Under the middle-of-the road and business-as-usual scenarios, a multitude of nations and their people are at risk of food insecurity (in terms of food availability). Without sustainable irrigation expansion, global self-sufficiency ratios will worsen. Although climate change plays a role, self-sufficiency ratios are highly sensitive to population growth estimates and dietary changes based on socio-economic pathways pursued. Future societies' resilience against global challenges such as climate change hinges on successful implementation of policies, actions and development strategies (Andrijevic *et al* 2019). Hence, investing in girls' education and expanding people's access to family-planning services in the developing world where populations are projected to increase (Abel *et al* 2016); and reducing global meat consumption in emergent economies, in addition to sustainably increasing agricultural production will be essential measures for countries working towards resilience and sustainability in the face of climate change.

1.7 References

Abel G J, Barakat B, Samir K C and Lutz W, 2016. Meeting the Sustainable Development Goals leads to lower world population growth. *Proceedings of the National Academy of Sciences*, *113*(50), pp.14294-14299.

Aggarwal P, Vyas S, Thornton P and Campbell B M 2019 How much does climate change add to the challenge of feeding the planet this century? *Environ. Res. Lett.* **14** 043001

Alexandratos N and Bruinsma J 2012 *World Agriculture towards 2030/2050: the 2012 revision* (Rome) Online: www.fao.org/economic/esa

Andrijevic M, Crespo Cuaresma J, Muttarak R and Schleussner C-F 2019 Governance in socioeconomic pathways and its role for future adaptive capacity *Nat. Sustain.* Online: https://doi.org/10.1038/s41893-019-0405-0

Brown L R, 2012. Full planet, empty plates: the new geopolitics of food scarcity. WW Norton & Company. New York.

Cassidy E S, West P C, Gerber J S and Foley J A 2013 Redefining agricultural yields: From tonnes to people nourished per hectare *Environ. Res. Lett.* **8**

D'Odorico P, Carr J A, Davis K F, Dell'Angelo J and Seekell D A 2019a Food Inequality, Injustice, and Rights *Bioscience* **69** 180–90

D'Odorico P, Carr J, Dalin C, Dell'Angelo J, Konar M, Laio F, Ridolfi L, Rosa L, Suweis S, Tamea S and Tuninetti M 2019b Global virtual water trade and the hydrological cycle: patterns, drivers, and socio-environmental impacts *Environ. Res. Lett.* **14** 053001

D'Odorico P, Davis K F, Rosa L, Carr J A, Chiarelli D, Dell'Angelo J, Gephart J, MacDonald G K, Seekell D A, Suweis S and Rulli M C 2018 The Global Food-Energy-Water Nexus *Rev. Geophys.* **56** 456–531

D'Odorico P, Carr J A, Laio F, Ridolfi L and Vandoni S 2014 Feeding humanity through global food trade *Earth's Future.* **2** 458–69

Davis K F, D'Odorico P and Rulli M C 2014 Moderating diets to feed the future *Earth's Futur.* **2** 559–65

Davis K F, Rulli M C, Seveso A and D'Odorico P 2017 Increased food production and reduced water use through optimized crop distribution. *Nature Geoscience.* **10**(12), p.919.

Deutsch C A, Tewksbury J J, Tigchelaar M, Battisti D S, Merrill S C, Huey R B and Naylor R L 2018 Increase in crop losses to insect pests in a warming climate *Science (80-.).* **361** 916–9

Elliott J, Müller C, Deryng D, Chryssanthacopoulos J, Boote K J, Büchner M, Foster I, Glotter M, Heinke J, Iizumi T, Izaurralde R C, Mueller N D, Ray D K, Rosenzweig C, Ruane A C and Sheffield J 2015 The Global Gridded Crop Model Intercomparison: data and modeling protocols for Phase 1 (v1.0) *Geosci. Model Dev* **8** 261–77

Erisman, J.W., Sutton, M.A., Galloway, J., Klimont, Z. and Winiwarter, W., 2008. How a 533 century of ammonia synthesis changed the world. *Nature Geoscience*, *1*(10), p.636.

Fader M, Gerten D, Krause M, Lucht W and Cramer W 2013 Spatial decoupling of agricultural production and consumption: Quantifying dependences of countries on food imports due to domestic land and water constraints *Environ. Res. Lett.* **8**

Falkenmark M, and Rockström J 2004 Balancing water for humans and nature: The new approach in ecohydrology. London & Sterling, VA: *Earthscan*.

FAO 2002 *The State of Food Insecurity in the World 2001.* Rome

FAO 2017a FAOSTAT Online Database Online: http://www.fao.org/faostat/en/#data/FBS

Fitton N, Alexander P, Arnell N, Bajzelj B, Calvin K, Doelman J, Gerber J S, Havlik P, Hasegawa T, Herrero M, Krisztin T, van Meijl H, Powell T, Sands R, Stehfest E, West P C and Smith P 2019 The vulnerabilities of agricultural land and food production to future water scarcity *Glob. Environ. Chang.* **58** 101944

Foley J A, Ramankutty N, Brauman K A, Cassidy E S, Gerber J S, Johnston M, Mueller N D, O'Connell C, Ray D K, West P C, Balzer C, Bennett E M, Carpenter S R, Hill J, Monfreda C, Polasky S, Rockström J, Sheehan J, Siebert S, Tilman D and Zaks D P M 2011 Solutions for a cultivated planet *Nature* **478** 337–42

Fricko O, Havlik P, Rogelj J, Klimont Z, Gusti M, Johnson N, Kolp P, Strubegger M, Valin H, Amann M, Ermolieva T, Forsell N, Herrero M, Heyes C, Kindermann G, Krey V, McCollum D L, Obersteiner M, Pachauri S, Rao S, Schmid E, Schoepp W and Riahi K 2017 The marker quantification of the Shared Socioeconomic Pathway 2: A middle-of-the-road scenario for the 21st century *Glob. Environ. Chang.* **42** 251–67

Fujimori S, Hasegawa T, Masui T, Takahashi K, Herran D S, Dai H, Hijioka Y and Kainuma M 2017 SSP3: AIM implementation of Shared Socioeconomic Pathways *Glob. Environ. Chang.* **42** 268–83

Garnett T, Appleby M C, Balmford A, Bateman I J, Benton T G, Bloomer P, Burlingame B, Dawkins M, Dolan L, Fraser D, Herrero M, Hoffmann I, Smith P, Thornton P K, Toulmin C, Vermeulen S J and Godfray H C J 2013 Sustainable intensification in agriculture: Premises and policies *Science (80-.).* **341** 33–4

Gephart J A, Davis K F, Emery K A, Leach A M, Galloway J N and Pace M L, 2016. The environmental cost of subsistence: optimizing diets to minimize footprints. *Science of the Total Environment*, *553*, pp.120-127.

Gerten D, Heck V, Jägermeyr J, Bodirsky B L, Fetzer I, Jalava M, Kummu M, Lucht W, Rockström J, Schaphoff S and Schellnhuber H J 2020. Feeding ten billion people is possible within four terrestrial planetary boundaries. *Nature Sustainability*, pp.1-9.

Godfray H C J, Beddington J R, Crute I R, Haddad L, Lawrence D, Muir J F, Pretty J, Robinson S, Thomas S M and Toulmin C 2010 Food security: The challenge of feeding 9 billion people *Science (80-.).* **327** 812–8

IPCC, 2014: *Climate Change 2014: Synthesis Report. Contribution of Working Groups I, II and III to the Fifth Assessment Report of the Intergovernmental Panel on Climate Change* [Core Writing Team, R.K. Pachauri and L.A. Meyer (eds.)]. IPCC, Geneva, Switzerland, 151 pp.

Holt-Giménez E, Shattuck A, Altieri M, Herren H and Gliessman S 2012 We Already Grow Enough Food for 10 Billion People... and Still Can't End Hunger *J. Sustain. Agric.* **36** 595–8

Jägermeyr J, Gerten D, Schaphoff S, Heinke J, Lucht W and Rockström J 2016 Integrated crop water management might sustainably halve the global food gap *Environ. Res. Lett.* **11** 025002

Jalava M, Kummu M, Porkka M, Siebert S and Varis O 2014 Diet change—a solution to reduce water use? *Environ. Res. Lett.* **9** 074016

Kinnunen, P., Guillaume, J.H., Taka, M., D'Odorico, P., Siebert, S., Puma, M.J., Jalava, M. and Kummu, M., 2020. Local food crop production can fulfil demand for less than one-third of the population. *Nature Food*, *1*(4), pp.229-237.

Kummu M, de Moel H, Porkka M, Siebert S, Varis O and Ward P J 2012 Lost food, wasted resources: Global food supply chain losses and their impacts on freshwater, cropland, and fertiliser use *Sci. Total Environ.* **438** 477–89

Kummu M, Fader M, Gerten D, Guillaume J H, Jalava M, Jägermeyr J, Pfister S, Porkka M, Siebert S and Varis O, 2017. Bringing it all together: Linking measures to secure nations' food supply. *Current opinion in environmental sustainability*, *29*, pp.98-117.

Lobell D B, Cassman K G and Field C B, 2009. Crop yield gaps: their importance, magnitudes, and causes. *Annual review of environment and resources*, *34*, pp.179-204.

Lobell D B and Gourdji S M 2012 The influence of climate change on global crop productivity *Plant Physiol.* **160** 1686–97

Macdonald G K 2013 Eating on an interconnected planet *Environ. Res. Lett.* **8**

Marchand P, Carr J A, Dell'Angelo J, Fader M, Gephart J A, Kummu M, et al. 2016 Reserves and trade jointly determine exposure to food supply shocks. *Environmental Research Letters.* **11**(9), 095009. https://doi.org/10.1088/1748-9326/11/9/095009

Mueller N D, Gerber J S, Johnston M, Ray D K, Ramankutty N and Foley J A 2012 Closing yield gaps through nutrient and water management *Nature* **490** 254–7

Müller C, Elliott J, Chryssanthacopoulos J, Arneth A, Balkovic J, Ciais P, Deryng D, Folberth C, Glotter M, Hoek S, Iizumi T, Izaurralde R C, Jones C, Khabarov N, Lawrence P, Liu W, Olin S, Pugh T A M, Ray D K, Reddy A, Rosenzweig C, Ruane A C, Sakurai G, Schmid E, Skalsky R, Song C X, Wang X, De Wit A and Yang H 2017 Global gridded crop model evaluation: Benchmarking, skills, deficiencies and implications *Geosci. Model Dev.* **10** 1403–22

O'Neill B C, Kriegler E, Riahi K, Ebi K L, Hallegatte S, Carter T R, Mathur R and van Vuuren D P 2014 A new scenario framework for climate change research: The concept of shared socioeconomic pathways *Clim. Change* **122** 387–400

OECD/FAO 2019 *OECD-FAO Agricultural Outlook 2019-2028* (Rome: OECD /FAO) Online: https://doi.org/10.1787/agr_outlook-2019-en

Ostberg S, Schewe J, Childers K and Frieler K 2018 Changes in crop yields and their variability at different levels of global warming *Earth Syst. Dyn.* **9** 479–96

Phalan B, Balmford A, Green R E and Scharlemann J P W 2011 Minimising the harm to

biodiversity of producing more food globally *Food Policy* **36**

Popp A, Calvin K, Fujimori S, Havlik P, Humpenöder F, Stehfest E, Bodirsky B L, Dietrich J P, Doelmann J C, Gusti M and Hasegawa T 2017 Land-use futures in the shared socio-economic pathways. *Global Environmental Change*, *42*, pp.331-345.

Porkka M, Kummu M, Siebert S and Varis O, 2013. From food insufficiency towards trade dependency: a historical analysis of global food availability. *PloS one*, *8*(12), p.e82714.

Pretty J 2018 Intensification for redesigned and sustainable agricultural systems *Science (80-.).* **362**

Puma M J, Bose S, Chon S Y and Cook B I 2015 Assessing the evolving fragility of the global food system *Environ. Res. Lett.* **10**

Ray D K, Mueller N D, West P C and Foley J A 2013 Yield Trends Are Insufficient to Double Global Crop Production by 2050 ed J P Hart *PLoS One* **8** e66428

Riahi K, van Vuuren D P, Kriegler E, Edmonds J, O'Neill B C, Fujimori S, Bauer N, Calvin K, Dellink R, Fricko O, Lutz W, Popp A, Cuaresma J C, KC S, Leimbach M, Jiang L, Kram T, Rao S, Emmerling J, Ebi K, Hasegawa T, Havlik P, Humpenöder F, Da Silva L A, Smith S, Stehfest E, Bosetti V, Eom J, Gernaat D, Masui T, Rogelj J, Strefler J, Drouet L, Krey V, Luderer G, Harmsen M, Takahashi K, Baumstark L, Doelman J C, Kainuma M, Klimont Z, Marangoni G, Lotze-Campen H, Obersteiner M, Tabeau A and Tavoni M 2017 The Shared Socioeconomic Pathways and their energy, land use, and greenhouse gas emissions implications: An overview *Glob. Environ. Chang.* **42** 153–68

Rojas M, Lambert F, Ramirez-Villegas J and Challinor A J 2019 Emergence of robust precipitation changes across crop production areas in the 21st century *Proc. Natl. Acad. Sci. U. S. A.* **116** 6673–8

Rosa, L., Chiarelli, D.D., Rulli, M.C., Dell'Angelo, J. and D'Odorico, P., 2020. Global agricultural economic water scarcity. *Science Advances*, *6*(18), p.eaaz6031.

Rosa L, Chiarelli D D, Tu C, Rulli M C and D'Odorico P 2019 Global unsustainable virtual water flows in agricultural trade *Environ. Res. Lett.*

Rosa L, Rulli M C, Davis K F, Chiarelli D D, Passera C and D'Odorico P 2018 Closing the yield gap while ensuring water sustainability *Environ. Res. Lett.* **13**

Rosenzweig C, Elliott J, Deryng D, Ruane A C, Müller C, Arneth A, Boote K J, Folberth C, Glotter M, Khabarov N, Neumann K, Piontek F, Pugh T A M, Schmid E, Stehfest E, Yang H and Jones J W 2014 Assessing agricultural risks of climate change in the 21st century in a global gridded crop model intercomparison. *Proc. Natl. Acad. Sci. U. S. A.* **111** 3268–73

Schleussner C F, Deryng D, Müller C, Elliott J, Saeed F, Folberth C, Liu W, Wang X, Pugh T A M, Thiery W, Seneviratne S I and Rogelj J 2018 Crop productivity changes in 1.5 °c and 2 °c worlds under climate sensitivity uncertainty *Environ. Res. Lett.* **13**

Seekell D, Carr J, Dell'Angelo J, D'Odorico P, Fader M, Gephart J, Kummu M, Magliocca N, Porkka M, Puma M, Ratajczak Z, Rulli M C, Suweis S and Tavoni A 2017 Resilience in the global food system *Environ. Res. Lett.* **12** 025010

Sen A. 1981 Poverty and famines: An essay on entitlement and deprivation. Oxford: *Oxford University Press*.

Springmann M, Clark M, Mason-D'Croz D, Wiebe K, Bodirsky B L, Lassaletta L, ... and Jonell M 2018 Options for keeping the food system within environmental limits. *Nature.* **562**(7728), 519.

Suweis S, Carr J A, Maritan A, Rinaldo A, and D'Odorico P 2015 Resilience and reactivity of global food security. *Proceedings of the National Academy of Sciences.* **112**(22), 6902–6907.

Taylor K E, Stouffer R J and Meehl G A 2012 An overview of CMIP5 and the experiment design *Bull. Am. Meteorol. Soc.* **93** 485–98

Tilman D, Balzer C, Hill J and Befort B L 2011 Global food demand and the sustainable intensification of agriculture *Proc. Natl. Acad. Sci. U. S. A.* **108** 20260–4

United Nations 2018 *The Sustainable Development Goals Report 2018*

United Nations 2019 World Population Prospects 2019 Online: https://population.un.org/wpp/

Van Ittersum M K, Cassman K G, Grassini P, Wolf J, Tittonell P and Hochman Z 2013 Yield gap analysis with local to global relevance-A review *F. Crop. Res.* **143** 4–17

van Vuuren D P, Edmonds J, Kainuma M, Riahi K, Thomson A, Hibbard K, Hurtt G C, Kram T, Krey V, Lamarque J F, Masui T, Meinshausen M, Nakicenovic N, Smith S J and Rose S K 2011 The representative concentration pathways: An overview *Clim. Change* **109** 5–31

van Vuuren D P, Stehfest E, Gernaat D E H J, Doelman J C, van den Berg M, Harmsen M, de Boer H S, Bouwman L F, Daioglou V, Edelenbosch O Y, Girod B, Kram T, Lassaletta L, Lucas P L, van Meijl H, Müller C, van Ruijven B J, van der Sluis S and Tabeau A 2017 Energy, land-use and greenhouse gas emissions trajectories under a green growth paradigm *Glob. Environ. Chang.* **42** 237–50

Vogel E, Donat M G, Alexander L V., Meinshausen M, Ray D K, Karoly D, Meinshausen N and Frieler K 2019 The effects of climate extremes on global agricultural yields *Environ. Res. Lett.* **14**

Warszawski L, Frieler K, Huber V, Piontek F, Serdeczny O and Schewe J 2014 The Inter-Sectoral Impact Model Intercomparison Project (ISI–MIP): Project framework *Proc. Natl. Acad. Sci.* **111** 3228–32

1.8 Supplementary Information -Extended Methods

Self-Sufficiency Ratios

We define self-sufficiency as the ability of a country to meet the caloric demand of its population through domestic food production in a given year. The country-specific self-sufficiency ratios (SSR) are measured as the total estimated kcal production divided by the total estimated kcal demand of each individual country for the years *x*=2030, 2050, 2080, and 2100 (Equation 1).

$$SSR_{year\ x,country\ n} = \frac{projected\ production_{x,n}}{projected\ demand_{x,n}} \quad (1)$$

Projected production is function of sustainable irrigation intensification and projected changes in yield due to climate change. Projected demand is a function of dietary changes and population growth forecasts. A country is considered self-sufficient if it has an SSR of 1 or greater (>1 indicates a surplus), while a country with an SSR less than 1 is not self-sufficient. Self-Sufficiency ratios inform us about which countries may produce enough crops to meet their domestic demand, and which will likely depend on international food trade and food supply stocks to feed their population (Puma *et al* 2015, Suweis *et al* 2015; Marchand *et al* 2016; Seekell *et al* 2017).

Sustainable Yield Gap Closure through Sustainable Irrigation Intensification

Irrigation practices are classified as unsustainable when their water consumption exceeds local renewable water availability (Rosa *et al* 2018). In these conditions, irrigation uses water that should be allocated to environmental flows and therefore contributes to environmental degradation and groundwater depletion (Rosa *et al* 2019). The Rosa *et al* 2018 paper assessed calorie production per crop class as the product of crop yield (tons per hectare), crop calorie content (kcal per tons), and crop harvested area (hectares). Current and maximized crop yields were taken from Monfreda *et al* 2008 and Mueller *et al* 2012, respectively. Calorie content for each crop was taken from D'Odorico *et al* 2014. Crop harvested areas were taken from Portman *et al* 2010. For each of the 22 crop classes considered in this study (Portmann *et al* 2010; Rosa *et al* 2018), the extent of sustainable irrigated production in the year 2000 and additional production potential with yield gap closure were taken from Rosa *et al* 2018.

Since 100% yield gap closure is generally neither economically feasible nor environmentally desirable (Van Ittersum *et al* 2013), we assumed 80% sustainable yield gap closure globally as the basis for future projections of global crop yields. Here we define sustainable production (P_s) for each crop class (i) as the sum of total rain-fed production (circa 2000) ($P_{rf,2000}$), sustainable irrigated production (circa 2000) ($P_{irr,2000}$), and additional potential production that could be available under an 80% yield gap closure scenario ($P_{80\%}$) (Equation 2).

$$P_{s,i} = P_{rf,2000,i} + P_{irr,2000,i} + P_{80\%,i} \quad (2)$$

Food Waste and Other Uses

Crop-specific and country-specific data for crop losses (i.e. food waste) and biofuels use were taken from the FAOSTAT Food Balance Sheets (FAO 2017a). The five-year average of the fraction of losses (l) and other uses (i.e. biofuels) (b) were calculated for the five most recent years of available data (2009 -2013) and assumed to be the current values. To our knowledge, there are no available projections of food waste and biofuel production in the 21st century, hence, we assumed that the current fraction of food waste and biofuels will apply for the remainder of the

21st century. The calories expected to be lost or allocated for other uses based on the designated percentages were subtracted from the sustainable production for each country per crop under the 80% yield gap closure scenario to derive the available yield in kilocalories for food and feed ($P_{available}$) (Equation 3).

$$P_{available,i} = P_{s,i} \times (1 - l_i - b_i) \quad (3)$$

Projected Yields with Climate Change

Currently, estimates of percent change in yields due to climate change are mainly available for the four major crops (maize, rice, wheat, and soybean) (e.g., Warszawski *et al* 2014; Ostberg *et al* 2018), which account for 70% of global calorie production (D'Odorico *et al* 2014). Percent yield change estimates were derived for the four major crops under three Representative Concentration Pathways (RCP) scenarios (RCP 2.6, RCP 6.0, and RCP 8.5) from years 2030 to 2100 for 10 global regions from the Inter-Sectoral Impact Model Intercomparison Project (ISIMIP) in the context of the Coupled Model Intercomparison Project, Phase 5 (Rosenzweig *et al* 2014, Warszawski *et al* 2014, Taylor *et al* 2012, van Vuuren *et al* 2011). Since yield estimates vary among the five global gridded crop models (GGCMs) (GEPIC, LPJ-GUESS, LPJmL, PEGASUS, and pDSSAT) forced by the bias-corrected climate model projections of the HadGEM2-ES Global Climate Model (GCM) used in this analysis, the multi-model mean of percent yield change (ΔY_{clim}) for the four major crops was calculated for the three RCPs. The regional mean percent yield change was then applied to the countries that lie within each respective region. The projected yields accounting for climate change for maize, rice, wheat and soybean were then added to the current available yield data of the remaining 18 crops (without climate change) to find the projected total crop production ($P_{total,cc}$) for every country, year, and RCP scenario (Equation 4).

$$P_{total,cc} = \sum_{i=1}^{4}\left[P_{available,i} + (P_{available,i} \times \Delta Y_{clim})\right] + \sum_{i=5}^{22} P_{available,i} \quad (4)$$

The effects of climate change on crop yields was accounted only for the four major crops.

Dietary changes and Population Growth

From the SSP database developed by the International Institute for Applied Systems (IIASA), we gathered agricultural demand data for five major global regions (OECD, Former Soviet Union, Latin America, Asia, and Middle East and Africa) under three SSP scenarios – SSP1, SSP2, and SSP3. Under SSP1, diets with low-animal calorie shares prevail; under SSP2 caloric consumption and animal calorie shares converge towards moderate levels; and under SSP3 diets with high animal shares prevail (Riahi *et al* 2017, van Vuuren *et al* 2017, Fricko *et al* 2017, Fujimori *et al* 2017, Popp *et al* 2017). The yearly animal-based consumption and vegetal-based consumption percentages of per capita diets were extrapolated from the IIASA agricultural demand data (SSP Database Version 2.0) (Riahi *et al* 2017; Popp *et al* 2017). The fraction of animal-based diet per capita for a given year and region based on SSP-IAM data was calculated through equation (5):

$$A_{x,r} = \frac{a_{x,r}}{c_{x,r} - e_{x,r}} \quad (5)$$

where $A_{x,r}$ represents the fraction of animal-based consumption in diets for the year *x* and region *r* of interest, *a* is the per capita livestock demand, *c* is the total per capita crop demand, and *e* represents the per capita demand of crop for energy from the SSP Database (in million tons of dry mass/yr / million). Hence, the fraction of vegetal-based diet ($V_{x,r}$) per capita was defined as (Equation 6):

$$V_{x,r} = \left(1 - A_{x,r}\right) \quad (6)$$

Where V_{xr} represents the fraction of crop demand for direct human consumption for year *x* and region *r*. The final diet composition fractions were assigned to each country based on its region.

Following the calculation of diet composition percentages for three SSP scenarios, we proceeded to calculate the total projected annual caloric demand in kcal per capita for each country. In order to calculate the crop calorie demand from animal products (i.e., the feed demand), the plant to animal caloric conversion factors (q) per country and the initial fraction of total animal calories from feed ($r_{initial}$) were taken from (Davis *et al* 2014). The fraction of total animal calories from feed for future years was assessed subtracting the grass-fed fraction of animal calories, and assuming that the amount of grass fed animal calorie demand will remain constant [i.e., equal to $A_{initial,n}\ (1 - r_{initial,n})$] in the future, as shown in equation 7:

$$r_{x,n} = \frac{A_{x,n} - A_{initial,n}\ (1 - r_{initial,n})}{A_{x,n}} \quad (7)$$

where $r_{x,n}$ is the fraction of total animal calories from feed for country *n* in year *x*. $A_{x,n}$ is the fraction of animal-based diet of the country and year evaluated, $A_{initial,n}$ is the initial fraction of animal-based diet (circa 2000) for country *n*, and $r_{initial,n}$ represents the initial fraction of total animal calories from feed (circa 2000) for country *n*.

For human well-being, an individual should consume at or above an average daily energy requirement, F_{wb}, estimated at 2327 kcal per capita per day (e.g., D'Odorico *et al* 2019a). Thus, the per capita caloric demand from animal-based products (K) was calculated following Equation 8:

$$K = F_{wb} \times q \times r_{x,n} \times A_{x,n} \quad (8)$$

where (q) is the country-based the plant to animal caloric conversion factor. Per capita caloric demand from crops for direct human consumption was estimated as the product of F_{wb} and $V_{x,n}$. $A_{x,n}$ and $V_{x,n}$ are based on the SSP scenario evaluated. By summing the per capita caloric demand from animal-based products and crops, and then multiplying the resultant daily caloric value by 365 days, we assessed the annual projected per capita caloric demand per country for years 2030 to 2100 under SSP 1, SSP 2, and SSP 3. We estimated the total annual projected caloric demand (D) per country for years 2030 to 2100 by multiplying the per capita demand estimates (based on SSP scenarios) by the estimated population of a country under the respective United Nations population variant (*var*) (Equation 9).

$$D = \left[K + \left(F_{wb} \times V_{x,n}\right)\right] \times 365\ days \times Population_{var} \quad (9)$$

Population estimates were taken from the United Nations 2019 World Population Prospects for all 165 countries included in this study (United Nations 2019). The UN Population Prospects include low, medium, and high population variants. Based on the basic underlying assumptions of each SSP scenario, we paired each SSP with the appropriate population variant – SSP 1 was paired with the low population variant, SSP 2 was paired with the medium population variant, and SSP 3 with the high population variant (Riahi *et al* 2017). Supplementary Figure 5 displays an example analysis using the methodological framework used in this study.

1.9 Supplementary Figures

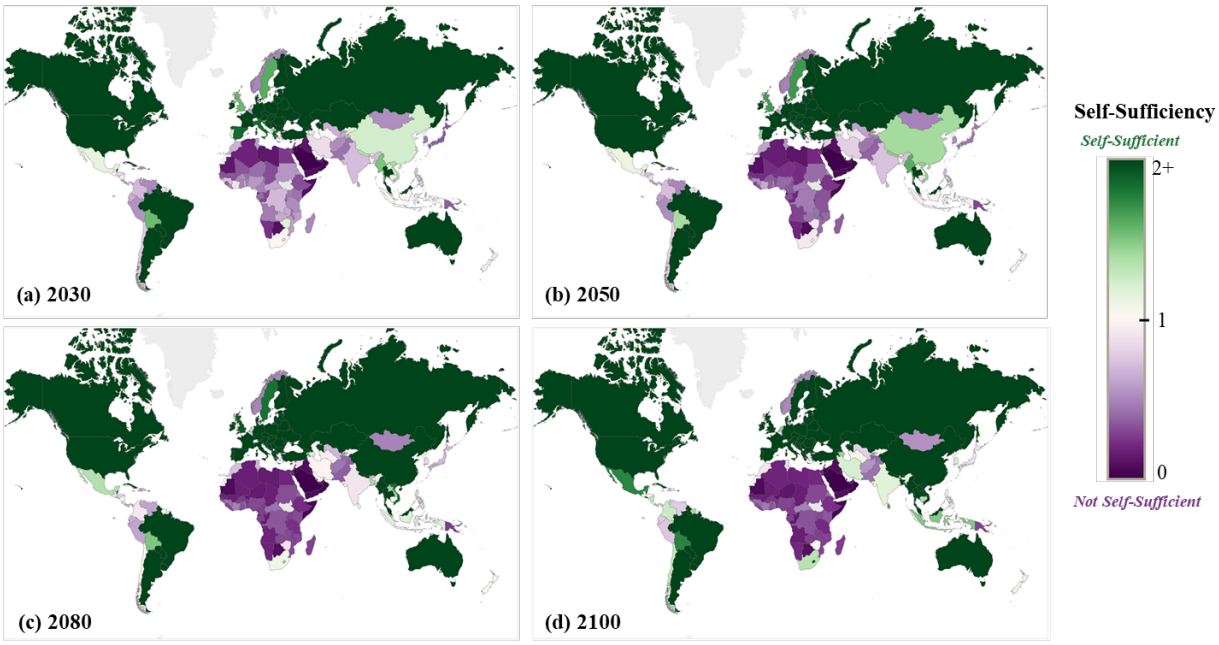

Supplementary Figure 1. Global self-sufficiency ratios under sustainability scenario from 2030 to 2100. This figure displays country-specific self-sufficiency ratios for the sustainability scenario in years 2030, 2050, 2080 and 2100. A country is considered self-sufficient if it has an SSR of 1 or greater (>1 indicates a surplus) shown in green, while a country with an SSR of less than 1 will not be self-sufficient (purple).

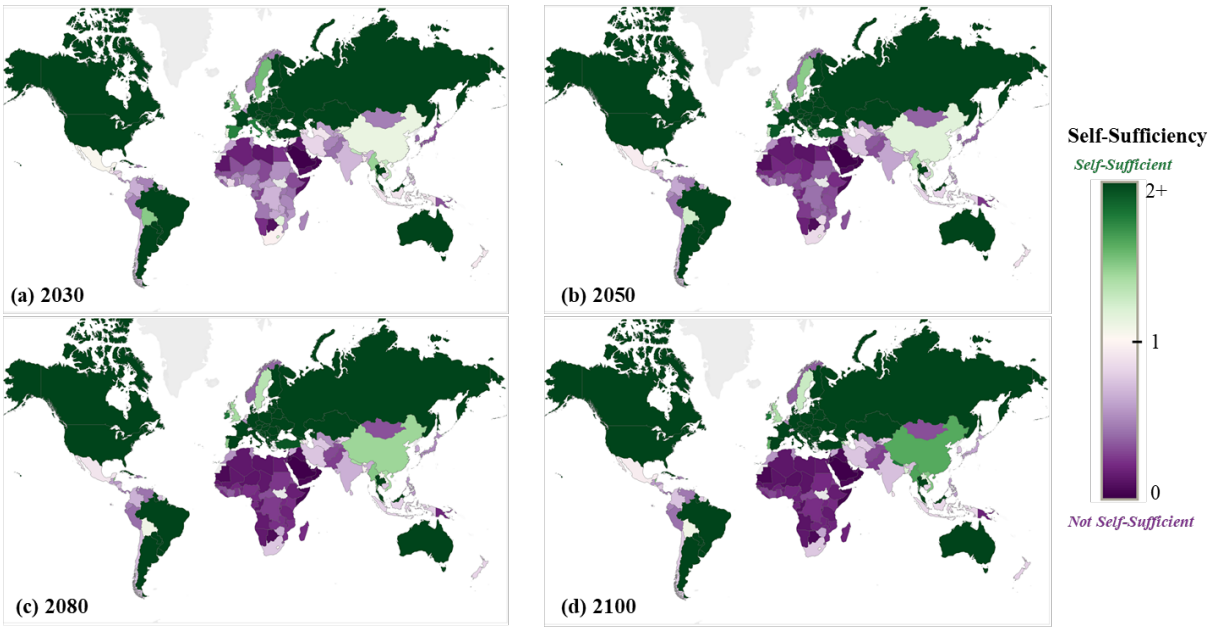

Supplementary Figure 2. Global self-sufficiency ratios under middle-of-the-road scenario from 2030 to 2100. This figure displays country-specific self-sufficiency ratios for the middle-of-the-road scenario in years 2030, 2050, 2080 and 2100. A country is considered self-sufficient if it has an SSR of 1 or greater (>1 indicates a surplus) shown in green, while a country with an SSR of less than 1 will not be self-sufficient (purple).

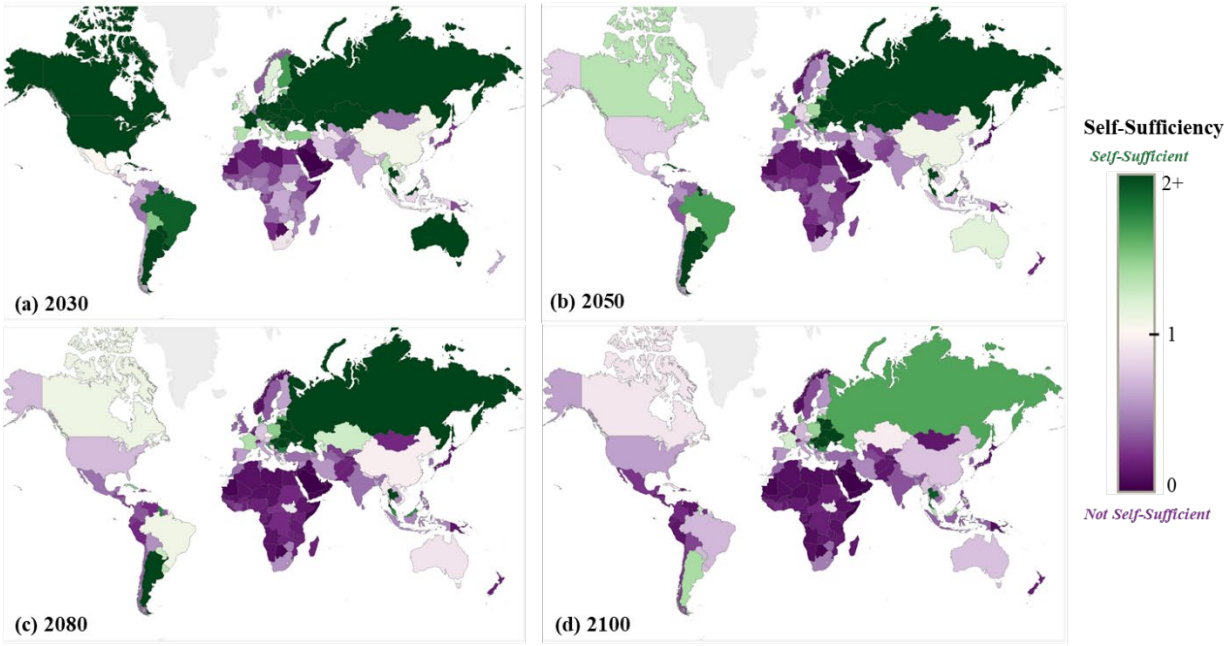

Supplementary Figure 3. Global self-sufficiency ratios under Business-as-usual scenario from 2030 to 2100. This figure displays country-specific self-sufficiency ratios for the business-as-usual scenario in years 2030, 2050, 2080 and 2100. A country is considered self-sufficient if it has an SSR of 1 or greater (>1 indicates a surplus) shown in green, while a country with an SSR of less than 1 will not be self-sufficient (purple).

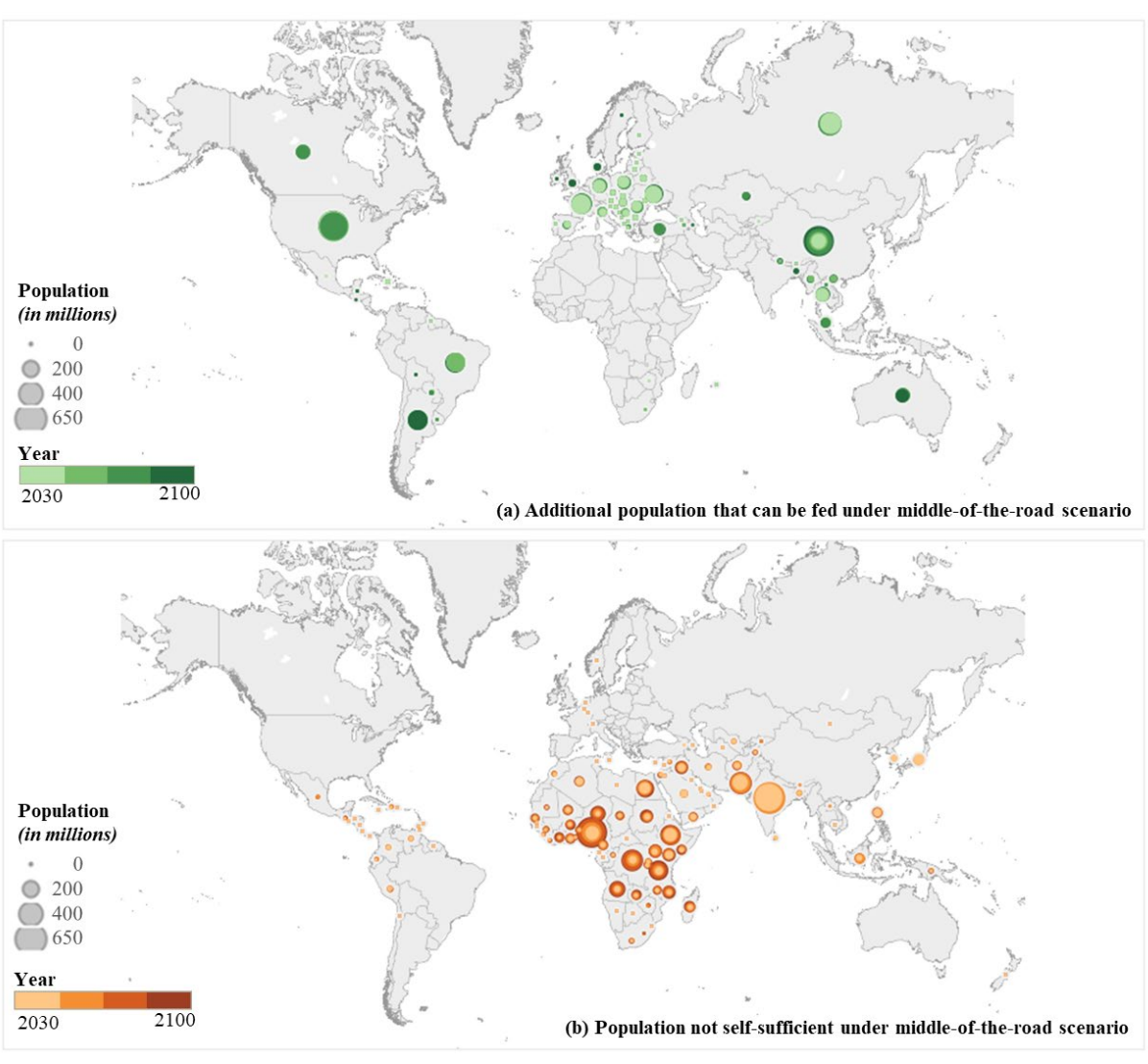

Supplementary Figure 4. Excess population that can be fed (a) and population for which caloric demand will not be met (b) (in millions of people) from years 2030 to 2100 under middle-of-the-road scenario. (a) country-specific additional population that could be fed under sustainable yield gap closure based on excess crop production. (b) population whose food demand will not be met through domestic food production in each country. Population (in millions) is represented by the varying bubble sizes. The years are represented by the respective color scales with the lightest shade for year 2030 and the darkest shade for 2100. If a country has a deficit in one year and excess another, it will appear on both panels. This figure represents the middle-of-the-road scenario.

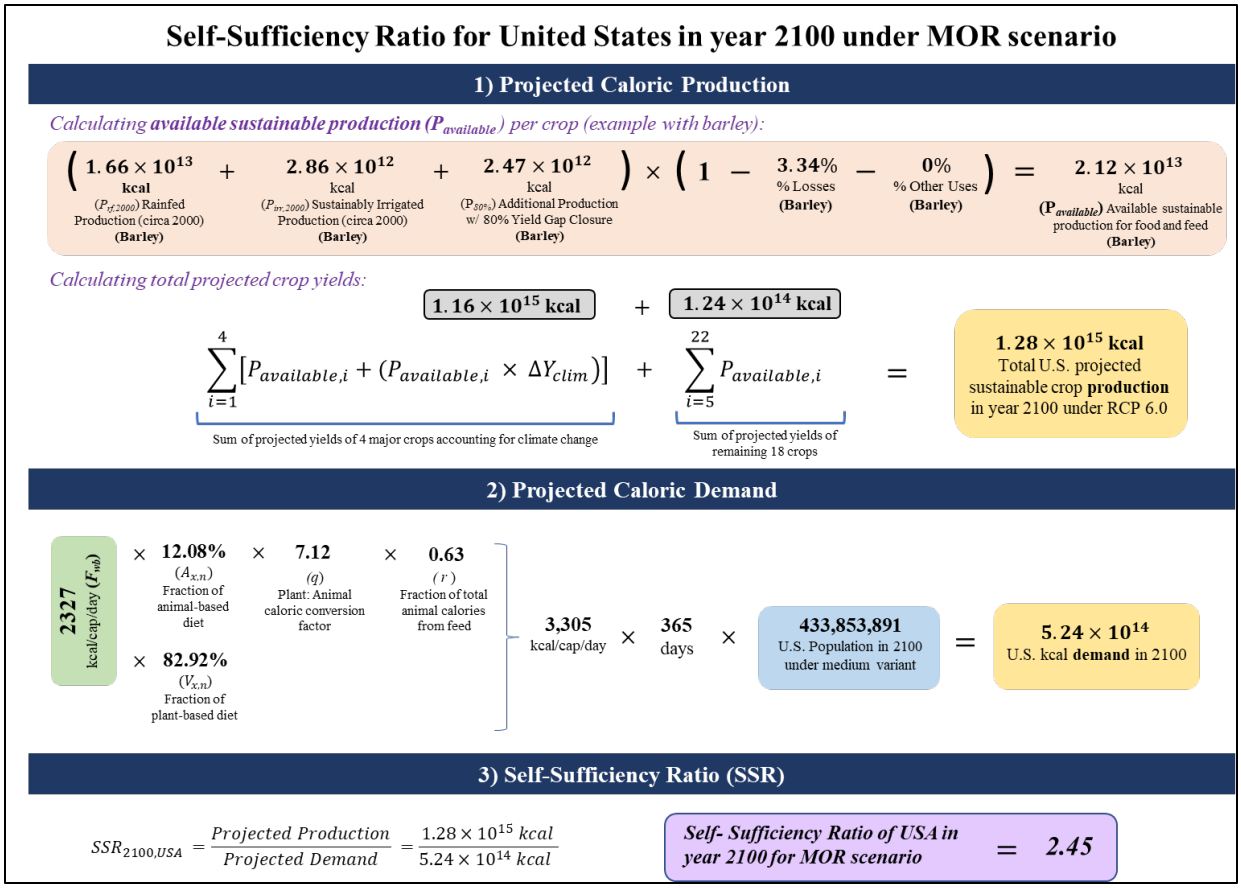

Supplementary Figure 5. Self-sufficiency ratio calculation for the United States in year 2100 under a Middle-of-Road scenario.

1.10 Supplementary References

D'Odorico P, Carr J A, Davis K F, Dell'Angelo J and Seekell D A 2019a Food Inequality, Injustice, and Rights *Bioscience* **69** 180–90

D'Odorico P, Carr J A, Laio F, Ridolfi L and Vandoni S 2014 Feeding humanity through global food trade *Earth's Future.* **2** 458–69

Davis K F, D'Odorico P and Rulli M C 2014 Moderating diets to feed the future *Earth's Futur.* **2** 559–65

FAO 2017a FAOSTAT Online Database Online: http://www.fao.org/faostat/en/#data/FBS

Fricko O, Havlik P, Rogelj J, Klimont Z, Gusti M, Johnson N, Kolp P, Strubegger M, Valin H, Amann M, Ermolieva T, Forsell N, Herrero M, Heyes C, Kindermann G, Krey V, McCollum D L, Obersteiner M, Pachauri S, Rao S, Schmid E, Schoepp W and Riahi K 2017 The marker quantification of the Shared Socioeconomic Pathway 2: A middle-of-the-road scenario for the 21st century *Glob. Environ. Chang.* **42** 251–67

Fujimori S, Hasegawa T, Masui T, Takahashi K, Herran D S, Dai H, Hijioka Y and Kainuma M 2017 SSP3: AIM implementation of Shared Socioeconomic Pathways *Glob. Environ. Chang.* **42** 268–83

Marchand P, Carr J A, Dell'Angelo J, Fader M, Gephart J A, Kummu M, et al. 2016 Reserves and trade jointly determine exposure to food supply shocks. *Environmental Research Letters.* **11**(9), 095009. https://doi.org/10.1088/1748-9326/11/9/095009

Monfreda C, Ramankutty N and Foley J A 2008 Farming the planet: 2. Geographic distribution of crop areas, yields, physiological types, and net primary production in the year 2000 *Global Biogeochem. Cycles* **22**

Mueller N D, Gerber J S, Johnston M, Ray D K, Ramankutty N and Foley J A 2012 Closing yield gaps through nutrient and water management *Nature* **490** 254–7

Ostberg S, Schewe J, Childers K and Frieler K 2018 Changes in crop yields and their variability at different levels of global warming *Earth Syst. Dyn.* **9** 479–96

Popp A, Calvin K, Fujimori S, Havlik P, Humpenöder F, Stehfest E, Bodirsky B L, Dietrich J P, Doelmann J C, Gusti M and Hasegawa T 2017 Land-use futures in the shared socio-economic pathways. *Global Environmental Change*, *42*, pp.331-345.

Portmann F T, Siebert S and Döll P 2010 MIRCA2000-Global monthly irrigated and rainfed crop areas around the year 2000: A new high-resolution data set for agricultural and hydrological modeling *Global Biogeochem. Cycles* **24** n/a-n/a

Puma M J, Bose S, Chon S Y and Cook B I 2015 Assessing the evolving fragility of the global food system *Environ. Res. Lett.* **10**

Riahi K, van Vuuren D P, Kriegler E, Edmonds J, O'Neill B C, Fujimori S, Bauer N, Calvin K, Dellink R, Fricko O, Lutz W, Popp A, Cuaresma J C, KC S, Leimbach M, Jiang L, Kram T, Rao S, Emmerling J, Ebi K, Hasegawa T, Havlik P, Humpenöder F, Da Silva L A, Smith S,

Stehfest E, Bosetti V, Eom J, Gernaat D, Masui T, Rogelj J, Strefler J, Drouet L, Krey V, Luderer G, Harmsen M, Takahashi K, Baumstark L, Doelman J C, Kainuma M, Klimont Z, Marangoni G, Lotze-Campen H, Obersteiner M, Tabeau A and Tavoni M 2017 The Shared Socioeconomic Pathways and their energy, land use, and greenhouse gas emissions implications: An overview *Glob. Environ. Chang.* **42** 153–68

Rosa L, Chiarelli D D, Tu C, Rulli M C and D'Odorico P 2019 Global unsustainable virtual water flows in agricultural trade *Environ. Res. Lett.*

Rosa L, Rulli M C, Davis K F, Chiarelli D D, Passera C and D'Odorico P 2018 Closing the yield gap while ensuring water sustainability *Environ. Res. Lett.* **13**

Rosenzweig C, Elliott J, Deryng D, Ruane A C, Müller C, Arneth A, Boote K J, Folberth C, Glotter M, Khabarov N, Neumann K, Piontek F, Pugh T A M, Schmid E, Stehfest E, Yang H and Jones J W 2014 Assessing agricultural risks of climate change in the 21st century in a global gridded crop model intercomparison. *Proc. Natl. Acad. Sci. U. S. A.* **111** 3268–73

Seekell D, Carr J, Dell'Angelo J, D'Odorico P, Fader M, Gephart J, Kummu M, Magliocca N, Porkka M, Puma M, Ratajczak Z, Rulli M C, Suweis S and Tavoni A 2017 Resilience in the global food system *Environ. Res. Lett.* **12** 025010

Suweis S, Carr J A, Maritan A, Rinaldo A, and D'Odorico P 2015 Resilience and reactivity of global food security. *Proceedings of the National Academy of Sciences.* **112**(22), 6902–6907.

Taylor K E, Stouffer R J and Meehl G A 2012 An overview of CMIP5 and the experiment design *Bull. Am. Meteorol. Soc.* **93** 485–98

United Nations 2019 World Population Prospects 2019 Online: https://population.un.org/wpp/

Van Ittersum M K, Cassman K G, Grassini P, Wolf J, Tittonell P and Hochman Z 2013 Yield gap analysis with local to global relevance-A review *F. Crop. Res.* **143** 4–17

van Vuuren D P, Edmonds J, Kainuma M, Riahi K, Thomson A, Hibbard K, Hurtt G C, Kram T, Krey V, Lamarque J F, Masui T, Meinshausen M, Nakicenovic N, Smith S J and Rose S K 2011 The representative concentration pathways: An overview *Clim. Change* **109** 5–31

van Vuuren D P, Stehfest E, Gernaat D E H J, Doelman J C, van den Berg M, Harmsen M, de Boer H S, Bouwman L F, Daioglou V, Edelenbosch O Y, Girod B, Kram T, Lassaletta L, Lucas P L, van Meijl H, Müller C, van Ruijven B J, van der Sluis S and Tabeau A 2017 Energy, land-use and greenhouse gas emissions trajectories under a green growth paradigm *Glob. Environ. Chang.* **42** 237–50

Warszawski L, Frieler K, Huber V, Piontek F, Serdeczny O and Schewe J 2014 The Inter-Sectoral Impact Model Intercomparison Project (ISI–MIP): Project framework *Proc. Natl. Acad. Sci.* **111** 3228–32

CHAPTER 2

Future food security in Africa under climate change

Reference: Beltran-Peña, A., & D'Odorico, P. (2022). Future food security in Africa under climate change. Earth's Future, 10, e2022EF002651. https://doi.org/10.1029/2022EF002651

2.1 Abstract

Africa is a major hotspot of food insecurity with climate change and population growth as major drivers. Irrigation expansion can sustainably increase agricultural productivity and adapt crops to climate change. We use agro-hydrological, climate, and socio-economic models to quantify crop production with irrigation expansion and perform food security analyses for different adaptation scenarios for African countries under baseline and 3°C warmer climate conditions. We find that under a 3°C warmer climate the total food production in Africa can only feed 1.35 billion people, when the continent's population is expected to reach 3.5 billion, leaving a food deficit equivalent to 2.15 billion people. Increasing agricultural productivity with irrigation alone will not be enough to achieve food self-sufficiency. Therefore, future food demand will likely be met by other means such as cropland expansion or greater reliance on imports which would further expose African populations to uncertainty from the volatility in global food prices.

2.2 Introduction

The African continent is affected by malnutrition and food insecurity. In 2020, over 811 million people globally, including 282 million Africans (21% of the continent's population) faced undernourishment due to climate-related shocks, conflict, changes in land tenure and agrarian systems of production, high-income inequality and economic downturns worsened by the COVID-19 pandemic (FAO, IFAD, UNICEF, WFP and WHO 2021). Additionally, 426 million people do not have regular access to sufficient (and nutritious) food and are considered moderately food insecure (FAO, ECA and AUC 2021). As of 2020, forty percent of the world's stunted children live in Africa (FAO, ECA and AUC 2021). Stunting, which is typically defined as having height two standard deviations below the World Health Organization's median for that age group, is an indicator of chronic malnutrition and can have serious developmental and health consequences (De Onis and Branca 2016; Graves et al., 2019). At the same time, Africa is considered the region with one of the fastest population growth rates in the world and is predicted to reach a population of about 2.5 billion people by 2050 compared to 1.3 billion today (United Nations 2019). Population is already outstripping food supply in the Sahel Region (Graves et al., 2019) and increasing many countries' dependence on food imports (D'Odorico et al., 2014); crop production will need to be sustainably increased to prevent population from outpacing food supply (Beltran-Peña et al., 2020).

Aside from the reliance of African countries on agriculture for food, the agricultural sector also accounts for on average ~19% of their Gross Domestic Product (GDP, with some countries like Sierra Leone relying on agriculture for up to 61% of their GDP) and over 60% of full-time employment – making countries more susceptible to changes in agricultural production capability (ADBG 2019; World Bank, 2021; Pretty et al., 2012). For reference, agriculture accounts for just 1-3% of GDP for high income countries even if they are major agricultural producers such as the

United States (World Bank 2021). Indeed, Africa is a major hotspot for food insecurity and climate change vulnerability because most countries in Africa are not currently and will not be self-sufficient under a changing climate. Beltran-Peña et al., 2020 showed that this region will continue to be heavily reliant on imports throughout the 21st century. Population in this region is expected to grow significantly under middle-of-the-road and business-as-usual scenarios – increasing the number of people that may be food insecure (in terms of food availability) (Beltran-Peña et al., 2020). Anthropogenic climate change has already reduced total factor productivity by 34% since 1961 in Africa, where warmer regions (i.e. Sub-Saharan Africa) with low agricultural productivity suffer the greatest impacts (Ortiz-Bobea et al., 2021). In 2018, Ethiopia, Malawi, Kenya, Mozambique, Madagascar, Zambia, and Uganda were the most affected by climate shocks from adverse weather conditions, drought, floods, late or erratic rainfall (FAO, ECA and AUC 2020). The World Meteorological Organization reports that 2019 was among the three warmest years on record for the African continent – characterized by continued increasing temperatures, rising sea levels and impacts associated with extreme weather and climate events (WMO 2020). The Greater Horn of Africa and the Sahel are regions that experienced extreme shifts from dry conditions in 2018 to flooding due to heavy rainfall in 2019 while, undernourishment has increased by 45.6% in drought-prone sub-Saharan Africa since 2012 (WMO 2020). Climate warming will continue to drastically affect crop productivity with more severe effects in Sub-Saharan Africa – jeopardizing the well-being of vulnerable populations disproportionately (FAO, ECA and AUC 2021).

The degree to which the Earth's climate will warm above pre-industrial levels and by when is highly dependent on global climate action policies and programs enacted. The current Nationally Determined Contributions (NDCs) do not put us on track to meet the goals of the Paris Agreement to *"hold the increase in the global average temperature to well below 2°C above pre-industrial levels and to pursue efforts to limit the temperature increase to 1.5°C above pre-industrial levels"* and may give rise to an increase in temperature of at least 3°C above pre-industrial levels by the end of the century (UNFCCC 2015; UNEP 2020). According to the 2020 UNEP Emissions Gap Report, with the actual pre-COVID-19 policies in place, emissions will heighten by 2030 and the Earth may reach a warming of at least 3.5°C by 2100 (UNEP 2020). Scientists have agreed that, to limit global warming to 1.5°C, "global net anthropogenic CO_2 emissions must decline by about 45% from 2010 levels by 2030 and net zero must be reached around 2050" relying heavily on carbon dioxide removal technologies (IPCC 2018; Terlouw et al., 2021; Rosa et al., 2021a). The 2021 Glasgow Climate Pact acknowledges that unless NDCs become more ambitious reflected by enhanced mitigation, reaching net-zero CO_2 emissions, adaptation, and finance actions, the 1.5°C and 2°C targets of the Paris Agreement may soon be out of sight (UNFCCC 2021; IPCC 2021; Millar et al., 2017). This pact (agreed upon by nearly 200 countries) explicitly calls upon parties to transition towards low-emission energy systems, phase out fossil fuels, and to strengthen their NDCs in 2022 (UNFCCC 2021). In a race against time and the carbon budget, there is no certainty that these pledges will result in actionable policy urgently needed – thus a 3°C warmer future is not unlikely. At the same time, countries in the G20, account for approximately 80% of greenhouse gas emissions (GHG) while climate change disproportionately impacts underdeveloped countries and regions (IPCC 2018; O'Neill et al., 2017; Harrington et al., 2016; UNEP 2020). It is estimated that at 3°C African regions may make up 27-51% of the global exposed and vulnerable population to climate change (Byer et al., 2018).

Agricultural expansion onto new areas damages habitats, biodiversity, increases deforestation and causes other negative environmental impacts (Foley et al., 2011; Gibbs et al., 2010; Williams et al., 2021). Williams et al., (2021) project large increases in agricultural land area with significant

habitat losses throughout Sub-Saharan Africa by 2050. Therefore, sustainable agricultural intensification on current croplands through greater infrastructural investments (in sustainable irrigation expansion, power production and grid development, and roads), narrowing yield gaps on underperforming lands, and reducing food loss and waste is the preferred adaptation approach to improve the supply and consumption of agricultural products from current croplands despite the rising land scarcity and degradation in Africa (Foley et al., 2011; Mueller et al., 2012; Rosa et al., 2018; Goyal and Nash 2017; FAO, ECA, AUC 2021). Implementing water storage management infrastructure, adopting soil water conservation practices, planting more suitable crops, and intensifying agricultural production through sustainable irrigation expansion onto currently water-limited rainfed croplands are viable strategies for climate adaptation (Rosa et al., 2018; Rosa et al., 2020b; Rosa 2022). Today, only 6% of the total cultivated area in African countries is equipped for irrigation (You et al., 2010). In Sub-Saharan Africa, in up to 35% of currently rain-fed croplands, water resources will be locally available for an expansion of irrigation without negative environmental externalities on freshwater resources under a 3°C warmer climate (Rosa et al., 2020a). However, opportunities for irrigation differ by country and some regions will experience a reduction in areas suitable for irrigation (Elliot et al., 2014). Recent studies have highlighted that relatively large annual water storage will be required to maintain a current irrigation potential in a 3°C warming scenario; conversely, in the absence of such water storage, about 120 million hectares of African croplands will become unsuitable for sustainable irrigation expansion (Rosa et al., 2020a).

To date, it is still unclear to what extent the sustainable expansion of irrigation, access to water storage, and food loss and waste reduction strategies will affect food security in African countries. Here we expand recent food self-sufficiency analyses (Beltran-Peña et al., 2020) to account for the limits to sustainable irrigation expansion under climate change. We consider sustainable irrigation and freshwater storage potential, environmental flow requirements, future reliance on animal-based products for dietary consumption, estimates of population growth, and diverse pathways of food loss and waste. This study quantifies the future of food security in Africa under climate and societal change.

2.3 Methods

This study uses agro-hydrological, climate, and societal models to perform a food security and vulnerability analysis for forty-nine African countries under a 3°C warmer climate (compared to pre-industrial conditions) to determine potential adaptation strategies and the extent to which African countries will be reliant on external food sources to adequately feed their populations.

2.3.1 Crop Production and Availability

To determine the crop production potentially achievable under climate change, we use results from Rosa et al. (2020a) who estimated rainfed and irrigated crop production for 130 primary crops based on the global cropland extent of the MIRCA2000 dataset (Portmann et al., 2010). Their analysis determined the spatial extent of land suitable for sustainable irrigation expansion under baseline (long-term climatic data for the reference period for global agricultural data from 1996 to 2005 (Portmann et al., 2010)) and 3°C climate conditions. The analysis by Rosa et al (2020a) used in this study evaluated the ability of available water resources to meet the crop water demand both at the monthly timescale (assuming that short-term water deficits can be offset by reliance on small-scale water storages and water harvesting techniques) and at the annual time scale (i.e.,

assuming that seasonal water deficits can be compensated by using large reservoirs). In other words, a need for "large reservoirs" is found when at the annual time scale water availability is sufficient to meet the irrigation water demand while the monthly water balance shows periods of water scarcity. In these analyses the local water availability included surface and groundwater runoff and accounted for the need to preserve environmental flows.

Irrigation water requirements were determined (following Rosa et al., 2020a) as the additional water needed to meet crop water requirements and prevent water stress conditions in croplands where rainfed crop growth is water stressed (green water scarcity) (Brouwer and Heibloem 1986; Rosa et al., 2020b). The irrigation water requirements for a 3°C warmer climate were calculated using projections of monthly precipitation, evaporation, and runoff (using 30 by 30 arc-min resolution) from the GFDL-ESM2M, HadGEM2-ES, MIROC-ESM-CHEM global climate models in conjunction with the LPJmL, H8, and WATERGAP2 global hydrological models for the representative concentration pathway (RCP) 8.5 of the Coupled Model Intercomparison Project Phase 5 (CMIP 5) from the Inter-Sectoral Impact Model Intercomparison Project (Warszawski et al., 2014; Fekete et al., 2002; Harris et al., 2014; Climate Hazards Group 2015; Rosa et al., 2020a). Rainfed croplands facing green water scarcity but where irrigation water requirements do not exceed local water availability are considered suitable for sustainable irrigation expansion (Rosa et al., 2018). Following Rosa et al., (2020b), the maximum potential, current rainfed and current irrigated caloric production of each crop was then computed as the product of crop yield (in tons per hectare) from Monfreda et al. (2008) and Mueller et al. (2012); crop calorie content (in kilocalories per tons) from D'Odorico et al. (2014); and crop harvested area (in hectares) from Portmann et al. (2010).

Here, a yield gap is defined as the difference between water-limited potential yield and the actual yield that a farmer currently achieves on a cropland (Lobell et al., 2009; Rosa et al., 2018). Narrowing or closing yield gaps through sustainable irrigation expansion is an agricultural intensification strategy to boost crop production without threatening biodiversity-rich ecosystems through expansion of agricultural croplands (Beltran-Peña et al., 2020; Rosa et al., 2022; Van Ittersum et al., 2013). This study considers a target yield gap closure of 80 percent as the feasible limit proposed by Van Ittersum et al. (2016). In line with sustainable development goal 6.6 (protect and restore water related ecosystems), our study preserves 60 percent environmental flow requirements (EF) in all scenarios (80 percent EF considered under 3°C as well in supplementary materials).

The projected potential sustainable crop production, *P*, (in kcal) for each country (*c)* is calculated for six production adaptation scenario combinations *(s)* of climate (baseline or 3°C warmer climate), water maintained for environmental flow requirements (*EF)*, and water storage strategies *(WS)* (monthly or annual) following equation 1:

$$P_{c,s} = \left[R_{2000} + \left(I_{T,2000} - I_{U,2000}\right) + \left(I_{P,s} \times 0.8\right)\right] \quad (1)$$

Here, R_{2000} indicates rainfed caloric (kcal) production in year 2000, $\left(I_{T,2000} - I_{U,2000}\right)$ represents sustainable irrigated caloric (kcal) production in year 2000 calculated as the difference between total and unsustainable production. Additional caloric production (kcal) potential under sustainable irrigation expansion for scenario *s* at 80% yield gap closure is represented as $(I_{P,S} \times 0.8)$ with $I_{P,s}$ being equal to zero in areas unsuitable to sustainable irrigation, and otherwise equal to the production gap calculated as the sum of yield gaps times cultivated areas across all crops.

The amount of crop calories produced that are actually available for direct or indirect human consumption is heavily dependent on the quantity of food this is lost or wasted. The Food and Agriculture Organization of the United Nations (FAO) and the United Nations Environment Program (UNEP) are working together to develop the Food Loss Index (FLI) and the Food Waste Index (FWI) respectively to measure progress toward meeting this goal. The FAO defines food loss as "the decrease in the quantity or quality of food resulting from decisions and actions by food suppliers in the chain, excluding retail, food service providers, and consumers" (FAO 2019). The 2019 FAO State of Food and Agriculture Report provides the first estimates for the FLI and found that globally, 14 percent of food is lost. In the context of the FWI, the UNEP defines food waste as "food and the associated inedible parts removed from the human food supply chain in the retail, food service, and household sectors" (UNEP 2021a). The 2021 Food Waste Index Report estimates that 17 percent of total global food production may be wasted (11 per cent in households, 5 per cent in food service and 2 per cent in retail). Combining the global averages of the FAO FLI and the UNEP FWI, approximately 31 percent of food is lost and wasted. The current percentages of food loss in Northern and Sub-Saharan Africa were taken from the Food Loss Index (FAO 2019b). Globally, there is insufficient data on food waste and the measurement methods vary widely. Therefore, we applied the global percentages of food waste from the FWI uniformly across all African countries in this study. SDG 12.3 sets the target of halving per capita global food waste at the retail and consumer levels and reduce food losses along production and supply chains, including post-harvest losses by 2030 (U.N. DESA 2016). Given this SDG, we calculated the 25 percent and 50 percent reductions from current values for each indicator (table 1). The food loss and food waste percentage scenarios derived from the FLI and FWI are depicted as $FL_{\%}$ and $FW_{\%}$, where the percentage indicates the percent reduction (equations 2.1 and 2.2).

$$FL_{\%} = FL_{current} - (FL_{current} \times \%_{reduction}) \quad (2.1)$$

$$FW_{\%} = FW_{current} - (FW_{current} \times \%_{reduction}) \quad (2.2)$$

	Current	25% Reduction	50% Reduction
Food Loss			
North Africa	10.80%	8.10%	5.4%
Sub-Saharan Africa	14%	10.50%	7%
Food Waste			
Global	17%	12.75%	8.5%
TOTAL FOOD LOSS AND WASTE			
North Africa	27.8%	20.85%	13.9%
Sub-Saharan Africa	31%	23.25%	15.5%

Table 1. Food loss and waste percentages derived from FLI and FWI. Green shaded boxes indicate SDG combination of food loss and waste.

We consider 3 pathways for food loss and waste (h) – no reduction, a 25% reduction and a 50% reduction. In this study we assessed the projected crop availability, $P_{AVAILABLE,}$ (in kcal) for direct or indirect human consumption per country and production adaptation scenario accounting for 80% yield gap closure and different food loss and waste reduction pathways (h) following equation 3:

$$P_{AVAILABLE,c,s,h} = P_{c,s} \times (1 - FL_{\%} - FW_{\%}) \quad (3)$$

A schematic of the production and food loss/waste combinations considered in this study can be found in figure 1.

2.3.2 Nutrition Thresholds

Nutritional requirements for individuals to be free from hunger have been associated with a minimum daily energy (calorie) intake (*fh*) of 1,829 kcal per capita per day (D'Odorico et al., 2019; FAO, IFAD, UNICEF, WFP and WHO 2021; Roser and Ritchie 2013). According to the Food and Agriculture Organization of the United Nations, the minimum daily energy requirement of a population is the weighted average of the different demographic groups within that population (i.e. differences in age, sex, body mass index, etc.) (FAO, IFAD, UNICEF, WFP and WHO 2021; Roser and Ritchie 2013). Likewise, an individual would need to consume about 2,327 kcal per capita per day or more to be in a better state of well-being (*wb*) (D'Odorico et al., 2019; FAO 2014). These thresholds were adopted in this study as the base dietary consumption pathways (*x*) - meaning that we assume people consume at least 1,829 or 2,327 kcal per day depending on the dietary scenario.

2.3.3 Future Dietary Caloric Demand

This study assesses food security in African countries under a baseline and 3°C warmer climate. To estimate when the global average temperature is expected to exceed preindustrial conditions (1850-1900) by 3°C, we took the average year over a running mean timeframe of 10 years for the GFDL-ESM2M and MIROC 5 global climate models under CMIP5 RCP 8.5 from the Climate Analytics Warming Attribution Calculator (Climate Analytics; Taylor et al., 2012). Based on these criteria, we assume that the estimated year of exceedance for 3.0°C above pre-industrial levels is around 2075 (table 2). It is important to note that there is some uncertainty on the exact year in which these temperature levels will be reached across models. However, the IPCC AR6 report projects that 3.0°C above pre-industrial level will be exceeded between 2075 and 2076 under the newly defined SSP3-7.0 scenario (Fyfe et al., 2021). Hence our estimate coincides well with recent studies. This projected year of exceedance, 2075, was used as the reference year to calculate the caloric demand per country (based on projected dietary composition patterns and population) during the time we expect the climate will reach 3°C of warming above pre-industrial levels.

	GFDL-ESM2M	**MIROC-5**	**Average Year of Exceedance**
3.0°C	2077 – 2086	2063 – 2072	2075

Table 2: Estimated 10-year time frame and average year of exceedance for 3.0°C above pre-industrial levels for GFDL-ESM2M and MIROC 5 global climate models.

Projected animal-based dietary consumption patterns were derived from the quantified scenario matrix produced as a GLOBIOM model emulation by Frank *et al* 2021. Crop and livestock demand data was quantified for the SSP2 scenario in the GLOBIOM model (Frank et al., 2021). According to O'Neill et al., 2017b, SSP2 is a scenario in which, "social, economic, and technological trends follow historical patterns. Global and national institutions work toward but make slow progress in achieving sustainable development goals, there are no fundamental technological breakthroughs, environment systems experience degradation but there are some improvements, there is a decline in the overall intensity of resource and energy use, fossil fuel

dependance decreases slowly but there is no reluctance in using unconventional fossil fuels, and global population growth is moderate" (O'Neill et al., 2017b; Fricko et al., 2017). The fraction of animal-based products (*A)* consumed in a diet was calculated as the ratio between the food demand for livestock products (including eggs and dairy) and the total demand for both crops and livestock (in kcal/cap/day) for the Sub-Saharan and North African regions (represented by the Sub-Saharan Africa, *SSA,* and the Middle East and Africa, *MAF*, regions in GLOBIOM).

The per capita (direct and indirect) crop caloric demand ($D_{c,t,x}$) – i.e., food + feed crops – per country *c* in year *t* for dietary pathway *x* was determined through equation 4, as the sum of plant-based caloric demand (*v*) and animal-based caloric demand from feed (*f*). The annual per capita demand was computed by multiplying the daily per capita demand by 365 days.

$$D_{c,t,x} = (v_{c,t,x} + f_{c,t,x}) \times 365 \quad (4)$$

The daily calorie consumption from food crops, *v,* is calculated as the fraction of plant-based products consumed in a diet $(1 - A_{c,t})$ multiplied by the daily calorie uptake, d_x which is equal to 1,829 or 2,327 kcal/day, depending on the diet type (free from hunger or well-being, respectively) (equation 5). The daily calorie consumption from feed crops (i.e., consumed by feed-fed livestock), *f*, is assessed as the product of the direct animal-based calories consumed ($d_x \times A_{c,t}$), the plant to animal caloric conversion factor, *q*, and the fraction of total animal calories from feed-fed production in country *c* ($r_{c,t}$) (equation 6). Values of *q* are country-specific and are taken from Davis et al., (2014).

$$v_{c,t,x} = d_x \times (1 - A_{c,t}) \quad (5)$$

$$f_{c,t,x} = [(d_x \times A_{c,t}) \times q_c \times r_{c,t}] \quad (6)$$

The value of $r_{c,t}$ changes over time according to trends in livestock consumption. It is assumed that any increase in livestock consumption entails only an increase in feed-fed production while grass-fed production is assumed to remain constant. Therefore, if $r_{c,inital}$ is the initial value of $r_{c,t}$ (i.e., circa year 2000), the value of *r* at time *t* per country *c* is calculated through equation 7.

$$r_{c,t} = \frac{\left((d_x \times A_{c,t}) - (d_x \times A_{c,initial})\right) \times (1 - r_{c,initial})}{(d_x \times A_{c,t})} \quad (7)$$

where $r_{c,inital}$ is here taken from Davis et al., (2014) (Beltran-Peña et al., 2020). The total caloric demand of a country in a specific year depends on the projected population of that country in the year evaluated. Population projections were taken from the 2019 UN Population Prospects for the low and medium variants in the year (2075) (United Nations 2019) when climate warming is projected to surpass 3°C (Table 2).

2.3.4 Food Sufficiency

The number of people that can be fed (*Y*) in a given country (c) and year (t) with the projected food availability under each production adaptation strategy scenario (*s*), food loss and waste pathway (*h*), and dietary pathway (*x*) was estimated by dividing the amount of food produced by the amount of food needed to feed a person in that country for that year (equation 8).

$$Y_{c,t,s,h,x} = \frac{P_{AVAILABLE,c,s,h}}{D_{c,t,x}} = \frac{Production\ (kcal * year^{-1})}{Demand\ (kcal * cap^{-1} * year^{-1})} \quad (8)$$

2.3.5 Food Insufficiency

The number of people that can be fed was then subtracted from the projected population (low or medium variant) to determine the food insufficiency of a country. Food insufficiency here is defined as the remaining number of people that cannot be fed (N) per a given country (c), year (t), production adaptation strategy (s), food loss and waste pathway (h), dietary pathway (x), and population variant (p) (equation 9).

$$N_{c,t,s,h,x,p} = Population_{c,t,p} - Y_{c,t,s,h,x} \quad (9)$$

These numbers were also converted to percentages. Figure 1 maps out the different combinations of demand and production variables that make up the different adaptation strategy scenarios.

2.3.6 National Food Deficit

The food deficit (Z) (kcal) of a country is defined as the amount of food (expressed in kcal) demand that cannot be met by the domestic food production and will need to come from external sources or even agricultural expansion. This study accounts for a zero hunger (free from hunger diet) or well-being (with higher caloric consumption) diet in the per capita caloric demand. Food deficit is estimated by multiplying the number of people that cannot be fed (N) (depending on population variant) by the annual per capita kcal demand (D) of a country in the year specified under either and fh or wb base-diet (equation 10).

$$Z_{c,t,s,h,x,p} = N_{c,t,s,h,x,p} \times D_{c,t,x} \quad (10)$$

See supplementary materials figures S5a and S5b for a visual representation of the model framework and variable descriptions.

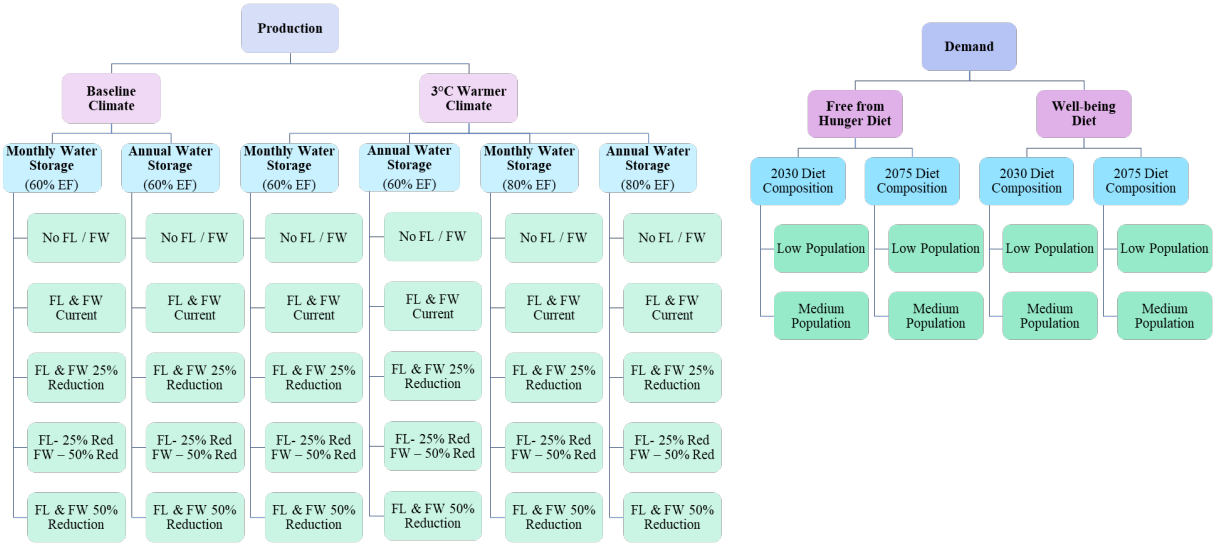

Figure 1. Scenario breakdown. This figure breaks down the different production and demand variables considered in this study. The adaptation strategy scenarios are made of distinct combinations of these variables.

2.3.7 Sustainable Development Goals Framework

A scenario was created to assess the extent to which African countries can domestically meet select sustainable development goals by 2075 and the magnitude of shortfalls. Our study considers only sustainable crop production through rainfed agricultural production, current sustainably

irrigated crop production, and additional production potential through sustainable irrigation expansion on currently rainfed croplands under a 3°C warmer climate. Additionally, in our analysis a minimum of 60% environmental flow requirements is preserved for ecosystem health, addressing SDG indicator 6.4 "to ensure sustainable withdrawals and supply of freshwater to address water scarcity" and SDG indicator 15.5 "to take urgent and significant action to reduce the degradation of natural habitats" (Liu et al., 2021; FAO 2019c; U.N. DESA 2016). Considering monthly and annual water storage potentials and strategies under a warmer climate based on Rosa et al (2020), corresponds to SDG 13 on climate action by "promoting mechanisms for raising capacity for effective climate change-related planning and management in least developed countries." By halving food waste at the retail and consumer levels and reducing food losses along the production and supply chains by 25%, SDG 12 "responsible consumption and production" would be met. To ensure zero hunger and zero malnutrition (SDG 2), every person in a country is assigned a well-being diet, where everyone consumes a minimum base diet of 2,327 kcal a day. We address SDG 5 "gender equality" to an extent by assuming a low population trajectory. Since 2075 is more than 50 years from now, we reckon that there is enough time to implement policies (e.g., to promote women education, employment, and socio-economic development) to reach a low population trajectory by the time climate reaches 3°C of warming. In short, crop production and availability for this scenario are determined based on sustainable irrigation expansion and monthly and annual water storage potential under a 3°C warmer climate, 60% environmental flow requirements preserved, 80% yield gap closure, and food loss and waste reduction of 25% and 50% respectively. Food demand is measured based on SSP2 animal-product consumption estimates, allocating every person with a well-being base diet, and the low population variant. Supplementary table S1 details how the specific SDG goal targets are accounted for in this scenario.

2.3.8 Regional Breakdown

As previously described, this study incorporates data from different sources. Due to data availability limitations, not all data is provided at the country level. Hence, each country was assigned the data values based on the regions they belong to (i.e. North Africa or Sub-Saharan Africa). The countries were then further subdivided into five African regions (North, South, East, West, and Central) according to the United Nations M49 standard (United Nations 1998) for statistical reporting purposes. The exceptions are Sudan and South Sudan which are both considered together and as part of Eastern Africa in this study due to data limitations. Each country is shown in only one region (United Nations 1998). The regional breakdown of the African countries considered in this study can be found in supplementary figure S4 and supplementary table S2. The results of this study are presented at the regional level and further expanded to the country level to demonstrate the practicability of this analysis in climate adaptation planning. Additional data can be found in the supplementary materials.

2.4 Results

2.4.1 Caloric Demand

According to the 2019 United Nations Population Prospect (medium variant), the population in Africa is expected to increase from 1.37 billion people in 2021 to 1.68 billion people in 2030 and 3.68 billion people by 2080 (United Nations 2019). Under the medium variant, Eastern and Western Africa are projected to experience the strongest population growth (roughly three-fold)

from 475 and 401 million people in 2020 to 1.34 and 1.24 billion people respectively in 2080. Central Africa's population is also projected to triple, while the Northern and Southern African regions will experience the lowest growth rates by comparison (figure 2a). The regional breakdown of countries is shown in supplementary table S2. Meanwhile, in line with historical patterns, economic growth, urbanization along with other factors will enable shifts towards diets with higher animal-sourced food products (OECD/FAO 2021).

Figure 2b presents the expected crop kilocalories production per capita per day required to meet either the free from hunger diet of 1,829 kcal/cap/day or the well-being diet of 2,327 kcal/cap/day for each of the five African regions. The change over time reflects the shift towards diets with higher animal-based product consumption (based on SSP2 projections of the GLOBIOM model). Northern Africa will continue to have a higher proportion of animal product in diets compared to the regions in Sub-Saharan Africa. However, Sub-Saharan Africa will experience the largest population growth which will continue to outstrip food supply.

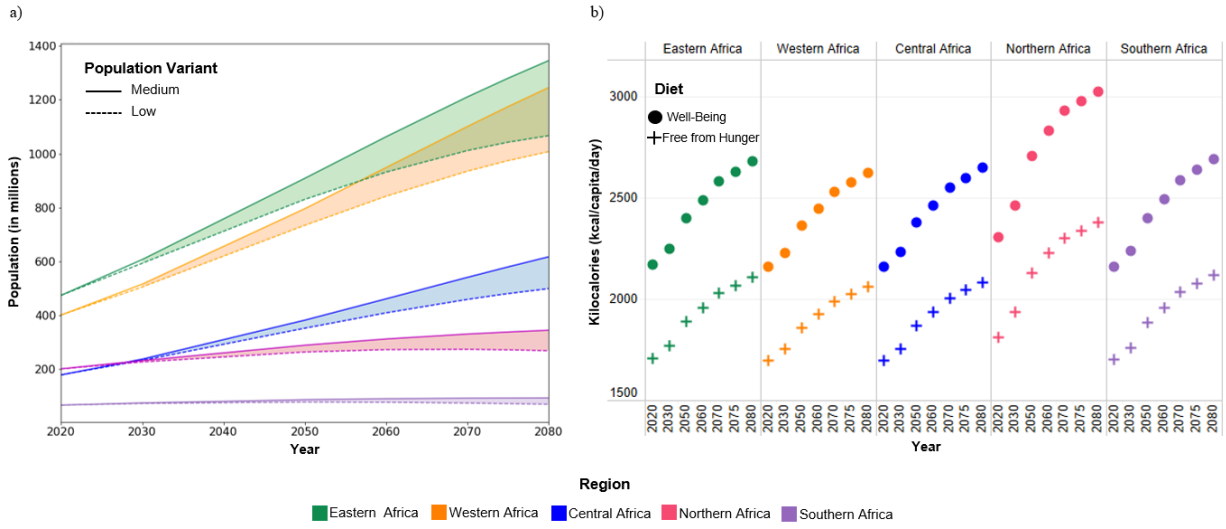

Figure 2. Population and dietary demand projections. Colors represent the five African regions. a. Population projections from 2020 to 2080 for the medium (solid line) and low (dashed line) population variants. b. Projected crop kilocalories required to meet daily per capita dietary demand (including feed-fed livestock products) for well-being (dot) and free from hunger (cross) diets from years 2020 to 2080.

2.4.2 Production with Food Loss and Waste Pathways

This study evaluated five potential food loss and food waste (FL&FW) pathways – no FL and no FW, current FL&FW, 25% reduction in FL&FW, 50% reduction in FL&FW, and the SDG goal of food loss at 25% and food waste at 50% reduction (figure 1). Even though it is not feasible to reach absolute zero food loss and waste, this scenario is included here as a refence point to demonstrate the impact food loss and waste have on the food calories available for human consumption. The pathway with no FL&FW also represents the total potential kcal production (figure 3, in grey) with 80% yield gap closure, under the various adaptation strategies (i.e. 3°C climate, 60% EF, Monthly WS) for each of the five African regions. Hence, the estimated food production and availability outcomes of each adaptation strategy under a 3°C warmer climate can be compared across the regions (figure 3A). Two baseline climate scenarios are included for

comparability. The potential caloric production is greatest in Western Africa for each strategy than in the other regions, followed by Eastern and Central Africa. Northern, and Southern Africa have lower production capabilities with nominal differences between adaptation strategies. It is of note that both regions are composed of countries with large desert areas which would partly explain the lower production. In most cases, annual water storage allows for greater food production than monthly water storage. The advantage is much greater in a 3°C warmer world for Eastern, Western, and Central Africa where annual water storage is a recommended adaptation measure (figure 3A). Likewise, under the baseline climate scenario, annual water storage allows for greater food calorie production than monthly water storage although the difference is much smaller for Northern and Southern Africa (figure 3A). For 3°C climate, we assessed food calorie production capacity when preserving 60% or 80% of environmental flow requirements in inland freshwater ecosystems. Although less crop production is possible when reserving more freshwater for ecosystems, this maybe a tradeoff that countries consider to further protect the environment. Unfortunately, not all calories produced can be used to meet food demand. The actual crop kilocalories available under the food loss and waste pathways are represented in figure 3A and supplementary table S3.

Reducing food loss and waste from current levels, will boost caloric availability and the number of people that can be fed. SDG 12.3 aims to reduce food loss and half food waste (shown in green). Figure 3A shows the impact of FL & FW reductions on food availability while figure 3B shows the impact of FL & FW reductions on the number of people that can be fed with a well-being diet in 2075 (the year projected to surpass 3°C) across the African continent. In the event the Earth's climate warms by 3°C above preindustrial levels, if 60% environmental flows are conserved and an annual water storage strategy is adopted, enough food will be produced domestically to feed (with a well-being diet of 2,327 kcal/cap/day) an estimated 851 million people in all of Africa if no food is lost or wasted. However, if the current rate of food loss (10.8% in Northern Africa; 14% in Sub-Saharan Africa) and food waste (17% all of Africa) remains unchanged, there will only be enough food available to feed 590 million people - 261 million people less than if there were no FL or FW. By reducing both FL and FW by 25%, the number of people potentially fed increases to 655 million (figure 3B). Meeting SDG 12.3, enough food would be available for approximately 691 million people. Taking it one step further and halving both FL and FW, this number increases to 720 million people fed in Africa through domestic food crop production. Our results present the extent to which reductions in food loss and waste can contribute to reducing hunger across the different agricultural adaptation strategies.

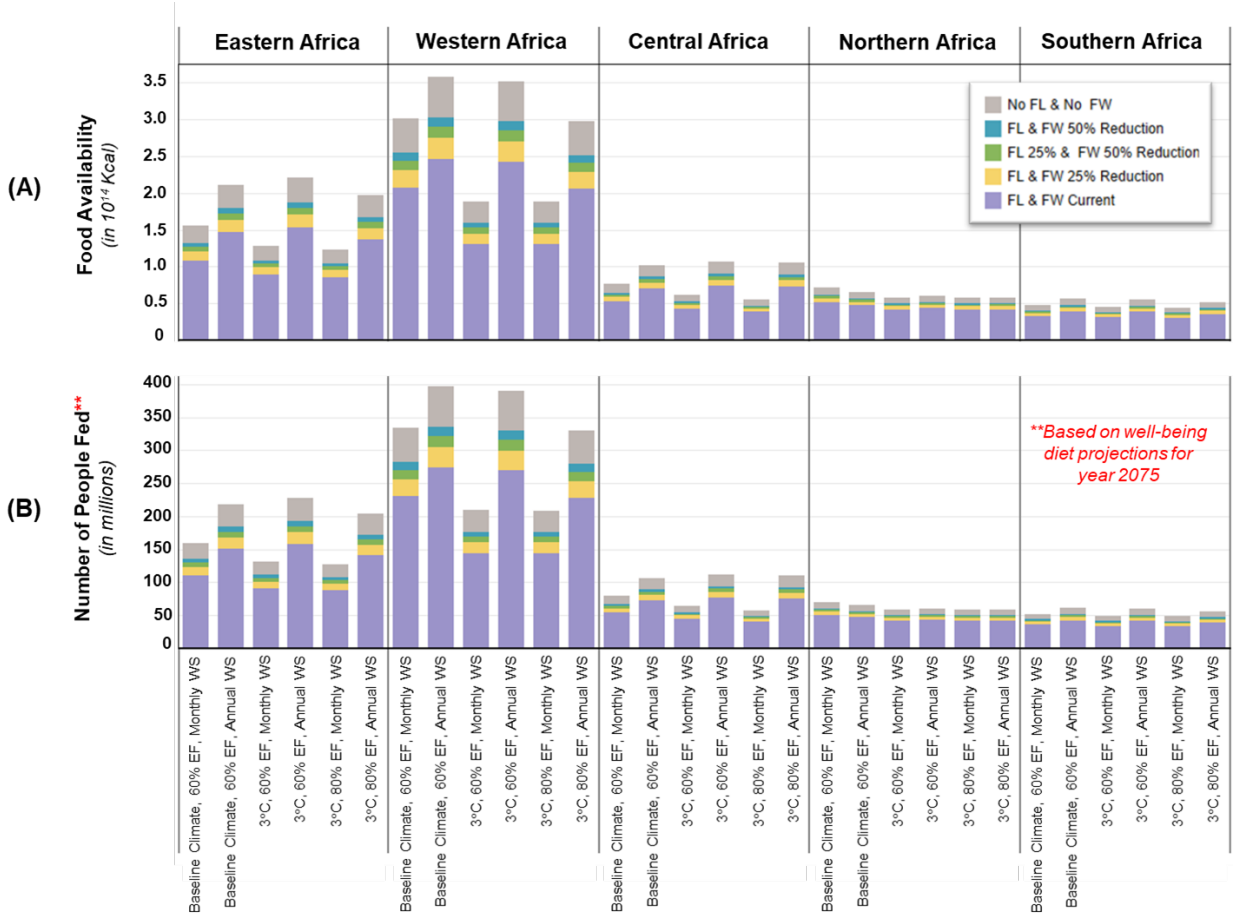

Figure 3. Regional food production and availability under different food loss and waste pathways. The colors represent the diverse food loss and waste pathways. Each bar within a region indicates a specific climate adaptation strategy scenario for crop production. Panel A shows the food available (in 10^{14} kilocalories) for direct or indirect human consumption while panel B displays the number of people that can be fed with a well-being diet (in year 2075) under each FL and FW pathway.

2.4.3 Potential futures for Africa in a 3°C warmer world

To understand the different potential outcomes of various adaptation strategy combinations in a 3°C warmer world, we estimated the number of people that could be fed (both with the fh and wb diet) with the potential calories produced under combinations of 60% or 80% EF (supplementary materials), annual or monthly WS. The percent of the population that can be fed was determined based on either the low or medium population variants. The percent of population that can be fed also depends on the minimum number of calories each person consumes as well as the population. We look at two scenarios with average food consumption corresponding to the "free from hunger" (each person consumes 1,829 kcal/day) or "well-being" diets (2,327 kcal/day). Depending on several factors, by 2075, a country's population may follow the low or medium population variant – influencing the percentage of the population that can be fed with the calories produced. Figure 4 details the results of these adaptation strategy combinations based on total food

production (not accounting for food loss or waste) when preserving 60% environmental flow requirements in terms of percent of the national population that can be fed split between monthly (left) and annual (right) water storage to allow for comparison. The plausible combinations of diet and population are differentiated by color. The corresponding results of the different adaptation strategies when 80% EF are preserved and how they compare with 60% EF are displayed in Supplementary Figures S1 and S2 respectively. Figure 4 presents the theoretical extent of countries' self-sufficiency under the different potential futures assuming none of the food produced domestically was lost or wasted. For example, if Ghana relies on monthly water storage, there will be enough food to feed 34% of Ghana's population with a well-being diet and medium population variant; 42% with the well-being diet and low population variant; 43% with the free from hunger diet and medium variant, and 53% with the free from hunger diet and low population variant. As expected, the annual water storage approach would allow to support a higher percentage of the population, reaching 46% of the population with the well-being diet and medium population variant; 57% with the well-being diet and low variant; 59% with the free from hunger diet and medium variant; or 72% with the free from hunger diet and low variant (figure 4).

Overall, if there were no food loss or waste, we found that relying on monthly water storage only five countries (Ghana, Lesotho, South Africa, Swaziland, and Zimbabwe) will be able to feed at least half of their population, but none will reach 100%. With annual water storage, ten countries will have enough food to feed at least 50% of their population and three (Lesotho, South Africa, and Swaziland) could have a surplus. In the "ideal case" scenario with the well-being diet, low population variant and annual water storage, seven African countries have enough to feed at least 50% of their population with four countries feeding more than 70%. Nonetheless, our results show that with monthly water storage 27 of the 49 countries evaluated in this study do not reach 20% and 5 of those (Botswana, Burundi, Comoros, Mauritania, and Somalia) cannot even feed 10% of their population in any population-diet combination. For most countries, implementing annual water storage techniques will increase their ability to feed people and strategize adaptation tactics. With annual water storage, 14 countries will not be able to feed 20% of their population (including four less than 10%) – less than with monthly water storage alone.

Importantly, the two diet scenarios are used here as a baseline to determine to what extent a country may achieve conditions of average self-sufficiency. Even when this happens, it doesn't mean that all people in that country are free from hunger or have access to the well-being diets. In other words, if on average food production is sufficient to meet free from hunger conditions or well-being food calorie needs per capita (depending on the diet scenario), inequalities in food access will lead to parts of the population consuming more than the average, leaving some groups or classes (typically the poor) with insufficient access (e.g., D'Odorico et al., 2019). The role of inequality in the analysis of food availability and countries' self-sufficiency is beyond the scope of this study, which does not look at food security impacts of country-specific food access, distribution, utilization, or stability patterns.

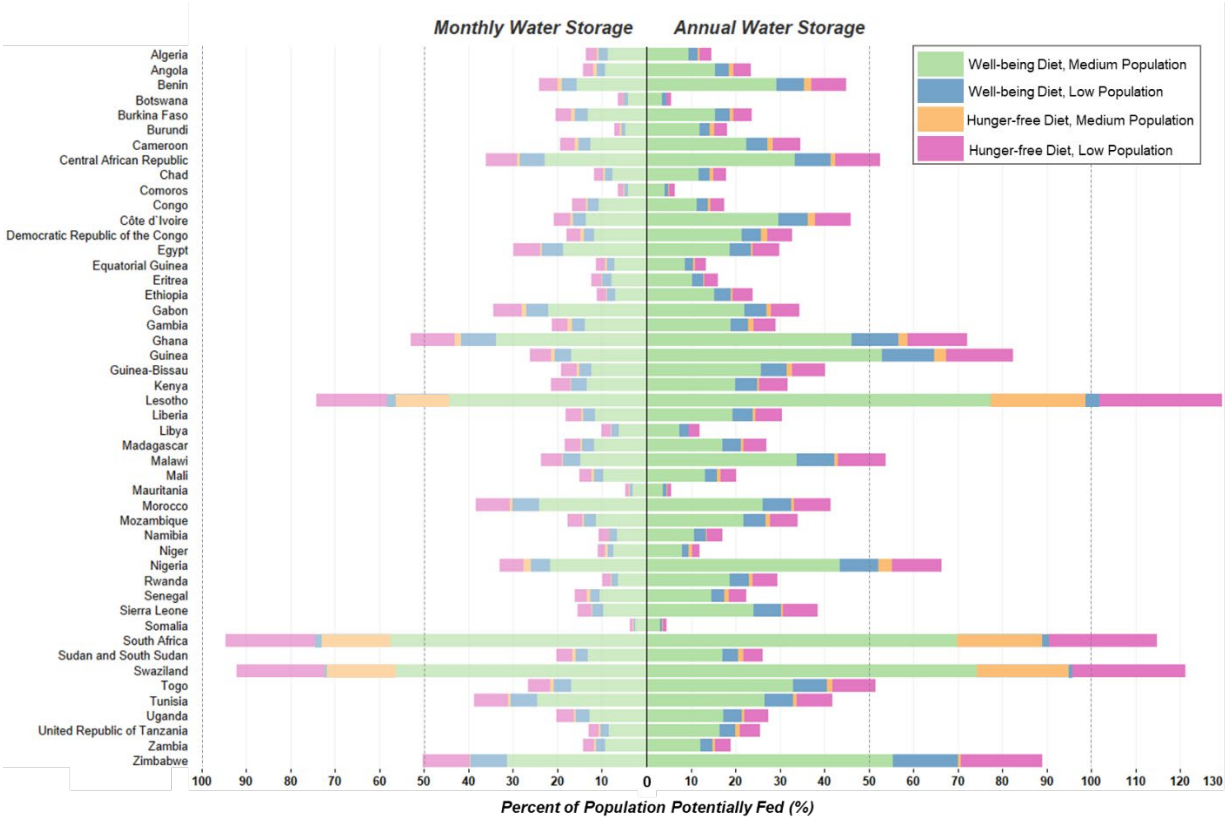

Figure 4. Percent of the population that could be fed (without food loss or waste) based on diverse adaptation strategies in a 3°C warmer world while preserving 60% environmental flow requirements. Four diet and population combinations are differentiated by color. Lighter shades represent results under monthly water storage (left) and darker shades are representative of annual water storage (right). Dashed lines indicate the 50% and 100% thresholds. The analyses in this figure are based on total domestic crop production available for human consumption not accounting for food lost or wasted.

2.4.4 2075 Outlook under Sustainable Development Goals

We determined the percent of a country's population (low trajectory) that can be fed with a well-being diet of 2,327 kcal per capita per day for both monthly and annual water storage strategies assuming irrigation is expanded in areas where it is sustainably possible while preserving 60% of environmental flows for ecosystem health; and efforts succeed to reduce food loss by a quarter and food waste by half compared to current levels in a 3°C future (figure 5). For all African countries storing water annually results in a much higher proportion of the population being fed with a well-being diet. For example, 52% of Guinea's population in 2075 can be fed if annual water storage techniques are implemented, compared to 17% with monthly storage. With an annual storage approach, five countries can feed over half of their population, three of which can feed over 70% (Lesotho, South Africa, and Swaziland). On the other hand, with a monthly water storage approach, only two countries can feed over 50% of their population. The countries with the greatest difference between the percent of population that can be fed with annual vs. monthly water storage are Guinea (Δ 36%), Lesotho (Δ 35%), Zimbabwe (Δ 25%), Nigeria (Δ 21%), and Malawi (Δ 19%).

Countries with a difference between the two water storage strategies of less than 1% are Algeria, Niger, Mauritania, Somalia, Congo, Egypt, Comoros, Gabon, and Botswana. The countries that will not be able to domestically produce sufficient calories to feed over 10% of their population regardless of water storage strategies are Algeria, Botswana, Comoros, Equatorial Guinea, Libya, Mauritania, Niger, and Somalia. These countries will continue to heavily rely on imports under both current and 3°C climate conditions (see table 3).

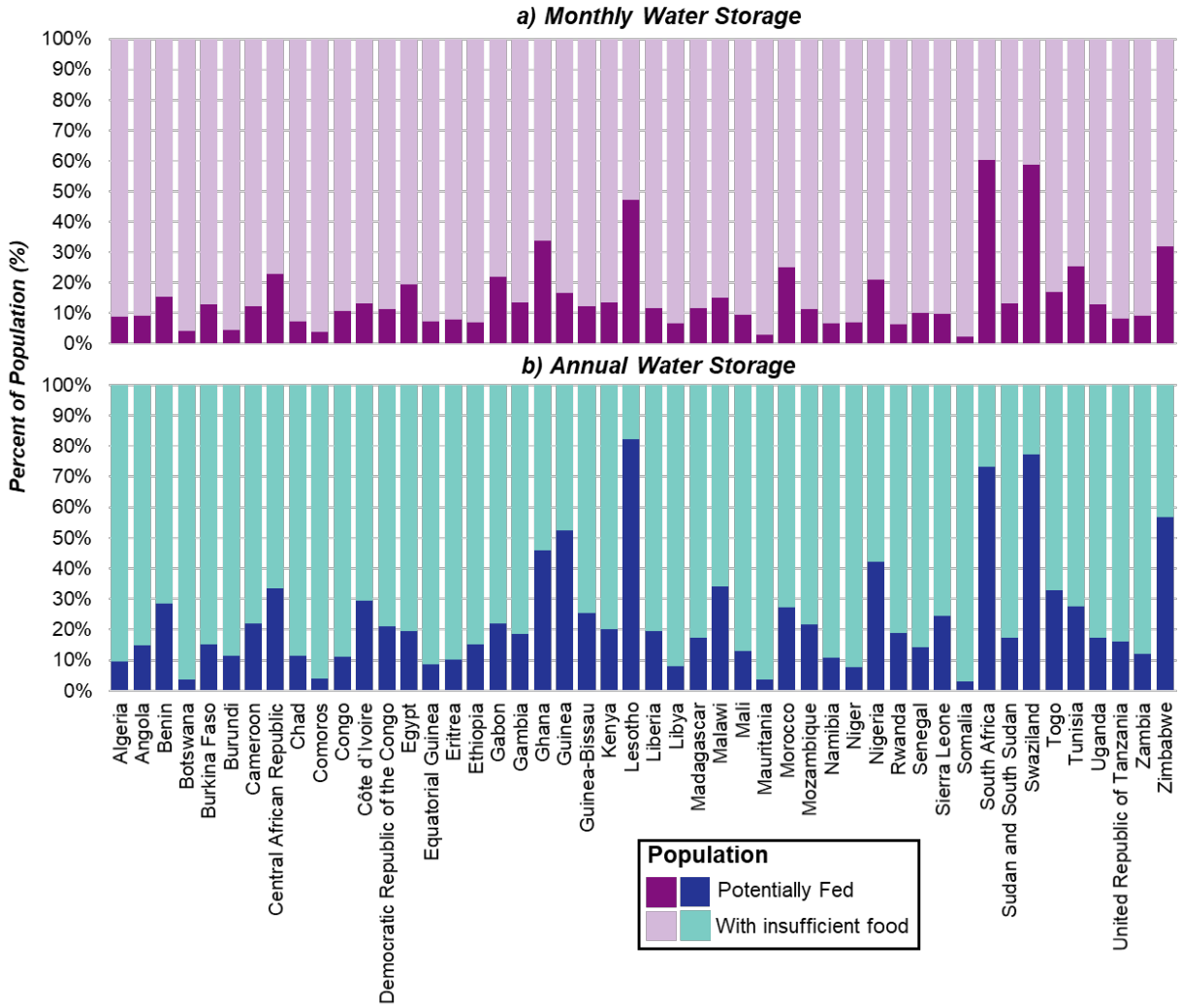

Figure 5. Percent of population that can or cannot be fed under the SDG scenario in a 3°C warmer climate based on a) monthly or b) annual water storage strategy. The SDG scenario considers a well-being diet, low population trajectory, 60% EF preserved, and FL 25% and FW 50% reduction. Dark shaded bars represent percent of population fed through domestic crop production. Light shaded bars represent percent not fed, but more specifically, the percent of population that still needs to be fed through imports or other means to meet SDG 2- zero hunger and malnutrition. This figure shows the results for 60% EF preserved. See supplementary figure S3 for results based on 80% EF reserved.

2.4.5 Caloric Deficits

We define *caloric deficit* as the number of calories needed to feed the remainder of a country's population whose dietary needs cannot be met through domestic crop production with a minimum daily consumption of either 1,829 or 2,327 kcal. As mentioned earlier, this accounts for the additional crop calories it takes to produce animal-based calories (which depends on fraction of animal-based products in diets). Access to water storage systems, food waste/food loss rates, and the fraction of runoff allocated to environmental needs (i.e., as environmental flows) determine a country's rate of crop production and the associated food supply. Based on the adaptation strategy (e.g., water storage) and dietary goal pursued as well as population trajectory reached, the number of people and subsequently the caloric deficit differ. Considering only annual water storage and well-being diets, in addition to 25% food loss and 50% food waste reduction (SDG), table 3 displays the caloric deficit and the corresponding number of people under three main scenarios for each region, while supplementary table S4 displays the caloric deficit by country.

2.4.6 Reference Scenario - Baseline Climate Conditions in 2030

According to the IPCC special report on global warming of 1.5°C, global warming is likely to reach 1.5°C between 2030 and 2052 if it continues to increase at the current rate" (IPCC 2018). The reference period for global agricultural data from Portmann et al., (2010) is years 1996 to 2005. According to the Global Land-Ocean Temperature Index of the NASA's Goddard Institute for Space Studies, the Earth had warmed by approximately 0.68°C above preindustrial levels by 2005 (our baseline climate condition) (NASA/GISS 2021). Thus, we created a frame of reference assuming baseline climate conditions remained in year 2030 and the SDG scenario framework was effectuated. Since 2030 is just around the corner, this projection is paired with the medium population to give conservative estimates. Hence, according to this analysis, in 2030 Africa would need to import 73.2×10^{13} kcal of crops, corresponding to the food needed to feed 881 million people with a well-being diet. Regionally, Eastern Africa would need external supply of food for 399 million people, followed by Northern Africa (170 million people), Western Africa (157 million people), and Central Africa (137 million people). Ethiopia, Egypt, the Democratic Republic of Congo, Algeria, Kenya, and Tanzania would have the greatest caloric deficits in 2030 with baseline climatic conditions (table 3).

2.4.7 At 3°C with SDG framework

The subsequent two scenarios in table 3 forecast the caloric deficits under a 3°C warmer climate (~year 2075) with an annual water storage approach and if the SDG framework is sustained (low population, well-being diet, food loss and waste reduction of 25% and 50% respectively). They differ only on the percentage of environmental flow requirements (60% or 80%) maintained. Looking at the 60% EF approach, Eastern and Western Africa will be in the toughest position, needing to procure (import) 84.3×10^{13} and 61.3×10^{13} kcal from outside sources to feed their populations. These food deficits correspond to the food needed to feed 857 and 658 million people, respectively, followed by Central Africa and Northern Africa with a food deficit of 390 and 221 million people. Comparatively, the relatively low food deficit of Southern Africa can be explained by the lower population density in the region. Nigeria (282 million people), Ethiopia (183 million people), the Democratic Republic of Congo (191 million people), Tanzania (142 million people), and Egypt (128 million people) will have the worst caloric deficits in the continent. In total, at a time when Africa's population is projected to reach 3.5 billion people, 207.2×10^{13} kcal for food and feed will need to be procured in Africa to feed 2.15 billion people (total projected African

population of the food deficit expressed in number of people) on the continent who cannot be provided for with domestic production. The difference in the number of people that cannot be fed through domestic production between the 60% EF and 80% EF strategy in all of Africa is 75 million people. Note that these scenario combinations are assuming that we reduce food loss by 25% and food waste by 50% from current levels as per the SDGs, curtailing food loss and waste more would further reduce the caloric deficit to an extent.

	Current Climate 60% Environmental Flows *(Year 2030, Medium Population)*		**3°C Climate, 60% Environmental Flows** *(Year 2075, Low Population)*		**3°C Climate, 80% Environmental Flows** *(Year 2075, Low Population)*	
Region	**Caloric Deficit** *(in 10^{13} kcal)*	**Number of People Equivalent** *(in millions)*	**Caloric Deficit** *(in 10^{13} kcal)*	**Number of People Equivalent** *(in millions)*	**Caloric Deficit** *(in 10^{13} kcal)*	**Number of People Equivalent** *(in millions)*
Central Africa	11.2	136.7	37.4	390.5	37.5	391.8
Eastern Africa	33.0	399.2	84.3	857.0	86.2	877.0
North Africa	14.7	169.6	22.0	221.4	22.2	223.0
South Africa	1.5	18.8	2.3	24.0	2.6	27.4
Western Africa	12.8	156.6	61.3	657.8	65.7	706.4
All Africa	73.2	880.9	207.2	2,150.7	214.1	2,225.6

Table 3. Regional food deficit and people equivalent for baseline and 3°C warmer climate. All three pathways represented in this table were formulated under the assumption that SDG food loss and waste (25%/50% reduction), the well-being diet, and annual water storage strategies are adopted. The results for the two environmental flow requirement targets (60% or 80% conservation) are presented for only a 3°C warmer climate.

2.5 Discussion

Our results echo the well-known dilemma that Africa is facing – population growth and food demand are outpacing the domestic agricultural production potential. We estimate that under a 3°C warmer climate with sustainable agricultural practices and reducing food loss and waste to achieve SDG 12.3, the total food production in Africa will only suffice to feed 1.35 billion people, at a time when the continent's population is expected to reach 3.5 billion, leaving a food deficit for 2.15 billion people. Africa holds just 9% of the world's surface water, while accounting for over 17% of the world's total population (Pekel et al., 2016; United Nations 2019). Meanwhile, croplands constitute 10% of the total land area on the African continent (Latham et al., 2014). However, over half (58.4%) of African croplands are located on drylands, where crop production is becoming increasingly difficult due to 'water shortages, land degradation, climate change and persistent poverty' (Latham et al., 2014; Tilman and Clark 2015; Sarukhán el al., 2005; Cherlet et al., 2018). Under climate change, in wet tropical regions drylands are expected to become wetter, while in Northern and Southern Africa, subtropical drylands will expand, and semi-arid zones may shift to arid or hyper-arid zones (Fischer et al., 2007; Safriel et al., 2005; Cherlet et al., 2018). Thus, Rosa et al., (2020a) determined how the suitability of current global croplands for sustainable irrigation would change under 1.5°C and 3°C levels of warming above pre-industrial levels. By accounting for sustainable irrigation expansion potential on current croplands for 130

primary crops, modelling water storage potentials (Rosa et al., 2020a), narrowing the yield gaps in underperforming lands, and simulating various food loss and waste reduction strategies, we are able to assess the number of people that could be potentially fed through sustainable agricultural intensification and the degree to which each country will be reliant on external food sources to meet the needs of their people as diets shift and population grows. Beltran-Peña et al., 2020 revealed that today, almost no African country is self-sufficient and as the Earth warms, they will be further unable to meet the food demands of their population through domestic production alone. Here we quantify the caloric deficit based on production potential, dietary trends, and population growth. The fraction of the population that cannot be fed under the SDG scenario (figure 5) are indicative of import dependency that is required in each African country in order to meet SDG goal 2- zero hunger and malnutrition, while addressing SDG goals 5 (gender equality), 6 (clean water and sanitation), 12 (responsible consumption and production), 13 (climate action), and 15 (life on land). We project that Eastern and Western Africa will have the greatest import needs, but the actual demand and deficit can be lessened with more sustainable consumption patterns as well as by using annual water storages to rely on water stocks accumulated during the wet season for irrigation during dry periods of the growing season(s). Storages associated with surface reservoirs can be problematic because of concerns related to environmental impacts, safety, size of these investment infrastructure, increasing dependence on foreign credit, dispossession of rural indigenous communities, and loss of rural livelihoods (Carr et al., 2017; Tatlhego and D'Odorico, 2021; Muller et al., 2021). While we refrain from venturing in the heated debate on the pros and cons of large dam infrastructure and whether they are needed for economic development of these countries (Scudder, 2017), we point to the fact that water storage can also be achieved through managed aquifer recharge, farm-scale detention ponds (e.g., Van Der Zaag and Gupta, 2008; He et al., 2021), or small-scale reservoirs that could be less challenging both environmentally and financially (Ross and Hasnain 2018; Sprenger et al., 2017). These options need to be adequately explored as a possible pathway for irrigation development in Africa.

2.5.1 Consumption Trends

The change in demand for animal-based products over time assessed in this study is based on the economic growth projections of SSP 2 in which "Gross Domestic Product (GDP) follows regional historical trends, with global average income (i.e., average GDP/capita) reaching about 60,000 (year-2005 USD/capita) by the end of the century. SSP 2 sees an increase of global average income by a factor 6 and depicts a future of global progress where developing countries achieve significant economic growth" (Fricko et al., 2017; Riahi et al., 2017; Dellink et al., 2017). According to Dellink et al., 2017, GDP per capita is projected to increase in all African countries considered in this study. Economic growth and rising incomes enable households to purchase foods with higher caloric and protein content (i.e. vegetables and animal products) which consequently drives up the demand for animal feed (D'Odorico et al., 2018; Tilman et al., 2011; Bennett 1941; OECD/FAO 2021; FAO, ECA and AUC. 2021). Our model considers these increases in dietary demand (figure 2). Diverting crop products for feed-fed livestock production (we are assuming that grass-fed production remains constant to prevent overgrazing), reduces the crop calories available for direct human consumption and increases environmental impacts. In fact, we find that at 3°C none of the countries evaluated, will be able to meet the food demand of their populations through domestic production alone (figures 4 and 5). The OECD/FAO Agricultural Outlook predicts that poultry and beef will account for the majority of meat imports in Africa to

account for domestic supply deficits due to consumption growth outpacing domestic production (OECD/FAO 2021).

With the projected rise in Africa's population from 1.37 billion people in 2021 to 3.5 billion people in 2075, changes in diets towards higher animal product consumption will strain the supply chain – augmenting the importance of reducing food losses and waste which increases crops available for direct or indirect human dietary consumption from current croplands (United Nations 2019). Before the development of the FAO Food Loss and UN Food Waste Indices, the 2011 FAO report by the Swedish Institute for Food and Biotechnology, was the only study that estimated food lost and wasted throughout all stages of the food supply chain and across all food production sectors and has been widely cited by subsequent studies (FAO 2011; FAO 2019; Gustavsson et al., 2013; Kummu et al., 2012). Contrary to popular belief, the UN Food Waste Index found that household per capita food waste generation is similar across country income groups, indicating the importance of addressing food waste in all countries (it was previously thought that food waste primarily occurred in developed nations while food loss was predominant in developing nations) (UNEP 2021a). Sustainable Development Goal 12 aims to ensure sustainable consumption and production by halving global food waste and reducing food losses by 2030 (U.N. DESA 2016). Here we take it a step further and calculate the additional calories that would become available by halving both food losses and waste. We found that halving both food loss and waste from current levels, will allow more food to be available to feed an additional 130 million Africans in a 3°C future (figure 3). Hence, rebalancing diets with an overall lower fraction of animal products with an increase in poultry consumption in lieu of beef or other ruminant meats – a trend already observed around the world (Davis et al., 2015); and increased nutritional plant-based foods in addition to significantly reducing food loss and waste, will boost the number of people that can be fed through domestic production along with reducing import needs, the financial cost, and environmental impacts of diets (FAO, IFAD, UNICEF, WFP and WHO. 2020; FAO, ECA and AUC. 2021; Mekonnen and Hoekstra 2012; Nijdam et al., 2012**)**.

Additionally, improving socio-economic conditions (i.e. empowering women, reducing the gender gap), investing in infrastructure, and sustainably intensifying food production are essential interventions to improve availability and demand ratios (FAO, ECA, AUC 2021; Graves et al., 2019; van Maanen et al., 2022). The intensification of food production, however, may strongly affect rural livelihoods, as small-holder farmers have more limited access to credit and financial resources to invest in high yield technology (e.g., irrigation, fertilizers, mechanization, concentrated livestock systems) and are therefore more likely to be displaced by agribusiness corporations. Low-technology agro-ecological methods, however, have been shown to be capable of sustaining higher yields (Altieri et al., 2012), and small-holders have been found to produce more (on a per unit area basis) than large scale farming (Herrero et al., 2017; Ricciardi et al., 2018).

2.5.2 Trade Implications

Africa is a net importer of agricultural products (i.e. cereals, meat, dairy products) and annually imports about 80 billion USD of food products, of which less than 20% is from intra-African trade (FAO and AUC 2021). In our reference scenario (with baseline climate conditions) estimates a caloric deficit equivalent of 881 million people in Africa by year 2030. However, considering with global warming of 3°C, more animal products in diet compositions, and population growth the projected caloric deficit equivalent in year 2075 increases to 2.15 billion people in Africa. It is important to note that, under a changing climate, some countries outside of Africa may not have the resources to export food products and may experience deficits as well while others will have a

surplus (Beltran-Peña et al., 2020). This poses two important questions that should be further explored. First, affordability - will countries be able afford to import the additional food needed to meet their population's demand? Second, to what extent can international trade be an adaptation mechanism? Janssens et al., 2021 demonstrates that 'trade policies influence the sensitivity of hunger to climate change' and calls for better trade agreements with lower tariffs and preventing border restrictions while using cautions to avoid food price increases due to lower availability in exporting regions' (Janssens et al., 2021). On the other hand, it was also noticed that lack of tariffs has often allowed relatively cheap imports of agricultural products (often subsidized by foreign governments) to outcompete and displace local production systems in Africa, thereby limiting self-sufficiency, food sovereignty, rural livelihoods, and the sustainable use of water resources (Friedmann, 1993; D'Odorico et al., 2019b). Moreover, trade-dependency may limit the resilience of food systems, as observed in recent food crises when some countries adopted export bans as a tool to control escalating domestic food prices, while leaving import-dependent countries scrambling for agricultural commodities (Seekell et al., 2017; FAO, 2021). Improving intra-African trade is a top priority for the African Union Commission's Department of Agriculture, Rural Development, Blue Economy and Sustainable Development so that local stakeholders including farmers, small and medium agri-businesses, women and youth can benefit from the market while removing trade barriers among African countries (FAO and AUC 2021). Still, if agricultural adaptation measures, stronger policies and infrastructural investments, and trade, are insufficient to meet future food demand under a changing climate, voluntary migrations or involuntary displacements may ensue which in turn may lead to lower agricultural productivity (McLeman 2014; McLeman 2019; Payne 2013; Cherlet et al., 2018; FAO, ECA and AUC. 2021).

2.5.3 Limitations

There are four main pillars of food security – availability, access, utilization, and stability (FAO 2008). They are all essential in ensuring food security of a population. However, the scope of this study only addresses the availability pillar – particularly production potential and trade dependency. The division between the free from hunger and well-being diets is an initial, but limited attempt to address nutritional quality of diets. A hunger-free diet allocates just enough daily calories (1,829 kcal) for people to not experience calorie intake deficits and thus hunger (addressing the SDG zero hunger target). A well-being diet allocates 2,327 kcal daily per person. The assumption is that the greater caloric allowance also implies the possibility of consuming more diverse food products (partially addresses the zero malnutrition SDG target). Further work is required to assess the nutritional quality of diets consumed and what will be required to ensure access to sufficient and nutritious diets. We consider 130 primary crops (Portmann et al., 2010) used for direct human consumption as well as for feed. Climate change is accounted for in terms of the irrigation area suitable for sustainable irrigation in a 3°C warmer climate. This study does not account for crop migration or the effects of CO_2 fertilization (Sloat et al., 2020). Importantly, irrigation expansion and a sustainable intensification of agriculture will require additional energy inputs, which could have added energy implications for African countries, such as energy import dependency and local energy access (Rosa et al., 2021b). Besides water availability, nutrients are another major factor limiting crop production in African countries with high soil nutrient depletion and investments in soil fertility replenishment are needed to improve crop production (Sanchez 2002). This study, however, does not assess the limitations of soil nutrient depletion or potential of soil fertility improvement on crop production.

The Sustainable Development Goals are set for year 2030. However, we are not on track to meet these goals by the set timeline (United Nations, 2021). There may be more ambitious targets for year 2075 and beyond, but since future targets and international agreements are not yet predictable, this study applies the SDG goals beyond 2030. Additionally, we present the data and our findings based on the population data for year in which 3°C above preindustrial levels is expected to be reached by the GFDL-ESM2M and MIROC 5 global climate models (~2075). However, the year we surpass 3°C is not certain and thus the results of this analysis may differ slightly depending on the population numbers of the actual year 3°C is reached.

Thus far, data availability for food loss and waste estimates around the world have been insufficient and reliant on extrapolations of data from few countries where limited data is available, but possibly outdated. The UNEP and FAO have recognized this challenge and created the Food Loss and Food Waste Indices to improve data reporting methods for countries to keep track of progress towards SDG 12.3 (FAO 2019; UNEP 2021a). Here we use the most recent estimates of food loss and waste, but there are still uncertainties in these estimates which will only improve with increased reporting over time.

The SDGs are here used as a framework to analyze and interpret the results of our study. These goals are here taken as a given without investigating their merit. We did not assess the process that went into their definition, who contributed to it, to what extent the rural poor, indigenous communities, and more in general those who should (or would be expected to) benefit from "sustainable development" had a voice in this process. While the SDGs are here used to build a narrative on food security in Africa a more critical analysis of the SDG framework is beyond the scope of this study. We also understand and acknowledge the importance of local community engagement and community-centered approaches before implementing any adaptation and mitigation measures.

2.6 Conclusion

Ending hunger and malnutrition is the second target of the United Nations Sustainable Development Goals. Our work evaluated the feasibility of meeting this goal through sustainable irrigation intensification on currently rainfed croplands in African countries in a 3°C warmer climate considering changes in consumption patterns and population growth. Furthermore, we estimated the difference in production potential by implementing various strategies of runoff water storage and environmental flow requirements. Finally, this study determines the amount of food that each country will still need to acquire from other methods (i.e. agricultural expansion) or external sources in order to adequately feed their populations while taking into account other SDGs.

Our findings show the existence of a mismatch between population and food demand growth and agricultural production across the African continent. It also stresses how African populations would be hardly able to predominantly rely on local food production, in disagreement with the claims of local food movements. Interestingly, the analysis of the global patterns of international food trade (D'Odorico et al., 2014) indicate that African countries are poorly integrated in the global agricultural market, which could limit their resilience to production shocks. The results of this study provide a preliminary assessment of the potential for sustainable agricultural intensification and water storage capacities under climate change in Africa; as well as data on the potential extents of future import needs based on varying consumption (including food loss and food waste) patterns to local decision makers.

2.7 References

African Development Bank Group (ADBG) 2019. 2019 Annual Report. (Available at: https://www.afdb.org/en/annual-report-2019)

Altieri, M. A., Funes-Monzote, F. R., & Petersen, P. (2012). Agroecologically efficient agricultural systems for smallholder farmers: Contributions to food sovereignty. Agronomy for Sustainable Development, 32(1), 1–13. https://doi.org/10.1007/s13593-011-0065-6Ayanlade, A. and Radeny, M., 2020. COVID-19 and food security in Sub-Saharan Africa: implications of lockdown during agricultural planting seasons. *npj Science of Food*, *4*(1), pp.1-6.

Beltran-Peña, A., Rosa, L. and D'Odorico, P., 2020. Global food self-sufficiency in the 21st century under sustainable intensification of agriculture. *Environmental Research Letters*, *15*(9), p.095004.

Bennett, M. K. (1941). *Wheat studies of the Food Research Institute, vols 12 and 18*. Stanford, CA: Stanford University.

Bonilla-Cedrez, C., Chamberlin, J. and Hijmans, R.J., 2021. Fertilizer and grain prices constrain food production in sub-Saharan Africa. *Nature Food*, pp.1-7.

Brenton, P. & Chemutai, V. Trade Responses to the COVID-19 Crisis in Africa, World Bank (2020).

Brouwer, C. and Heibloem, M., 1986. Irrigation water management: irrigation water needs. *Training manual*, *3*. FAO Rome.

Byers, E., Gidden, M., Leclère, D., Balkovic, J., Burek, P., Ebi, K., Greve, P., Grey, D., Havlik, P., Hillers, A. and Johnson, N., 2018. Global exposure and vulnerability to multi-sector development and climate change hotspots. *Environmental Research Letters*, *13*(5), p.055012.

Carr, C.J., 2017. *River basin development and human rights in eastern africa—A policy crossroads* (p. 240). Springer Nature.

Cherlet, M., Hutchinson, C., Reynolds, J., Hill, J., Sommer, S., von Maltitz, G. (Eds.), *World Atlas of Desertification*, Publication Office of the European Union, Luxembourg, 2018.

Climate Analytics. Warming Attribution Calculator. Available at: http://wlcalc.climateanalytics.org/choices

Climate Hazards Group 2015, Climate Hazards Group CHIRPSv2.0. https://www.chc.ucsb.edu/data/chirps. Accessed October 23, 2020.

D'Odorico, P., Carr, J.A., Laio, F., Ridolfi, L. and Vandoni, S., 2014. Feeding humanity through global food trade. *Earth's Future*, *2*(9), pp.458-469.

D'Odorico, P., Davis, K.F., Rosa, L., Carr, J.A., Chiarelli, D., Dell'Angelo, J., Gephart, J., MacDonald, G.K., Seekell, D.A., Suweis, S. and Rulli, M.C., 2018. The global food-energy-water nexus. *Reviews of geophysics*, *56*(3), pp.456-531.

D'Odorico, P., Carr, J.A., Davis, K.F., Dell'Angelo, J. and Seekell, D.A., 2019. Food inequality, injustice, and rights. Bioscience, 69(3), pp.180-190.

D'Odorico, P., Carr, J., Dalin, C., Dell'Angelo, J., Konar, M., Laio, F., Ridolfi, L., Rosa, L., Suweis, S., Tamea, S. and Tuninetti, M., 2019b. Global virtual water trade and the hydrological cycle: patterns, drivers, and socio-environmental impacts. *Environmental Research Letters*, *14*(5), p.053001.

Davis, K.F., D'Odorico, P. and Rulli, M.C., 2014. Moderating diets to feed the future. *Earth's Future*, *2*(10), pp.559-565.

Davis, K.F., K. Yu, M. Herrero, P. Havlik, J. A. Carr, P. D'Odorico, "Trends and trade-offs of livestock's environmental impacts, Environm. Res. Lett., 10, 125013, 2015.

De Onis, M. and Branca, F., 2016. Childhood stunting: a global perspective. *Maternal & child nutrition*, *12*, pp.12-26.

Dellink, R., Chateau, J., Lanzi, E. and Magné, B., 2017. Long-term economic growth projections in the Shared Socioeconomic Pathways. *Global Environmental Change*, *42*, pp.200-214.

Elliott, J., Deryng, D., Müller, C., Frieler, K., Konzmann, M., Gerten, D., Glotter, M., Flörke, M., Wada, Y., Best, N. and Eisner, S., 2014. Constraints and potentials of future irrigation water availability on agricultural production under climate change. *Proceedings of the National Academy of Sciences*, *111*(9), pp.3239-3244.

FAO, 2008. An Introduction to the Basic Concepts of Food Security. FAO, Rome. Retrieved from <http://www.fao.org/3/al936e/al936e00.pdf>.

FAO 2011. Global food losses and food waste – Extent, causes and prevention. Rome.

FAO 2014. Food security indicators. November 17 2014 revision. Rome.

FAO 2019. *The State of Food and Agriculture 2019. Moving forward on food loss and waste reduction.* Rome. License: CC BY-NC-SA 3.0 IGO.

FAO 2019b. Food Loss Index. Online statistical working system for loss calculations. (Available at http://www.fao.org/food-loss-and-food-waste/flw-data).

FAO 2019c. Incorporating environmental flows into "water stress" indicator 6.4.2: guidelines for a minimum standard method for global reporting (report) (Rome) p 32 (Available at: http://www.fao.org/documents/card/en/c/ca3097en/)

FAO 2021. The State of Agriculture in the World. Rome.

FAO and AUC. 2021. *Framework for boosting intra-African trade in agricultural commodities and services.* Addis Ababa.

FAO, ECA and AUC. 2020. *Africa Regional Overview of Food Security and Nutrition 2019.* Accra.

FAO, ECA and AUC. 2021. Africa regional overview of food security and nutrition 2020: Transforming food systems for affordable healthy diets. Accra, FAO.

FAO, IFAD, UNICEF, WFP and WHO. 2020. The State of Food Security and Nutrition in the World 2020. Transforming food systems for affordable healthy diets. Rome, FAO. https://doi.org/10.4060/ca9692en

FAO, IFAD, UNICEF, WFP and WHO. 2021. The State of Food Security and Nutrition in the World 2021. Transforming food systems for food security, improved nutrition and affordable healthy diets for all. Rome, FAO. https://doi.org/10.4060/cb4474en

Fekete, B.M., Vörösmarty, C.J. and Grabs, W., 2002. High-resolution fields of global runoff combining observed river discharge and simulated water balances. *Global Biogeochemical Cycles*, *16*(3), pp.15-1.

Fischer, G., Tubiello, F.N., Van Velthuizen, H. and Wiberg, D.A., 2007. Climate change impacts on irrigation water requirements: Effects of mitigation, 1990–2080. *Technological Forecasting and Social Change*, *74*(7), pp.1083-1107.

Foley, J.A., Ramankutty, N., Brauman, K.A., Cassidy, E.S., Gerber, J.S., Johnston, M., Mueller, N.D., O'Connell, C., Ray, D.K., West, P.C. and Balzer, C., 2011. Solutions for a cultivated planet. *Nature*, *478*(7369), pp.337-342.

Frank, S., Gusti, M., Havlík, P., Lauri, P., DiFulvio, F., Forsell, N., Hasegawa, T., Krisztin, T., Palazzo, A. and Valin, H., 2021. Land-based climate change mitigation potentials within the agenda for sustainable development. *Environmental Research Letters*, *16*(2), p.024006.

Fricko, O., Havlik, P., Rogelj, J., Klimont, Z., Gusti, M., Johnson, N., Kolp, P., Strubegger, M., Valin, H., Amann, M. and Ermolieva, T., 2017. The marker quantification of the Shared Socioeconomic Pathway 2: A middle-of-the-road scenario for the 21st century. *Global Environmental Change*, *42*, pp.251-267.

Friedmann, H., 1993. The political economy of food: a global crisis. *New left review*, (197), pp.29-57.

Fyfe, J.; Fox-Kemper, B.; Kopp, R.; Garner, G. (2021): Summary for Policymakers of the Working Group I Contribution to the IPCC Sixth Assessment Report - data for Figure SPM.8 (v20210809). NERC EDS Centre for Environmental Data Analysis, *09 August 2021*. doi:10.5285/98af2184e13e4b91893ab72f301790db. http://dx.doi.org/10.5285/98af2184e13e4b91893ab72f301790db

Gibbs, H.K., Ruesch, A.S., Achard, F., Clayton, M.K., Holmgren, P., Ramankutty, N. and Foley, J.A., 2010. Tropical forests were the primary sources of new agricultural land in the 1980s and 1990s. *Proceedings of the National Academy of Sciences*, *107*(38), pp.16732-16737.

Goyal, A. & Nash, J. 2017. Reaping Richer Returns: Public Spending Priorities for African Agriculture Productivity Growth. Africa Development Forum series [online]. Washington, DC, World Bank Group.

Graves, A., Rosa, L., Nouhou, A.M., Maina, F. and Adoum, D., 2019. Avert catastrophe now in Africa's Sahel. *Nature.*

Gustavsson, J., Cederberg, C., Sonesson, U. & Emanuelsson, A. 2013. *The methodology of the FAO study: "Global food losses and food waste – extent, causes and prevention". FAO, 2011*. SIK report No. 857. Lund, Sweden, Swedish Institute for Food and Biotechnology (SIK).

Harrington, L.J., Frame, D.J., Fischer, E.M., Hawkins, E., Joshi, M. and Jones, C.D., 2016. Poorest countries experience earlier anthropogenic emergence of daily temperature extremes. *Environmental Research Letters*, *11*(5), p.055007.

Harris, I.P.D.J., Jones, P.D., Osborn, T.J. and Lister, D.H., 2014. Updated high-resolution grids of monthly climatic observations–the CRU TS3. 10 Dataset. *International journal of climatology*, *34*(3), pp.623-642.

He, X., Bryant, B.P., Moran, T., Mach, K.J., Wei, Z. and Freyberg, D.L., 2021. Climate-informed hydrologic modeling and policy typology to guide managed aquifer recharge. *Science Advances*, *7*(17), p.eabe6025.

Herrero, M., Thornton, P.K., Power, B., Bogard, J.R., Remans, R., Fritz, S., Gerber, J.S., Nelson, G., See, L., Waha, K. and Watson, R.A., 2017. Farming and the geography of nutrient production for human use: a transdisciplinary analysis. *The Lancet Planetary Health*, *1*(1), pp.e33-e42.

Hoekstra, A.Y. and Mekonnen, M.M., 2012. The water footprint of humanity. *Proceedings of the national academy of sciences*, *109*(9), pp.3232-3237.

IPCC, 2018: Summary for Policymakers. In: Global Warming of 1.5°C. An IPCC Special Report on the impacts of global warming of 1.5°C above pre-industrial levels and related global greenhouse gas emission pathways, in the context of strengthening the global response to the threat of climate change, sustainable development, and efforts to eradicate poverty [Masson-Delmotte, V., P. Zhai, H.-O. Pörtner, D. Roberts, J. Skea, P.R. Shukla, A. Pirani, W. Moufouma-Okia, C. Péan, R. Pidcock, S. Connors, J.B.R. Matthews, Y. Chen, X. Zhou, M.I. Gomis, E. Lonnoy, T. Maycock, M. Tignor, and T. Waterfield (eds.)]. In Press

IPCC, 2021: Summary for Policymakers. In: Climate Change 2021: The Physical Science Basis. Contribution of Working Group I to the Sixth Assessment Report of the Intergovernmental Panel on Climate Change [Masson-Delmotte, V., P. Zhai, A. Pirani, S.L. Connors, C. Péan, S. Berger, N. Caud, Y. Chen, L. Goldfarb, M.I. Gomis, M. Huang, K. Leitzell, E. Lonnoy, J.B.R. Matthews, T.K. Maycock, T. Waterfield, O. Yelekçi, R. Yu, and B. Zhou (eds.)]. In Press

Janssens, C., Havlík, P., Krisztin, T., Baker, J., Frank, S., Hasegawa, T., Leclère, D., Ohrel, S., Ragnauth, S., Schmid, E. and Valin, H., 2021. International trade is a key component of climate change adaptation. *Nature Climate Change*, pp.1-2.

Kummu, M., de Moel, H., Porkka, M., Siebert, S., Varis, O. & Ward, P.J. 2012. Lost food, wasted resources: global food supply chain losses and their impacts on freshwater, cropland, and fertiliser use. *Science of the Total Environment*, 438: 477–489.

Latham, J., Cumani, R., Rosati, I. and Bloise, M., 2014. Global land cover share (GLC-SHARE) database beta-release version 1.0-2014. *FAO: Rome, Italy*.

Liu, X., Liu, W., Liu, L., Tang, Q., Liu, J. and Yang, H., 2021. Environmental flow requirements largely reshape global surface water scarcity assessment. Environmental Research Letters, 16(10), p.104029.

Liu, Z., Ciais, P., Deng, Z., Lei, R., Davis, S.J., Feng, S., Zheng, B., Cui, D., Dou, X., Zhu, B. and Guo, R., 2020. Near-real-time monitoring of global CO 2 emissions reveals the effects of the COVID-19 pandemic. *Nature communications*, *11*(1), pp.1-12.

Lobell, D.B., Cassman, K.G. and Field, C.B., 2009. Crop yield gaps: their importance, magnitudes, and causes. *Annual review of environment and resources*, *34*, pp.179-204.

McLeman, R. *Climate and Human Migration: Past Experiences, Future Challenges* (Cambridge Univ. Press, 2014).

McLeman, R., 2019. International migration and climate adaptation in an era of hardening borders. *Nature Climate Change*, *9*(12), pp.911-918.

Mekonnen, M.M. and Hoekstra, A.Y., 2012. A global assessment of the water footprint of farm animal products. *Ecosystems*, *15*(3), pp.401-415.

Millar, R.J., Fuglestvedt, J.S., Friedlingstein, P., Rogelj, J., Grubb, M.J., Matthews, H.D., Skeie, R.B., Forster, P.M., Frame, D.J. and Allen, M.R., 2017. Emission budgets and pathways consistent with limiting warming to 1.5 C. *Nature Geoscience*, *10*(10), pp.741-747.

Monfreda, C., Ramankutty, N. and Foley, J.A., 2008. Farming the planet: 2. Geographic distribution of crop areas, yields, physiological types, and net primary production in the year 2000. *Global biogeochemical cycles, 22(1).Vancouver*

Mueller, N.D., Gerber, J.S., Johnston, M., Ray, D.K., Ramankutty, N. and Foley, J.A., 2012. Closing yield gaps through nutrient and water management. *Nature*, *490*(7419), pp.254-257.

Müller, M.F., Penny, G., Niles, M.T., Ricciardi, V., Chiarelli, D.D., Davis, K.F., Dell'Angelo, J., D'Odorico, P., Rosa, L., Rulli, M.C. and Mueller, N.D., 2021. Impact of transnational land acquisitions on local food security and dietary diversity. *Proceedings of the National Academy of Sciences*, *118*(4).

NASA's Goddard Institute for Space Studies (NASA/GISS), 2021. Global Land-Ocean Temperature Index. Retrieved from: https://climate.nasa.gov/vital-signs/global-temperature/

Nijdam, D., Rood, T. and Westhoek, H., 2012. The price of protein: Review of land use and carbon footprints from life cycle assessments of animal food products and their substitutes. *Food policy*, *37*(6), pp.760-770.

O'Neill, B.C., Oppenheimer, M., Warren, R., Hallegatte, S., Kopp, R.E., Pörtner, H.O., Scholes, R., Birkmann, J., Foden, W., Licker, R. and Mach, K.J., 2017a. IPCC reasons for concern regarding climate change risks. *Nature Climate Change*, *7*(1), pp.28-37.

O'Neill, B.C., Kriegler, E., Ebi, K.L., Kemp-Benedict, E., Riahi, K., Rothman, D.S., van Ruijven, B.J., van Vuuren, D.P., Birkmann, J., Kok, K. and Levy, M., 2017b. The roads ahead: Narratives for shared socioeconomic pathways describing world futures in the 21st century. *Global environmental change*, *42*, pp.169-180.

OECD/FAO (2021), OECD-FAO Agricultural Outlook 2021-2030, OECD Publishing, Paris, https://doi.org/10.1787/19428846-en.

Ortiz-Bobea, A., Ault, T.R., Carrillo, C.M., Chambers, R.G. and Lobell, D.B., 2021. Anthropogenic climate change has slowed global agricultural productivity growth. *Nature Climate Change*, *11*(4), pp.306-312.

Payne, W., 2013. New Research Approaches to improve drylands agriculture to deliver a more prosperous future. *CGIAR Dryland Systems Research Program*. Addis Ababa, Ethiopia

Pekel, J.F., Cottam, A., Gorelick, N. and Belward, A.S., 2016. High-resolution mapping of global surface water and its long-term changes. *Nature*, *540*(7633), pp.418-422.

Portmann F T, Siebert S and Döll P 2010 MIRCA2000—global monthly irrigated and rainfed crop areas around the year 2000: a new high-resolution data set for agricultural and hydrological modeling *Global Biogeochem. Cycles* **24** GB1001

Pretty, J.N., Williams, S. and Toulmin, C., 2012. *Sustainable intensification: increasing productivity in African food and agricultural systems*. Routledge.

Riahi, K., Van Vuuren, D.P., Kriegler, E., Edmonds, J., O'neill, B.C., Fujimori, S., Bauer, N., Calvin, K., Dellink, R., Fricko, O. and Lutz, W., 2017. The Shared Socioeconomic Pathways and their energy, land use, and greenhouse gas emissions implications: An overview. *Global environmental change*, *42*, pp.153-168.

Ricciardi, V., Ramankutty, N., Mehrabi, Z., Jarvis, L. and Chookolingo, B., 2018. How much of the world's food do smallholders produce?. *Global food security*, *17*, pp.64-72.

Rosa, L., Rulli, M.C., Davis, K.F., Chiarelli, D.D., Passera, C. and D'Odorico, P., 2018. Closing the yield gap while ensuring water sustainability. *Environmental Research Letters*, *13*(10), p.104002

Rosa, L., Chiarelli, D.D., Tu, C., Rulli, M.C. and D'Odorico, P., 2019. Global unsustainable virtual water flows in agricultural trade. *Environmental Research Letters*, *14*(11), p.114001.

Rosa, L., Chiarelli, D.D., Sangiorgio, M., Beltran-Peña, A.A., Rulli, M.C., D'Odorico, P. and Fung, I., 2020a. Potential for sustainable irrigation expansion in a 3 C warmer climate. *Proceedings of the National Academy of Sciences*, *117*(47), pp.29526-29534.

Rosa, L., Chiarelli, D.D., Rulli, M.C., Dell'Angelo, J. and D'Odorico, P., 2020b. Global agricultural economic water scarcity. *Science Advances*, 6(18), p.eaaz6031.

Rosa, L., Sanchez, D.L. and Mazzotti, M., 2021a. Assessment of carbon dioxide removal potential via BECCS in a carbon-neutral Europe. *Energy & Environmental Science*, *14*(5), pp.3086-3097.

Rosa, L., Rulli, M.C., Ali, S., Chiarelli, D.D., Dell'Angelo, J., Mueller, N.D., Scheidel, A., Siciliano, G. and D'Odorico, P., 2021b. Energy implications of the 21st century agrarian transition. *Nature Communications*, *12*(1), pp.1-9.

Rosa L. Adapting agriculture to climate change via sustainable irrigation: Biophysical potentials and feedbacks. *Environmental Research Letters*. 2022. **17** 063008. https://doi.org/10.1088/1748-9326/ac7408

Roser, M. and Ritchie, H., 2013. Food supply. *Our World in Data*.

Ross, A. and Hasnain, S., 2018. Factors affecting the cost of managed aquifer recharge (MAR) schemes. *Sustainable Water Resources Management*, *4*(2), pp.179-190.

Safriel, U, Adeel, Z, Niemeijer, D, Puigdefabregas, J, White, R, Lal, R, Winslow, M, Ziedler, J, Prince, S, Archer, E, King, C, Shapiro, B, Wessels, K, Nielsen, TT, Portnov, B, Reshef, I, Thornell,

J, Lachman, E & McNab, D 2005, Dryland systems. in R Hassan, R Scholes & N Ash (eds), Ecosystems and Human Well-being: Current State and Trends.: Findings of the Condition and Trends Working Group. vol. 1, Island Press, pp. 623-662. http://www.millenniumassessment.org/documents/document.291.aspx.pdf

Sanchez, P.A., 2002. Soil fertility and hunger in Africa. *Science*, *295*(5562), pp.2019-2020.

Sarukhán, J., Whyte, A., Hassan, R., Scholes, R., Ash, N., Carpenter, S.T., Pingali, P.L., Bennett, E.M., Zurek, M.B., Chopra, K. and Leemans, R., 2005. Millenium ecosystem assessment: Ecosystems and human well-being.

Scudder, T.T., 2012. *The future of large dams: Dealing with social, environmental, institutional and political costs*. Routledge.

Seekell, D., Carr, J., Dell'Angelo, J., D'Odorico, P., Fader, M., Gephart, J., Kummu, M., Magliocca, N., Porkka, M., Puma, M. and Ratajczak, Z., 2017. Resilience in the global food system. *Environmental Research Letters*, *12*(2), p.025010.

Sloat, L.L., Davis, S.J., Gerber, J.S., Moore, F.C., Ray, D.K., West, P.C. and Mueller, N.D., 2020. Climate adaptation by crop migration. *Nature communications*, *11*(1), pp.1-9.

Sprenger, C., Hartog, N., Hernández, M., Vilanova, E., Grützmacher, G., Scheibler, F. and Hannappel, S., 2017. Inventory of managed aquifer recharge sites in Europe: historical development, current situation and perspectives. *Hydrogeology Journal*, *25*(6), pp.1909-1922.

Tatlhego, M., and P. D'Odorico, "Are African irrigation dam projects for large-scale agribusiness or small-scale farmers?", *Environmental. Research Communications, in press. https://doi.org/10.1088/2515-7620/ac2263*

Taylor, K.E., Stouffer, R.J. and Meehl, G.A., 2012. An overview of CMIP5 and the experiment design. *Bulletin of the American meteorological Society*, *93*(4), pp.485-498.

Terlouw, T., Bauer, C., Rosa, L. and Mazzotti, M., 2021. Life cycle assessment of carbon dioxide removal technologies: A critical review. *Energy & Environmental Science*, *14*(4), pp.1701-1721.

Tilman, D., Balzer, C., Hill, J., & Befort, B. L. (2011). Global food demand and the sustainable intensification of agriculture. *Proceedings of the National Academy of Sciences of the United States of America*, **108**(50), 20,260–20,264. https://doi.org/10.1073/pnas.1116437108

Tilman, D. and Clark, M., 2015. Food, agriculture & the environment: Can we feed the world & save the earth?. *Daedalus*, *144*(4), pp.8-23.

U.N. DESA, 2016. Transforming our world: The 2030 agenda for sustainable development.

UNFCCC, 2015:Adoption of the Paris Agreement FCCC/CP/2015/L.9/Rev. 1 http://unfccc.int/resource/docs/2015/cop21/eng/l09r01.pdf

UNFCCC, 2021: Glasgow Climate Pact FCCC/PA/CMA/2021/L.16 https://unfccc.int/sites/default/files/resource/cma2021_L16_adv.pdf United Nations *1998 United Nations Standard Country Code, Series M: Miscellaneous Statistical Papers, No. 49*, New York: United Nations. https://unstats.un.org/unsd/methodology/m49/

United Nations 2019 *World population prospects 2019* https://population.un.org/wpp/

United Nations (2021). The Sustainable Development Goals Report 2021. New York.

United Nations Environment Programme (2020). *Emissions Gap Report 2020*. Nairobi.

United Nations Environment Programme (UNEP) (2021a). Food Waste Index Report 2021. Nairobi.

United Nations Environment Programme (2021b). Emissions Gap Report 2021: The Heat Is On – A World of Climate Promises Not Yet Delivered – Executive Summary. Nairobi

Van der Zaag, P. and Gupta, J., 2008. Scale issues in the governance of water storage projects. *Water Resources Research*, *44*(10).

Van Ittersum, M.K., Cassman, K.G., Grassini, P., Wolf, J., Tittonell, P. and Hochman, Z., 2013. Yield gap analysis with local to global relevance—a review. *Field Crops Research*, *143*, pp.4-17.

Van Ittersum, M.K., Van Bussel, L.G., Wolf, J., Grassini, P., Van Wart, J., Guilpart, N., Claessens, L., de Groot, H., Wiebe, K., Mason-D'Croz, D. and Yang, H., 2016. Can sub-Saharan Africa feed itself?. *Proceedings of the National Academy of Sciences*, *113*(52), pp.14964-14969.

van Maanen, N., Andrijevic, M., Lejeune, Q., Rosa, L., Lissner, T. and Schleussner, C.F., 2022. Accounting for socioeconomic constraints in sustainable irrigation expansion assessments. *Environmental Research Letters*.

Warszawski, L., Frieler, K., Huber, V., Piontek, F., Serdeczny, O. and Schewe, J., 2014. The inter-sectoral impact model intercomparison project (ISI–MIP): project framework. *Proceedings of the National Academy of Sciences*, *111*(9), pp.3228-3232.

Williams, D.R., Clark, M., Buchanan, G.M., Ficetola, G.F., Rondinini, C. and Tilman, D., 2021. Proactive conservation to prevent habitat losses to agricultural expansion. *Nature sustainability*, *4*(4), pp.314-322.

World Bank. "Agriculture, forestry, and fishing, value added (% of GDP)." *World Development Indicators.* The World Bank Group, 2021, data.worldbank.org/indicator/NV.AGR.TOTL.ZS. Accessed 13 Oct. 2021.

World Meteorological Organization (WMO), 2020. *State of the Climate in Africa 2019*. WMO-No. 1253

You, L., Ringler, C., Nelson, G., Wood-Sichra, U., Robertson, R., Wood, S., Guo, Z., Zhu, T. and Sun, Y., 2010. *What is the irrigation potential for Africa?* (No. 993). International Food Policy Research Institute (IFPRI).

2.8 Supplementary Tables

Sustainable Development Goal Targets	Corresponding SDG Scenario Assumption
SDG Goal 2 - Zero Hunger ***2.1*** End hunger and ensure access by all people to safe, nutritious, and sufficient food all year round. ***2.2*** End all forms of malnutrition. ***2.4*** Ensure sustainable food production systems and implement resilient agricultural practices.	***Well-Being Diet*** To ensure zero hunger and zero malnutrition, every person in a country is assigned a well-being diet, where everyone consumes a minimum base diet of 2,327 kcal a day. ***Sustainable Irrigation Expansion*** Only sustainable agricultural production and adaptation measures (i.e. water storage strategies) considered in this study.
SDG Goal 5 - Gender Equality ***5.6*** Ensure universal access to sexual and reproductive health and reproductive rights.	***Low Population Variant*** Given progress is made toward increasing access to sexual and reproductive health and rights in African countries we assume a low population variant by 2075.
SDG Goal 6 - Clean Water and Sanitation ***6.4*** Substantially increase water-use efficiency across all sectors and ensure sustainable withdrawals and supply of freshwater to address water scarcity and substantially reduce the number of people suffering from water scarcity. ***6.6*** Protect and restore water-related ecosystems, including mountains, forests, wetlands, rivers, aquifers, and lakes.	***Sustainable Crop Production*** Only current and potential crop production in areas where blue water availability exceeds blue water consumption and there is enough water to maintain environmental flows are considered. Crop production from current unsustainable irrigation is not considered. ***Environmental Flow Requirements*** 60% environmental flow requirements preserved to protect freshwater ecosystems and prevent biodiversity loss.
SDG Goal 12 - Responsible Consumption and Production ***12.3*** Halve per capita global food waste at the retail and consumer levels and reduce food losses along production and supply chains, including post-harvest losses.	***Food Loss and Waste*** Food loss 25% reduction and food waste 50% reduction compared to current levels based on Food Loss Index of the UN Food and Agriculture Organization and Food Waste Index of the UN Environment Program.
SDG Goal 13 - Climate Action ***13.1*** Strengthen resilience and adaptive capacity to climate-related hazards and natural disasters in all countries. ***13.B*** Promote mechanisms for raising capacity for effective climate change-related planning and management in least developed countries.	***Water Storage*** As a climate adaptation measure, large water storage techniques are developed and implemented to support annual water storage which can be used in dry periods.
SDG Goal 15 – Life on Land *15.1* Ensure the conservation, restoration and sustainable use of terrestrial and inland freshwater ecosystems and their services. *15.5* Take urgent and significant action to reduce the degradation of natural habitats, halt the loss of biodiversity and protect and prevent the extinction of threatened species.	***Environmental Flow Requirements*** 60% environmental flow requirements preserved to protect freshwater ecosystems and prevent biodiversity loss. ***Sustainable Irrigation Expansion*** Only sustainable agricultural production and adaptation measures (i.e. water storage strategies) considered in this study.

Table S1. Sustainable Development Goal targets and corresponding assumption for the SDG scenario composed in this study.

Country	Region	North or Sub-Saharan Africa
Algeria	Northern Africa	North Africa
Angola	Central Africa	Sub-Saharan Africa
Benin	Western Africa	Sub-Saharan Africa
Botswana	Southern Africa	Sub-Saharan Africa
Burkina Faso	Western Africa	Sub-Saharan Africa
Burundi	Eastern Africa	Sub-Saharan Africa
Cameroon	Central Africa	Sub-Saharan Africa
Central African Republic	Central Africa	Sub-Saharan Africa
Chad	Central Africa	Sub-Saharan Africa
Comoros	Eastern Africa	Sub-Saharan Africa
Côte d'Ivoire	Western Africa	Sub-Saharan Africa
Democratic Republic of the Congo	Central Africa	Sub-Saharan Africa
Egypt	Northern Africa	North Africa
Equatorial Guinea	Central Africa	Sub-Saharan Africa
Eritrea	Eastern Africa	Sub-Saharan Africa
Ethiopia	Eastern Africa	Sub-Saharan Africa
Gabon	Central Africa	Sub-Saharan Africa
Gambia	Western Africa	Sub-Saharan Africa
Ghana	Western Africa	Sub-Saharan Africa
Guinea	Western Africa	Sub-Saharan Africa
Guinea-Bissau	Western Africa	Sub-Saharan Africa
Kenya	Eastern Africa	Sub-Saharan Africa
Lesotho	Southern Africa	Sub-Saharan Africa
Liberia	Western Africa	Sub-Saharan Africa
Libya	Northern Africa	North Africa
Madagascar	Eastern Africa	Sub-Saharan Africa
Malawi	Eastern Africa	Sub-Saharan Africa
Mali	Western Africa	Sub-Saharan Africa
Mauritania	Western Africa	Sub-Saharan Africa
Morocco	Northern Africa	North Africa
Mozambique	Eastern Africa	Sub-Saharan Africa
Namibia	Southern Africa	Sub-Saharan Africa
Niger	Western Africa	Sub-Saharan Africa
Nigeria	Western Africa	Sub-Saharan Africa
Republic of Congo	Central Africa	Sub-Saharan Africa
Rwanda	Eastern Africa	Sub-Saharan Africa
Senegal	Western Africa	Sub-Saharan Africa
Sierra Leone	Western Africa	Sub-Saharan Africa
Somalia	Eastern Africa	Sub-Saharan Africa
South Africa	Southern Africa	Sub-Saharan Africa
Sudan	Eastern Africa	Sub-Saharan Africa
South Sudan	Eastern Africa	Sub-Saharan Africa

Swaziland	Southern Africa	Sub-Saharan Africa
Tanzania	Eastern Africa	Sub-Saharan Africa
Togo	Western Africa	Sub-Saharan Africa
Tunisia	Northern Africa	North Africa
Uganda	Eastern Africa	Sub-Saharan Africa
Zambia	Eastern Africa	Sub-Saharan Africa
Zimbabwe	Eastern Africa	Sub-Saharan Africa

Table S2. Regional breakdown of countries for this study.

A) Scenario: Current Climate, 60% Environmental Flow Requirements, Monthly Water Storage					
Region	No Food Loss or Waste	Current Food Loss and Waste	25% Reduction of Both Food Loss and Waste	Food Loss 25% Reduction, Food Waste 50% Reduction	Both Food Loss and Waste
Central Africa	6.73557E+13	4.64754E+13	5.16955E+13	5.45581E+13	5.69156E+13
Eastern Africa	1.19891E+14	8.27247E+13	9.20162E+13	9.71116E+13	1.01308E+14
Northern Africa	5.45952E+13	3.94177E+13	4.32121E+13	4.55324E+13	4.70064E+13
Southern Africa	4.1703E+13	2.87751E+13	3.20071E+13	3.37794E+13	3.5239E+13
Western Africa	2.66274E+14	1.83729E+14	2.04365E+14	2.15682E+14	2.25001E+14
B) Scenario: Current Climate, 60% Environmental Flow Requirements, Annual Water Storage					
Region	No Food Loss or Waste	Current Food Loss and Waste	25% Reduction of Both Food Loss and Waste	Food Loss 25% Reduction, Food Waste 50% Reduction	50% Reduction of Both Food Loss and
Central Africa	9.30918E+13	6.42334E+13	7.1448E+13	7.54044E+13	7.86626E+13
Eastern Africa	1.72863E+14	1.19276E+14	1.32673E+14	1.40019E+14	1.46069E+14
Northern Africa	5.12948E+13	3.70348E+13	4.05998E+13	4.27799E+13	4.41648E+13
Southern Africa	5.00724E+13	3.455E+13	3.84306E+13	4.05586E+13	4.23112E+13
Western Africa	3.2294E+14	2.22829E+14	2.47856E+14	2.61581E+14	2.72884E+14
C) Scenario: 3C, 60% Environmental Flow Requirements, Monthly Water Storage					
Region	No Food Loss or Waste	Current Food Loss and Waste	25% Reduction of Both Food Loss and Waste	Food Loss 25% Reduction, Food Waste 50% Reduction	Both Food Loss and Waste
Central Africa	5.31388E+13	3.66658E+13	4.0784E+13	4.30424E+13	4.49023E+13
Eastern Africa	9.58847E+13	6.61604E+13	7.35915E+13	7.76666E+13	8.10226E+13
Northern Africa	3.71132E+13	2.67957E+13	2.93751E+13	3.09524E+13	3.19545E+13
Southern Africa	3.8631E+13	2.66554E+13	2.96493E+13	3.12911E+13	3.26432E+13
Western Africa	1.54064E+14	1.06304E+14	1.18244E+14	1.24792E+14	1.30184E+14
D) Scenario: 3C, 60% Environmental Flow Requirements, Annual Water Storage					
Region	No Food Loss or Waste	Current Food Loss and Waste	25% Reduction of Both Food Loss and Waste	Food Loss 25% Reduction, Food Waste 50% Reduction	50% Reduction of Both Food Loss and
Central Africa	9.81075E+13	6.76942E+13	7.52975E+13	7.94671E+13	8.29009E+13
Eastern Africa	1.84074E+14	1.27011E+14	1.41277E+14	1.491E+14	1.55542E+14
Northern Africa	4.43749E+13	3.20387E+13	3.51227E+13	3.70087E+13	3.82068E+13
Southern Africa	4.91375E+13	3.39049E+13	3.77131E+13	3.98014E+13	4.15212E+13
Western Africa	3.17299E+14	2.18936E+14	2.43527E+14	2.57012E+14	2.68118E+14
E) Scenario: 3C, 80% Environmental Flow Requirements, Monthly Water Storage					
Region	No Food Loss or Waste	Current Food Loss and Waste	25% Reduction of Both Food Loss and Waste	Food Loss 25% Reduction, Food Waste 50% Reduction	50% Reduction of Both Food Loss and
Central Africa	4.66465E+13	3.21861E+13	3.58012E+13	3.77837E+13	3.94163E+13
Eastern Africa	9.14253E+13	6.30834E+13	7.01689E+13	7.40545E+13	7.72543E+13
Northern Africa	3.7001E+13	2.67147E+13	2.92863E+13	3.08588E+13	3.18578E+13
Southern Africa	3.80861E+13	2.62794E+13	2.92311E+13	3.08497E+13	3.21827E+13
Western Africa	1.53845E+14	1.06153E+14	1.18076E+14	1.24614E+14	1.29999E+14
F) Scenario: 3C, 80% Environmental Flow Requirements, Annual Water Storage					
Region	No Food Loss or Waste	Current Food Loss and Waste	25% Reduction of Both Food Loss and Waste	Food Loss 25% Reduction, Food Waste 50% Reduction	50% Reduction of Both Food Loss and
Central Africa	9.66197E+13	6.66676E+13	7.41556E+13	7.82619E+13	8.16436E+13
Eastern Africa	1.62457E+14	1.12095E+14	1.24686E+14	1.3159E+14	1.37276E+14
Northern Africa	4.00075E+13	2.88854E+13	3.1666E+13	3.33663E+13	3.44465E+13
Southern Africa	4.5219E+13	3.12011E+13	3.47056E+13	3.66274E+13	3.821E+13
Western Africa	2.6328E+14	1.81663E+14	2.02068E+14	2.13257E+14	2.22472E+14

Table S3. Total food calories available for human consumption under diverse food loss and waste pathways

	Current Climate 60% Environmental Flows *(Year 2030, Medium Population)*		**3C Climate, 60% Environmental Flows** *(Year 2075, Low Population)*		**3C Climate, 80% Environmental Flows** *(Year 2075, Low Population)*	
Country	**Caloric Deficiency** *(in 10^{11} kcal)*	**Number of People Equivalent** *(in millions)*	**Food Deficiency** *(in 10^{11} kcal)*	**Number of People Equivalent** *(in millions)*	**Food Deficiency** *(in 10^{11} kcal)*	**Number of People Equivalent** *(in millions)*
Algeria	395.9	42.0	598.3	50.4	602.9	50.8
Angola	242.9	29.9	863.1	92.7	863.1	92.7
Benin	44.9	5.6	185.9	21.4	213.4	24.6
Botswana	21.8	2.7	29.5	3.1	29.6	3.1
Burkina Faso	146.0	17.9	433.9	45.6	439.4	46.2
Burundi	93.0	11.4	272.7	28.8	287.4	30.3
Cameroon	148.3	18.0	461.7	46.4	461.7	46.4
Central African Republic	23.1	2.8	55.4	5.8	55.7	5.8
Chad	133.1	16.3	352.5	36.9	353.5	37.0
Comoros	8.1	1.0	14.0	1.5	14.0	1.5
Congo	44.3	5.5	108.2	11.6	108.2	11.6
Côte d`Ivoire	96.1	11.7	432.8	43.8	482.3	48.9
Democratic Republic of the Congo	496.6	60.7	1,843.3	191.1	1,854.1	192.2
Egypt	694.7	87.3	1,095.6	129.0	1,095.7	129.0
Equatorial Guinea	12.8	1.6	26.4	2.9	26.4	2.9
Eritrea	25.8	3.1	56.0	5.8	57.2	5.9
Ethiopia	868.3	105.0	1,857.6	182.7	1,884.7	185.3
Gabon	14.8	1.8	30.0	3.2	30.0	3.2
Gambia	15.7	1.9	44.7	4.7	44.7	4.7
Ghana	78.8	10.0	239.5	29.9	265.3	33.2
Guinea	-6.7	-0.8	132.5	14.5	132.7	14.5
Guinea-Bissau	10.7	1.3	26.9	2.9	26.9	2.9
Kenya	385.1	46.9	719.0	73.1	736.8	75.0
Lesotho	8.1	1.0	3.7	0.4	3.9	0.4
Liberia	36.6	4.5	80.7	8.4	80.7	8.4
Libya	58.9	7.0	59.3	6.2	60.1	6.3
Madagascar	196.0	23.9	514.1	52.9	515.6	53.1
Malawi	83.2	10.6	226.0	28.9	244.6	31.2
Mali	152.6	18.6	462.8	46.9	469.1	47.6
Mauritania	44.9	5.5	101.3	10.6	101.6	10.6
Morocco	238.7	24.4	351.8	27.8	362.0	28.6
Mozambique	193.7	23.9	579.2	62.3	585.4	63.0
Namibia	21.3	2.6	35.8	3.5	35.8	3.5
Niger	213.0	25.8	909.2	90.5	911.8	90.8
Nigeria	248.9	30.9	2,519.5	282.0	2,822.2	315.9
Rwanda	84.2	10.4	184.1	19.8	206.3	22.1
Senegal	119.8	14.5	359.0	35.0	362.0	35.3
Sierra Leone	50.0	6.1	91.3	9.5	91.3	9.5
Somalia	162.0	19.9	433.4	45.3	433.7	45.4
South Africa	101.0	12.5	153.1	16.7	184.6	20.1
Sudan and South Sudan	306.0	33.9	866.7	79.0	884.7	80.6
Swaziland	0.8	0.1	3.5	0.4	3.5	0.4

Togo	24.9	3.1	109.9	11.9	124.1	13.4
Tunisia	84.1	8.9	94.4	8.0	97.2	8.2
Uganda	319.8	39.5	743.4	80.7	749.9	81.4
United Republic of Tanzania	381.5	46.3	1,424.4	142.5	1476.2	147.6
Zambia	150.1	18.2	439.3	43.8	439.3	43.8
Zimbabwe	41.3	5.1	95.1	10.1	102.2	10.8

Table S4. Food calorie deficiency and population equivalent with annual water storage, SDG food loss and waste (25%/50% reduction) and well-being diet for 3 scenarios.

2.9 Supplementary Figures

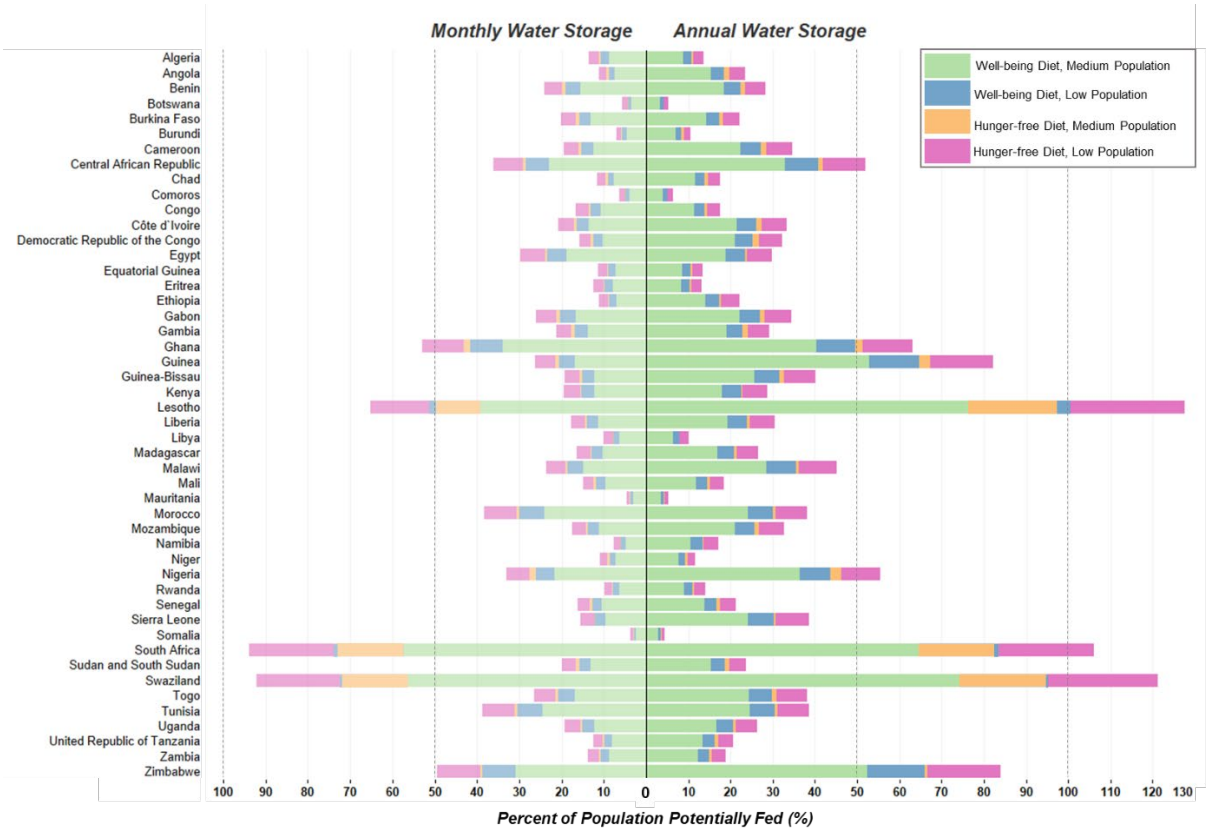

Figure S1. Percent of the population that can be fed based on diverse adaptation strategies in a 3°C warmer world while preserving 80% environmental flow requirements. Four diet and population combinations are differentiated by color. Lighter shades represent results under monthly water storage (left) and darker shades are representative of annual water storage (right). Dashed lines indicate the 50% and 100% thresholds.

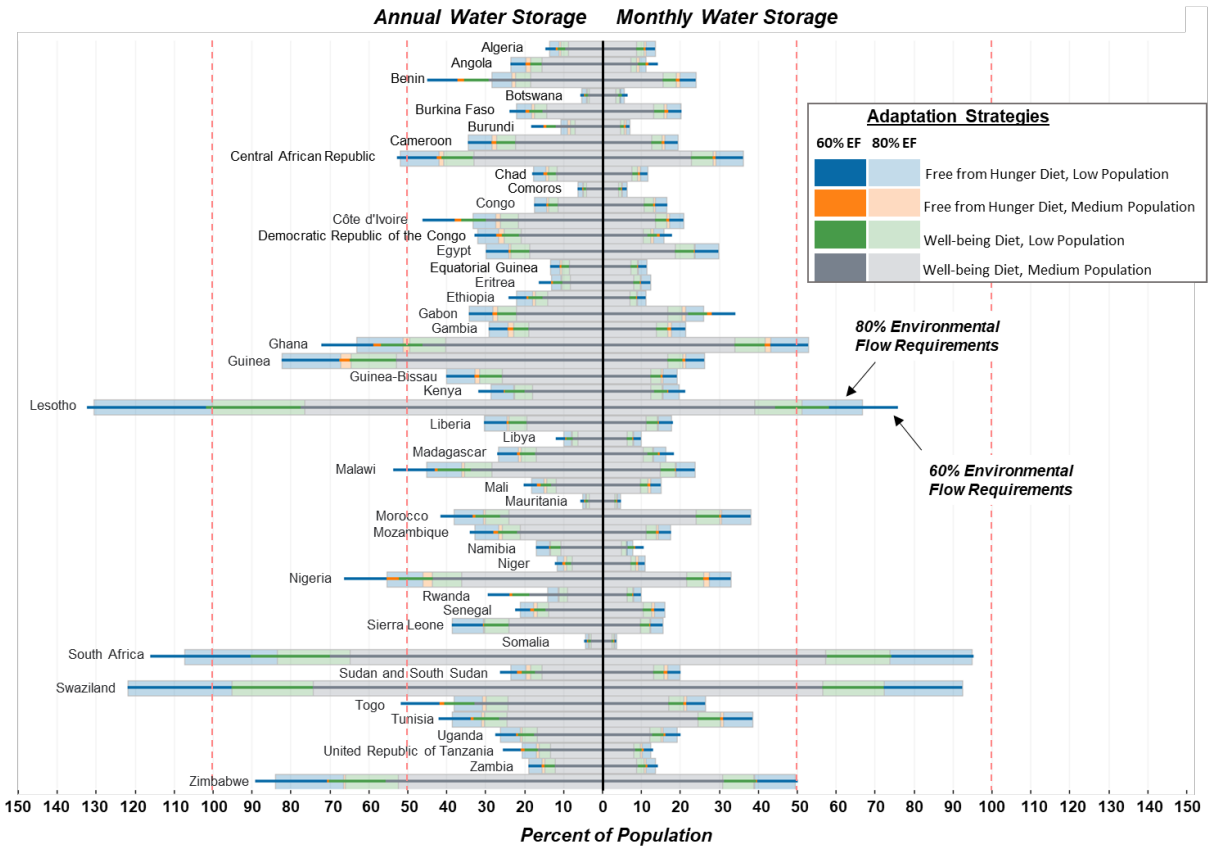

Figure S2. Sensitivity Analysis. Percent of population that can be fed in a 3°C warmer climate under specific adaptation strategies. The thin light bars represent scenarios with 80% EF, while the darker thin lines denote scenarios with 60% EF. As mentioned before, the more water allocated to the environment, less is available for agriculture resulting in less crop production. This explains why Benin, for example, can sustainably feed more people if it adopts annual water storage techniques and allocates 60% EF. For other countries, such as Guinea, the difference in the percentage of population that can be fed between 60% and 80% EF is almost negligible. In this case, the country may decide they can afford to allocate more water to environmental flows.

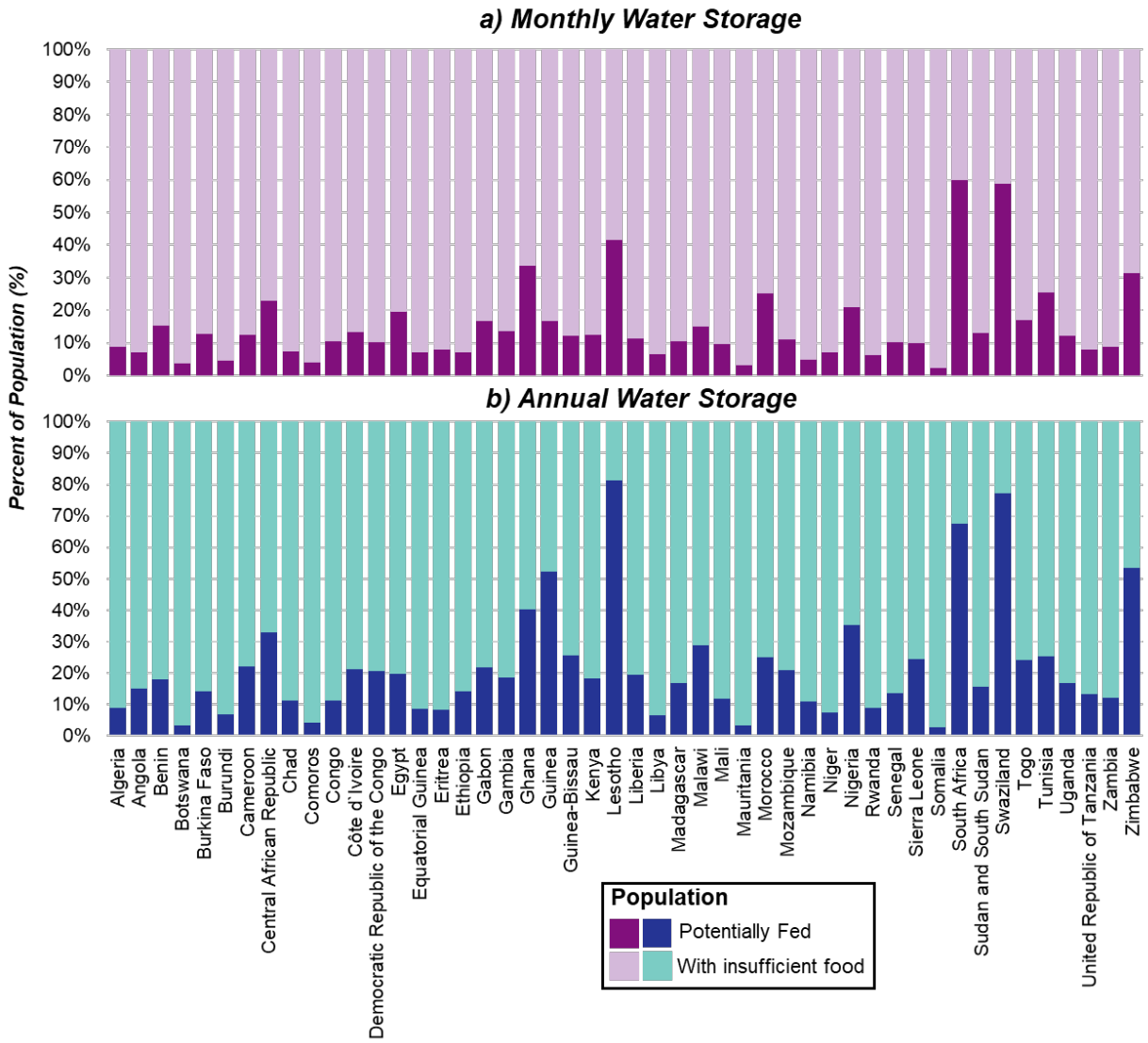

Figure S3. Percent of population that can or cannot be fed under SDG scenario in a 3°C warmer climate based on a) monthly or b) annual water storage strategy. Dark shaded bars represent percent of population fed through domestic crop production. Light shaded bars represent percent not fed, but more specifically, the percent of population that still needs to be fed through imports or other means to achieve zero hunger. This figure shows the results for 80% EF preserved.

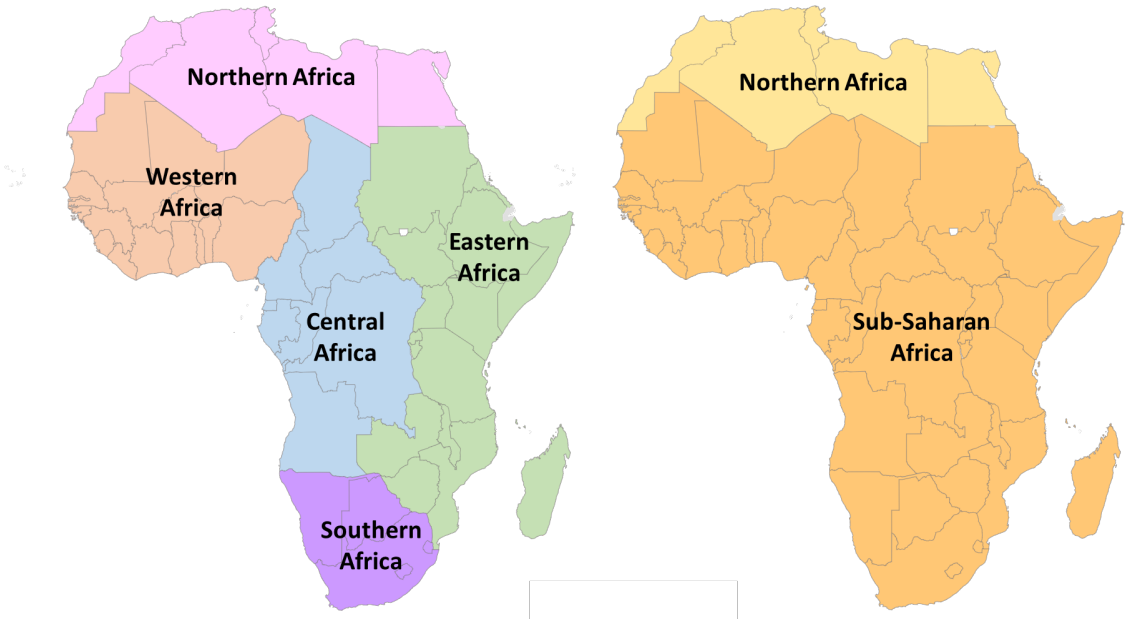

Figure S4. Regional breakdown of African counties used for this study.

Methodology Framework

1) Projected Potential Sustainable Crop Production and Availability ($kcal * year^{-1}$) for country *c*

Total projected potential sustainable crop production (kcal):

$$P_{c,s} = R_{2000} + (I_{T,2000} - I_{U,2000}) + (I_{P,s} \times 0.8)$$

Available sustainable production (kcal) for food and feed from crop after accounting for food loss and waste:

$$P_{AVAILABLE,c,s,h} = P_{c,s} \times (1 - FL_{\%} - FW_{\%})$$

$$FL_{\%} = FL_{current} - (FL_{current} \times \%_{reduction})$$
$$FW_{\%} = FW_{current} - (FW_{current} \times \%_{reduction})$$

Parameters *(s)*:
- *Water storage strategy:* annual or monthly
- *Climate:* baseline or 3°C
- *Environmental flows preserved:* 60% or 80%

Parameters *(h)*:
- *Food loss / waste reduction strategy:* none, 25% or 50%

2) Projected Caloric Demand ($kcal * cap^{-1} * year^{-1}$) for country *c* year *t*

Per capita daily (direct, *v*, and indirect, *f*,) crop caloric (kcal) demand – i.e., food + feed crops:

$$D_{c,t,x} = (v_{c,t,x} + f_{c,t,x}) \times 365$$

$$v_{c,t,x} = d_x \times (1 - A_{c,t}) \qquad f_{c,t,x} = [(d_x \times A_{c,t}) \times q_c \times r_{c,t}]$$

$$r_{c,t,x} = \frac{((d_x \times A_{c,t}) - (d_x \times A_{c,initial})) \times (1 - r_{c,initial})}{(d_x \times A_{c,t})}$$

Parameters *(x)*:
- *Diet type allocated:* free from hunger or well-being diet (1,829 or 2,327 kcal/day)

3) Food Sufficiency

Food Sufficiency: the number of people in a country that CAN be fed with sustainable domestic production under parameters considered)

$$Y_{c,t,s,h,x} = \frac{P_{AVAILABLE,c,s,h}}{D_{c,t,x}} = \frac{Production\ (kcal * year^{-1})}{Demand\ (kcal * cap^{-1} * year^{-1})}$$

4) Food Insufficiency

Food Insufficiency: the number of people in a country that CANNOT be fed with sustainable domestic production under parameters considered)

$$N_{c,t,s,h,x,p} = Population_{c,t,p} - Y_{c,t,s,h,x}$$

Parameters *(p)*:
- Population growth trajectory: low or medium variant

5) National Food Deficit

Food Deficit (kcal) of a country – the amount of food (expressed in kcal) demand that cannot be met by the domestic food production and will need to come from external sources or even agricultural expansion.

$$Z_{c,t,s,h,x,p} = N_{c,t,s,h,x,p} \times D_{c,t,x}$$

Parameters accounted for: *(c) = country; (t) = year; (s) = production adaptation scenario; (h) =food loss and waste reduction strategy; (x) = dietary pathway; (p) = population trajectory*

Figure S5a. Methodology framework.

Variables Defined

Parameters

NOTE: The following sub-variables represent the parameters that a variable in the above model is dependent on. As mentioned in the manuscript there are different potential scenarios per parameter as described below. The model framework above is meant to give a general representation of the methodology undertaken. These equations were assessed for every possible parameter combination (figure 1) and the results presented both in the manuscript and supplementary materials.

- c = country
- t = year
- s = production adaptation scenario combinations of climate (baseline or 3°C warmer climate), water maintained for environmental flow requirements (60% or 80%), and water storage strategies (monthly or annual).
- h = Food loss / waste reduction strategy: no reduction, 25% or 50% reduction from current levels
- x = Diet type allocated: free from hunger or well-being diet (1,829 or 2,327 kcal/day)
- p = Population growth trajectory: low or medium variant

Caloric Production and Availability

- $P_{c,s}$ = total projected potential sustainable crop production (kcal) per country c under production adaptation scenario s.
- $P_{AVAILABLE,c,s,h}$ = crop production (kcal) available per country for human consumption after accounting for food loss and waste.
- R_{2000} = rainfed caloric (kcal) production in year 2000 (from Rosa et al., 2020a).
- $\left(I_{T,2000} - I_{U,2000}\right)$ = sustainable irrigated caloric (kcal) production in year 2000 calculated as the difference between total and unsustainable production (Data from Rosa et al., 2020a).
- $(I_{P,s} \times 0.8)$ = Additional caloric production (kcal) potential under sustainable irrigation expansion for scenario s at 80% yield gap closure with $I_{P,z}$ being equal to zero in areas unsuitable to sustainable irrigation, and equal to the production gap calculated as the sum of yield gaps times cultivated areas across all crops. We describe the methodology used to determine the potential of sustainable irrigation expansion under different climate (data from CMIP5), environmental flows, and water storage strategies ($I_{P,z}$) in the methods section but refer to Rosa et al., 2020a for additional details.
- $FL_{\%}$ and $FW_{\%}$ = Percentage of food lost or wasted under reduction strategies (no reduction, 25% or 50% reduction from current levels) (we call this parameter h). The current food loss and food waste percentages were derived from the Food Loss Index (FAO 2019b) and Food Waste index (UNEP 2021a).

Caloric Demand

- $D_{c,t,x}$ = The per capita daily (direct and indirect) crop caloric (kcal) demand – i.e., food + feed crops – per country c in year t for diet type x. Consumption patterns may differ over time so we calculate it for each year.
- $v_{c,t,x}$ = The per capita daily direct crop caloric (kcal) demand – i.e., plant-based food consumption – per country c in year t for diet type x.
- $f_{c,t,x}$ = The per capita daily indirect crop caloric (kcal) demand – i.e., feed crops – per country c in year t for diet type x.
- d_x = the daily calorie uptake which is equal to 1,829 or 2,327 kcal/day, depending on the dietary pathway *(x)*– free from hunger or well-being, respectively (D'Odorico et al., 2019).
- $A_{c,t}$ = fraction of animal-based products consumed in a diet calculated as the ratio between the food demand for livestock products (including eggs and dairy) and the total demand for both crops and livestock (in kcal/cap/day) for the Sub-Saharan and North African regions – represented by the Sub-Saharan Africa, SSA, and the Middle East and Africa, MAF regions taken from GLOBIOM model (Frank et al 2021).
- $\left(1 - A_{c,t}\right)$ = the fraction of plant-based products consumed in a diet.
- $(d_x \times A_{c,t})$ = direct animal-based calories consumed per capita (kcal)
- q_c = plant to animal conversion factor (taken from Davis et al., 2014)
- $r_{c,t}$ = the fraction of total animal calories from feed-fed production in country c, year t. $r_{c,initial}$ is taken from Davis et al., (2014).

Food Sufficiency and Deficiency Estimates

- $Y_{c,t,s,h,x}$ = Number of people that CAN be fed in a given country *(c)* and year *(t)* with the projected food availability under production adaptation scenario (*s*) and dietary pathway *(x)*
- $N_{c,t,s,h,x,p}$ = Number of people that CANNOT be fed in a given country *(c)* and year *(t)* with the projected food availability under production adaptation scenario (*s*) and dietary pathway *(x)*
- $Population_{c,t,p}$ = Projected population in country *(c)*, year *(t)* which could be either the low or high population variants (p) of the 2019 United Nations Population Prospects (United Nations 2019).
- $Z_{c,t,s,x}$ = Food deficit (kcal) of a country – the amount of food (expressed in kcal) demand that cannot be met by the domestic food production (in a given country *(c)* and year *(t)* with the projected food availability under production adaptation scenario (*s*) and dietary pathway *(x))* and will need to come from external sources or even agricultural expansion.

Figure S5b. Methodology framework description of variables.

CHAPTER 3

Assessing the Impacts of Climate Change on Water Resources using Earth System Models to Project Hydroclimate Variability and Snowpack Changes in the California Sierra Nevada

Abstract:

The Sierra Nevada snowpack, responsible for 30% of California's water supply and providing irrigation water to 300,000 hectares of farmland, is under threat due to climate change. Projections indicate a decline in snowpack depths and an earlier onset of snowmelt, trends that are projected to persist and possibly accelerate into the mid-to-end of the 21st century. California's Sierra Nevada region is particularly susceptible to snow loss due to anthropogenic climate change, which could significantly affect water availability for crop yields – aggravating food security at a time when demand is projected to increase. Although previous studies have assessed the impacts of droughts, namely through changes in precipitation and evaporative demand, on agriculture separately, few have focused on directly linking the projected impacts of declining snowmelt on these interconnected systems. We develop a framework that combines variable resolution Earth System Models and crop-water models to assess water supply and demand vulnerability of California's water-food nexus to changing snow regimes in the Sierra Nevada under climate change.

3.1 Introduction

3.1.1 Sierra Nevada Snow and Climate

Mountains act as the world's water towers by capturing and storing freshwater as snow and ice during winter months, and subsequently releasing water as runoff during warmer seasons – supplying water to downstream areas (Immerzeel et al., 2020). Many studies suggest that under a changing climate, the fraction of precipitation falling as snow will decrease and the timing and spatiotemporal character of snowmelt will be altered. Rising temperatures intensify and warm atmospheric rivers, the dominant driver of precipitation in California, causing more precipitation to fall as rain at the expense of snow, thus raising the risk of rain on snow events (Maina et al., 2023; Ombadi et al., 2023), and shifting the snowline to higher elevations in mountainous regions (Davenport et al., 2020; Gonzales et al., 2019; Huang et al., 2020; Huang & Swain, 2022; Pörtner et al., 2022; Lynn et al., 2020; Payne et al., 2020; Siirila-Woodburn et al., 2021, Shulgina et al., 2023). These changes to the cryosphere associated with anthropogenic climate warming could have dire consequences for human populations and ecosystems reliant on highland freshwater stores if no mitigation and/or adaptation measures are implemented - notably for agricultural production.

The fraction of water used for irrigation supplied by snowmelt runoff will decrease in the 21st century (Qin et al., 2020). In the western United States, where nearly 75% of freshwater originates as mountain snowpack (Livneh & Badger, 2020), over 90% of monitoring sites show declines in snowpack depth and earlier melt timing (Mote et al., 2018). This is projected to continue into the mid-to-end of the 21st century and may even accelerate (Rhoades et al., 2018; Siirila-Woodburn et al., 2021, Cowherd et al., 2023). Under high-emission scenarios, snow water equivalent (SWE) – the amount of water stored in snowpacks – is expected to decline by ~45% by 2050 in the Sierra

Nevada (Siirila-Woodburn et al., 2021). According to Siirila-Woodburn et al., 2021, episodic (5 consecutive years) and persistent (10 consecutive years) low-to-no snow conditions are projected to occur in California in the late 2040s and 2050s respectively – making climate mitigation and adaptation a priority. Thus, an in-depth and comprehensive study on the extent to which food production may be impacted by climate change in areas where changes in rainfall cannot compensate for snowmelt loss is imperative.

3.1.2 California Agriculture

California's mountain ranges are important assets for its water supply. The Sierra Nevada is the primary source for California's State Water Project (SWP) and supplies 300,000 hectares of farmland with irrigation water (CDWR 2022). California's snow-dependent basins are actively threatened by anthropogenic climate change, which will reduce freshwater storage from snow (which typically supplies water during the dry season when downstream water demand is high) and in turn could significantly affect crop yields.

California is the largest agricultural producer in the United States and the country's largest agricultural exporter with an output valued at US $59.4 billion, one-third of which is derived from perennial crops (i.e., almonds, grapes, fruit trees) (Cooley et al., 2015; CDFA 2020). The state produces a third of the vegetables and two-thirds of the fruits consumed in the U.S. and exports approximately 32% of its agricultural production (Hong et al., 2020; CDFA 2021a). Furthermore, the agricultural sector supports 1.2 million jobs in the state of California (CFDA 2021a). Climate change is already causing disruptions for agricultural production. The drought that occurred in 2021 resulted in about 160,000 hectares of drought-idled cropland, further groundwater depletion, and economic losses of $1.7 billion and 14,600 jobs (Medellín-Azuara et al., 2022). Moreover, 30% of farmworker families in the state live below the poverty line and are disproportionately affected by economic shocks (USDL 2016).

Without adequate implementation of climate mitigation and adaptation measures, diminishing snowpack in the Sierra Nevada in response to climate change, will have serious implications for food security in California. The ensuing economic impacts could have dire consequences on the livelihoods of low-income communities of color who are the most vulnerable to climate change and economic shocks (Wehner et al., 2017).

3.1.3 Projecting Sierra Snowpack Loss with Earth System Models

Global climate models (GCMs) have been the primary tool to project future climate conditions. Yet, until recently, they have been limited in their utility in understanding the hydrologic cycle in mountainous regions because typical GCM spatial resolutions (~111 km) are far too coarse to explain complex mountainous land-atmosphere dynamics. This is compounded by the fact that state and regional water managers increasingly need more regionally specific data to make better informed decisions in a changing climate (Jagannathan et al., 2020). Hence, new approaches to regional climate modelling in mountain regions are crucial in projecting shifts in regional freshwater availability and the potential impacts to downstream food systems.

Although previous studies have assessed changes in snowpack or quantified the projected impacts of declining snowmelt on crop production, most of these studies are done globally with coarse resolution GCMs that highlight broad patterns of change (Huss et al., 2017; Mankin et al., 2015; Qin et al., 2020; Qin et al., 2022; Rauscher et al., 2008; Diffenbaugh et al., 2013). None have identified the interconnectedness of these systems and the role of downstream water storage in mitigating food production losses at a high spatiotemporal resolution – specifically in California.

Here, we aim to develop a framework to assess the vulnerability of the agricultural sector in a changing climate due to its reliance on snowmelt runoff at finer spatial resolutions. To provide more policy relevant insights, we isolate what is at stake for each warming level reached (i.e., +1.5°C, +2.0°C, and +3.0°C) throughout the 21st century. To provide more decision relevant information, we use the variable resolution Community Earth System Model (VR-CESM) and the regionally-refined-mesh Energy Exascale Earth System Model (RRM-E3SM) which provide high spatiotemporal estimates (14 km horizontal resolution, daily-to-hourly outputs) of historical and future projections of California's hydroclimate (Rhoades et al., 2018; Caldwell et al., 2019). These simulations allow us to quantify the impacts of climate change on water and food systems in California – accounting for changes in precipitation and snowpack trends in the Sierra Nevada. We then connect changes in headwater hydrology to water supply and demand tradeoffs in a possible future with more extreme, punctuated precipitation and low-to-no-snow conditions. Finally, we identify the risks posed by diminishing snowmelt runoff to irrigated crop production.

The objective of this study is to evaluate how climate change will affect the hydroclimate in the Sierra Nevada region and its consequences for water availability in California's Central Valley. The results of this research will provide California stakeholders and managers in the water, agricultural sector (e.g., California Department of Water Resources, California Department of Food and Agriculture, California Energy Commission, California Natural Resources Agency) with the high spatiotemporal resolution data and information necessary to develop a coordinated, integrated approach to building climate resilience as called for by the California Climate Adaptation Strategy (AB 1482).

3.2 Methods

3.2.1 Study Area

Our study area encompasses the Sacramento, San Joaquin, and Tulare watersheds spanning the western slopes of the Sierra Nevada and the Central Valley of California. The watershed boundaries are defined by the U.S. Geological Survey (USGS) Watershed Boundary Dataset hydrologic unit code level 6 (HUC 6) (U.S. Geological Survey, 2019). The HUC 6 watersheds were divided into mountain and valley regions based on a 90-meter digital elevation model resampled from the 30-meter resolution USGS National Elevation Dataset (Hanser 2008). The areas above the 1,000-meter elevation line are characterized as mountainous regions while areas below 1,000-m elevation are considered valley regions. Figure 1a shows the regional breakdown of the three HUC 6 watersheds. The Sierra Nevada is divided into the three basins to elucidate the distinct precipitation, snowpack, and runoff regimes in the northwest, central west, and southwest portions of the Sierra Nevada which are expected to face different timings and magnitudes of snow loss over the 21st century (Huning and AghaKouchak, 2018). We identified and categorized counties within our study area based on the USGS HUC 6 watersheds they belong to. Figure 1b showcases California counties in three HUC 6 watersheds for which we extracted irrigation water demand data from Ruess et al., 2022: Sacramento watershed (blue), San Joaquin watershed (orange), and Tulare watershed (green) (U.S. Census Bureau 2019).

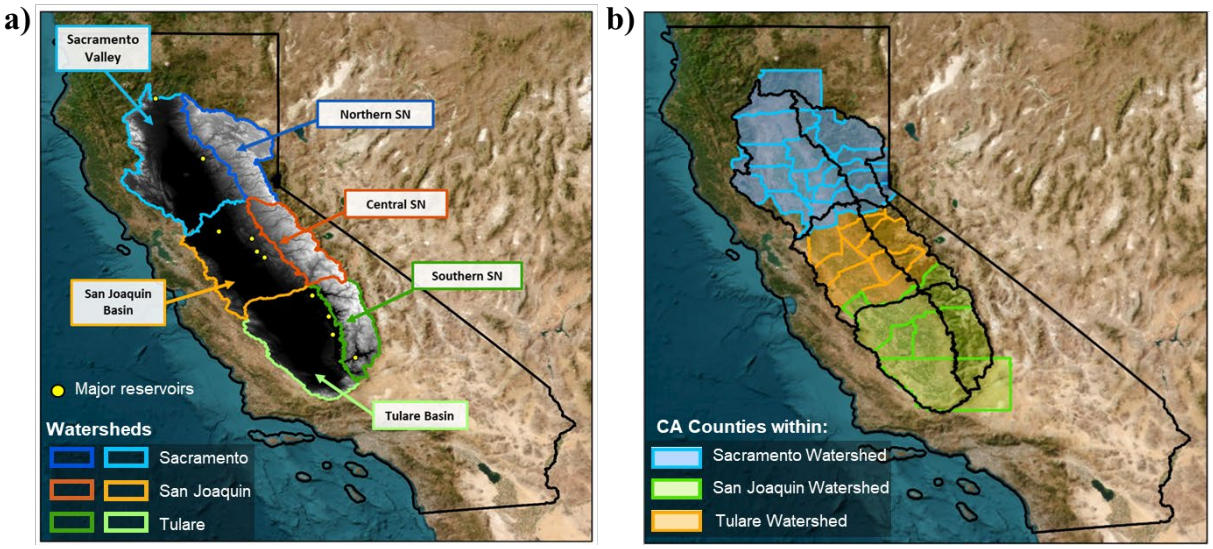

Figure 1. Study area. Figure 1 illustrates the regional breakdown of the USGS HUC6 watersheds into 6 distinct Sierra Nevada (SN) and Central Valley regions evaluated in this study as well as the locations of the 10 major dams in the state of California (https://water.usgs.gov/GIS/dsdl/reservoir_shp.zip). Figure 1b delineates the counties in California that fall within the Sacramento, San Joaquin, and Tulare watersheds used to assess agricultural production statistics using data from Ruess et al., 2022.

3.2.2 Model Description

The Community Earth System Model (CESM) is a global climate model developed at the National Center for Atmospheric Research (NCAR) that provides state-of-the-art computer simulations of the Earth's past, present, and future climate states. CESM consists of seven geophysical model components – atmosphere, sea-ice, land, river, ocean, land-ice, and ocean-wave (Danabasoglu et al., 2020). Here we use its variable-resolution grid capabilities (VR-CESM) for historical and future hydroclimate projections. Technical details of VR-CESM are presented in Xu et al., 2021. Analogous to VR-CESM, the United States Department of Energy's (DOE's) Energy Exascale Earth System Model version 2 (E3SMv2) has a unique capability for variable resolution modeling, Regionally Refined Mesh enabled E3SM (RRM-E3SM). We compare and contrast historical model outputs from RRM-E3SM and VR-CESM (Rhoades *et al* 2018; Caldwell et al., 2019) over California to contextualize hydroclimate variability due to model structural uncertainty (Lehner et al., 2020). Both VR-CESM and RRM-E3SM utilize the same grids with global horizontal resolutions of 111 km with a refinement patch of 14 km resolution over the contiguous U.S. Figure 2 highlights differences in representing California topography with conventional GCM horizontal resolutions (111 km), VR-CESM and RRM-E3SM (14 km) and observed (~90 m). Both E3SM and CESM simulations use prescribed sea-surface temperatures and sea ice extent following the protocols of the Atmosphere Model Intercomparison Project (AMIP; Gates et al., 1999; Bambach et al., 2022). Utilizing prescribed ocean conditions isolates atmosphere-land surface interactions, in contrast to simulations incorporating a fully coupled, prognostic ocean and sea-ice components (Rhoades et al., 2018).

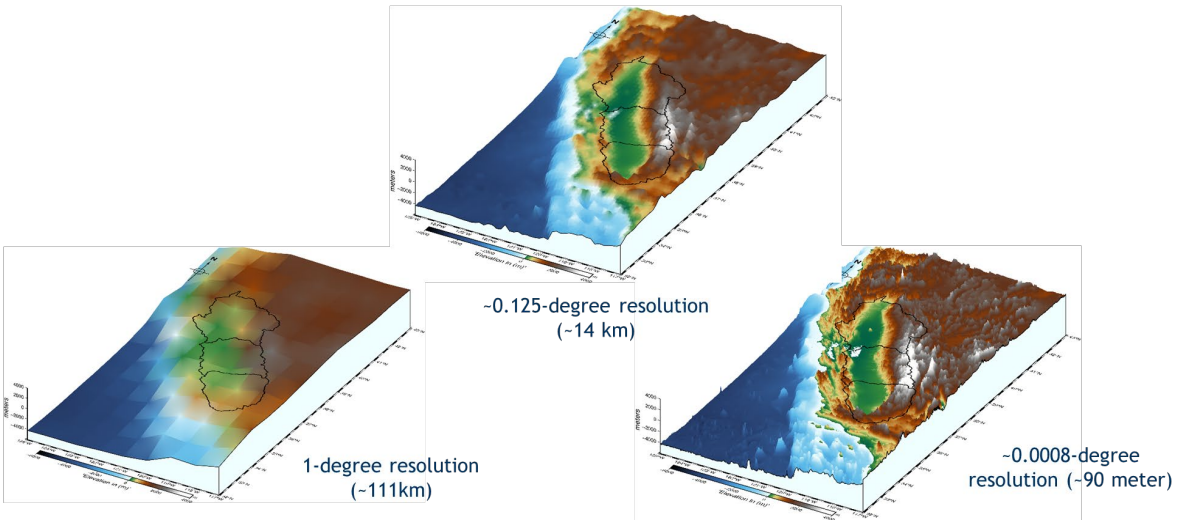

Figure 2. Model resolution. Differences in topographic representation across 111 km, 14 km, and 90 m horizontal resolutions over California. The study regions are outlined in black.

3.2.3 Climate Warming Assessment and Diagnostics

Annual mean global 2-m air temperature above the surface of the land, sea, and inland waters was derived from the Community Atmosphere Model (CAM) component of the Community Earth System Model 2 (CESM2) for years 1984 to 2100. CESM2 outputs were compared to those of the E3SM Atmosphere Model (EAM) for years 1985-2024. To evaluate the performance of the CAM and EAM simulations, we compared model outputs to the Fifth-generation of the European Centre for Medium-Range Weather Forecasts (ECMWF) atmospheric reanalysis, known as ERA5, from years 1940 to 2022 (Hersbach et al., 2023). For both CAM and EAM, 3-hourly and 6-hourly data (for ERA5, monthly averaged data) were averaged to the annual timescale then spatially averaged across the globe. Figure 3a depicts the annual 2-m global surface air temperature outputs of the CAM, EAM, and ERA5. EAM shows a slight cold-bias while CESM is slightly warmer than ERA5. Comparing the historical mean global temperatures for years 1984-2005, we find that EAM is 0.4℃ cooler than ERA5, and CAM is 0.3℃ warmer than the ERA5 observed global mean temperature of 14.2℃ (Table 1).

Global 2-m surface air temperature anomalies (T_{anom}) for each model/reanalysis were calculated by subtracting the historical (1984 -2005) global mean temperature (μ_{hist}) of the product by the temperature output for each year of data (Equations 1 and 2; Table 1).

(1) $$\mu_{hist} = \left(\frac{1}{22}\right) * \sum_{1984}^{2005} TSA$$

(2) $$T_{anom} = TSA_{yr} - \mu_{hist}$$

EAM, CAM, and ERA5 have similar rates of change (Figure 3b). In this study, the reference period is 1984-2005 due to missing years between 2006 and 2014 in CAM. For consistency this reference period was also utilized for EAM and ERA5. A common reference period used for comparing global climate analyses is 1951-1980. Table 1 indicates a temperature differential of 0.4℃ between the global temperature averages of ERA5 for the periods 1984-2005 and 1951-1980. Throughout

this study, any mention of a climate being 1.5°C, 2°C, or 3°C warmer pertains to CESM with the reference period of 1984-2005.

a) b)

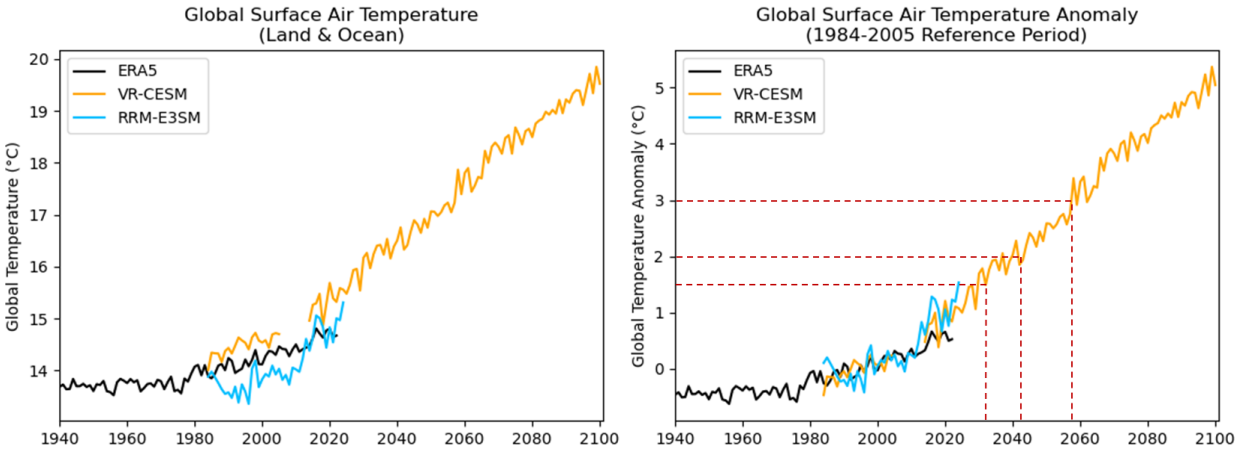

Figure 3. Global surface air temperature projections. a) annual 2-m global surface air temperatures of the VR-CESM (orange) and RRM-E3SM (blue) model projections compared with the ERA5 reanalysis dataset (black). b) annual 2-m global surface air temperature anomalies relative to a reference period (1985-2005). Dotted lines highlight logistic regression estimates of the warming levels and dates when they are reached.

Table 1. Historical global mean temperatures.

Reference Period	Global Mean Temperature		
	ERA5 (observed)	VR-CESM	RRM-E3SM
1984 - 2013	14.2 °C	n/a	13.8°C
1984 - 2005	14.2°C	14.5°C	13.8°C
1951 - 1980	13.8°C	n/a	n/a
Temperature Adjustment Factor for Reference Periods (based on observed data from ERA5)			
From 1984 - 2013 to 1951 - 1980 reference period			0.46°C
From 1984 - 2005 to 1951 - 1980 reference period			0.40°C

3.2.3.1 Logistic Regression

In this study, future hydroclimate projections were exclusively conducted using the variable-resolution community earth system model (VR-CESM) due to limited data availability for future years from RRM-E3SM at the time of analysis. Building upon the methodology by Rhoades et al. in 2022, we conducted a logistic regression statistical analysis to identify the year-of-emergence for each warming level. Logistic regression is a statistical analysis method that aims to establish a relationship between an explanatory variable (year) and the probability of the response variable

(surface air temperature anomaly) being 1. Using global 2-m surface air-temperature anomalies for each year from 1984 – 2100, we assessed whether the anomaly reached or exceeded the three warming thresholds evaluated in this study (1.5℃, 2℃, or 3℃). If the anomaly reached or surpassed the warming threshold, a value of 1 was assigned; otherwise, a value of 0 was assigned. Equation 3 outlines the conditions employed for each warming level. Due to the bounded nature of probabilities (from 0 to 1), logistic regression employs the logit function to model this relationship effectively (please refer to Rhoades et al. in 2022 for details).

$$T_{yr}^{1.5°C} = \begin{cases} 1 \text{ if } T_{anom} \geq 1.5℃ \\ 0 \text{ otherwise,} \end{cases}$$

(3)

$$T_{yr}^{2°C} = \begin{cases} 1 \text{ if } T_{anom} \geq 2℃ \\ 0 \text{ otherwise,} \end{cases}$$

$$T_{yr}^{3°C} = \begin{cases} 1 \text{ if } T_{anom} \geq 3℃ \\ 0 \text{ otherwise} \end{cases}$$

Figure 4 displays the logistic regression curves corresponding to the 1.5℃, 2℃, and 3℃ warming levels. We selected the first year for which the probability (P) of the global temperature reaching or surpassing each warming level (1.5℃, 2℃, or 3℃) was greater than or equal to 0.5. The 0.5 threshold represents a greater than random chance of occurrence. A 30-year interval centered around the first year in which $P \geq 0.5$ for each warming level was selected. These 30-year periods represent projected climate normal for 1.5℃, 2℃, or 3℃ climate change conditions.

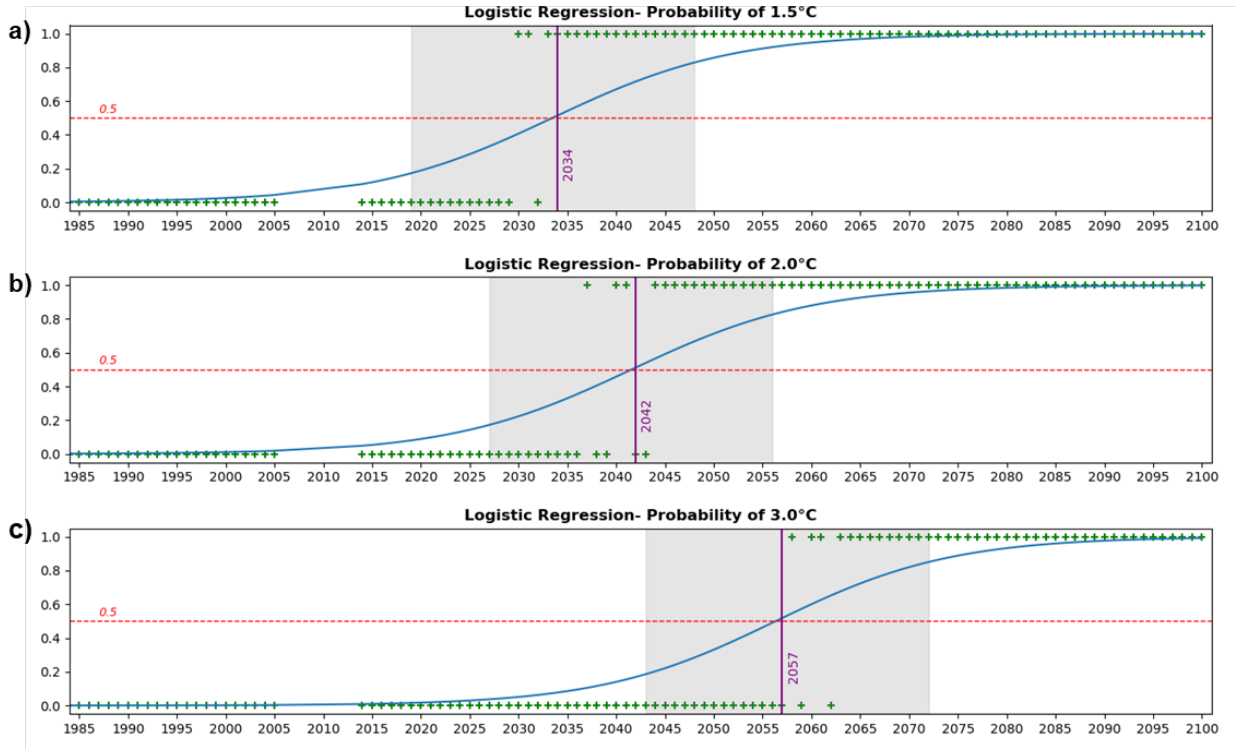

Figure 4. Logistic regression curves. Logistic regression curves for (a) 1.5°C, (b) 2°C, and (c) 3°C warming levels. The vertical purple line represents the year of P ≥ 0.5 exceedance for each warming level while the grey shaded area represents the 30-year interval around that year used for climatological analysis. Green crosses indicate whether each year in the dataset from 1985 to 2100 exceeds the warming level (yes = 1, no = 0).

Based on VR-CESM, the first years of P ≥ 0.5 for 1.5°C, 2°C, and 3°C are 2034, 2042, and 2057 respectively. The 30-year intervals representative of the climate normal under these warming levels are listed in Table 2. While the actual mean temperature anomalies (T_{anom}) for these time periods may not precisely align with the target warming levels, they serve as the most suitable representation based on the data.

Table 2. VR-CESM global warming levels. A description of the target warming levels accompanied by the corresponding 30-year intervals centered around the first year when exceeding those levels has a 50% probability. The table includes the average temperature change, both globally and within the study area, during the respective 30-year interval for each target warming level.

Target Warming Level	Probability (%)	First year with 50% probability of exceeding warming level	Interval	Interval Years	Global Mean Temperature Change (Interval Mean)	Regional Mean Temperature Change (Study Area)
1.5°C	50%	2034	30 years	2019 - 2048	*1.65°C*	*1.64°C*
2.0°C	50%	2042	30 years	2027 - 2056	*2.07°C*	*2.12°C*
3.0°C	50%	2057	30 years	2043 - 2072	*2.96°C*	*3.1°C*

3.2.3.2 Regional Climate Change

Annual mean 2-m surface air temperature for the 6 study regions encompassing the Sierra Nevada and Central Valley of California was derived using the VR-CESM Community Land Model (CLM) with 14-km resolution. As with the global mean temperature, VR-CESM CLM 6-hourly data was averaged to the annual timescale then spatially averaged across the six study regions. The annual data was then averaged for the corresponding 30-year intervals representative of the climate normal for the historical period, 1.5℃, 2℃, and 3℃ climate change. The regional mean temperature change across the entire study area, encompassing the Sierra Nevada and Central Valley, closely approximates the global mean temperature change corresponding to the target warming levels. For instance, Table 2 reveals a regional and global mean temperature change of approximately 1.64℃ and 1.65℃ respectively for the 1.5℃ target. Table 3 provides a breakdown of the regional variability of temperature anomalies across the six regions. Historically the mean temperature across the Sierra Nevada is 9.49℃ while the Central Valley is much warmer with an average temperature of 16.87℃. Given these historical means, the Sierras are projected to warm at a slightly faster rate (on average 0.4℃) than the Central Valley regions. The rate of warming increases significantly from the Northern Sacramento Valley to the Southern Tulare Basin. This could have more drastic impacts on water demand management in the southern regions.

Table 3. Breakdown of regional temperature change under global warming thresholds. Mean historical temperature and regional temperature change for six distinct regions in this study under 1.5℃, 2℃, and 3℃ global temperature scenarios. The table also includes the average regional temperature change for the entire Sierra Nevada and the Central Valley.

Regional Δ°C at Global Warming Thresholds for VR-CESM (Study Area Breakdown)				
Regions	**Historical Mean**	**Regional Δ°C @ Global 1.5°C**	**Regional Δ°C @ Global 2.0°C**	**Regional Δ°C @ Global 3.0°C**
Northern Sierra	9.6°C	2.2°C	2.7°C	3.8°C
Central Sierra	8.0°C	1.0°C	1.5°C	2.5°C
Southern Sierra	9.5°C	2.3°C	2.7°C	3.6°C
All Sierras Mean	***9.0°C***	***1.8°C***	***2.3°C***	***3.3°C***
Sacramento Valley	16.1°C	0.6°C	1.2°C	2.2°C
San Joaquin Basin	16.6°C	1.2°C	1.6°C	2.5°C
Tulare Basin	17.9°C	2.6°C	3.0°C	3.9°C
Central Valley Mean	***16.9°C***	***1.4°C***	***1.9°C***	***2.9°C***

Select variables from RRM-E3SM and VR-CESM model outputs were extracted and averaged from 3 or 6-hourly timesteps to daily means. These variables include 2-m surface air temperature, rainfall, snowfall, snow water equivalent, fraction of area covered by snow, snowmelt, total runoff, surface runoff, and evapotranspiration (*ET*) (sum of vegetation transpiration and evaporation from soil and canopy). The data used in this study was spatially averaged across the six shapefile regions of interest highlighted in Figure 1.

3.2.4 Snow water equivalent under climate change

To determine the climatological mean of April 1st SWE, we calculated the mean of the SWE values simulated on April 1st for each water year within the 30-year period for each warming level. This approach allowed us to estimate the average SWE magnitude expected on April 1st per warming scenario. To determine the average peak SWE for each warming level, we calculated the mean of SWE values on the days when the maximum peak SWE occurs for each water year throughout the corresponding 30-year period.

Additionally, we examined the difference in number of days between the day of peak SWE occurrence and April 1st, which we refer to as the 'April 1st delta.' This delta represents the number of days earlier than April 1st that peak SWE occurs. By analyzing the day of occurrence of peak SWE, we gain insights into the timing of peak snowpack accumulation and potential impact on water resources. To estimate the typical snow cover extent under different warming levels, the fraction of snow-covered area (F_{SCA}) on April 1st and the days of occurrence of peak SWE was assessed by averaging over the climatological periods to represent the corresponding average F_{SCA} expected on April 1st and the average timing of peak SWE. SWE volumes (VSWE) in km^3 were calculated following Patricola et al., 2020 based on shapefile area and fraction of snow-covered area.

Historical climatological SWE from RRM-E3SM and VR-CESM was compared to two observational datasets for the Sierra Nevada region for years 1985-2014: the Western United States UCLA Daily Snow Reanalysis, Version 1 (Margulis) which contains daily estimates of posterior (SWE), F_{SCA} and snow depth at ~500 m resolution (Fang et al., 2022; Margulis et al., 2016); and the ground measurement-based University of Arizona (UofASWE) gridded snow product over the contiguous US (CONUS) which provides SWE and snow depth at a horizontal resolution of 4 km (Zeng et al., 2018; Brunke et al., 2021). Figure 5a illustrates that RRM-E3SM underestimates peak SWE by approximately 40 mm and shows an earlier reduction compared to both the UCLA and UofASWE snow products. Despite this discrepancy, in all three datasets, maximum SWE occurs in March. VR-CESM more accurately captures the magnitude of SWE as observed in the two observational datasets but exhibits a more pronounced decline one month earlier (Figure 5b). As shown in Figure 5, historical VR-CESM SWE estimates more closely resemble observed conditions in the Sierra Nevada region and is thus employed as the baseline model for future projections.

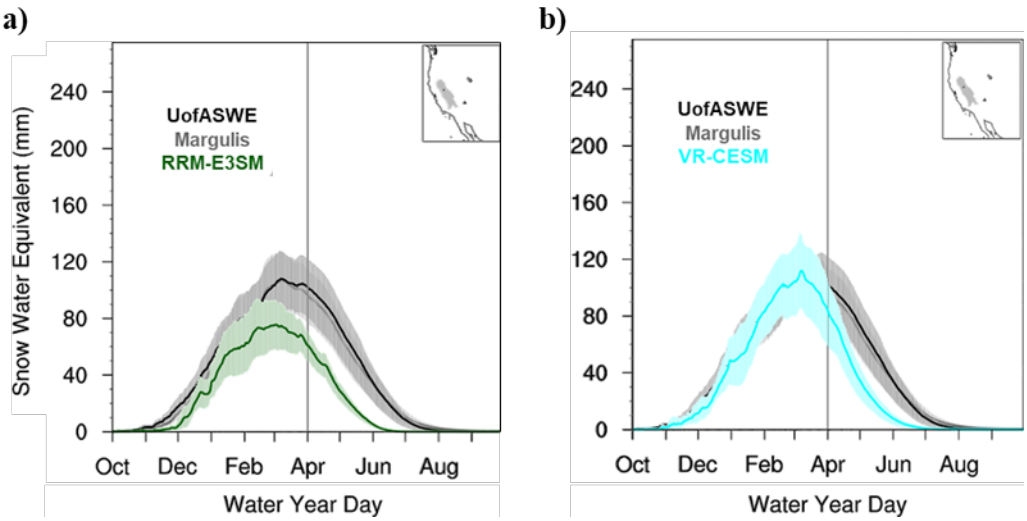

Figure 5. Comparison of snow water equivalent (SWE) between observational datasets and earth system models. a) RRM-E3SM SWE and b) VR-CESM outputs versus historical reanalysis SWE observational data from Margulis and UofASWE datasets.

3.2.5 Hydroclimate Trends

Using spatially and daily averaged data from RRM-E3SM and VR-CESM, which were aggregated into monthly sums, the monthly climatological mean was quantified for rain, snow, snowmelt, evapotranspiration, and runoff variables for the 30-year periods of each warming level. Additionally, the standard deviation and 95% confidence intervals were determined to assess the variability and uncertainty of the results. Due to data availability limitations, RRM-E3SM is utilized as a historical comparison to VR-CESM for the period spanning 1985-2013. Analysis for future warming levels were exclusively performed with VR-CESM.

In addition, several hydrologic metrics were computed to further investigate the characteristics of the hydroclimate in USGS HUC 6 watershed encompassing the California Sierra Nevada and Central Valley. Total precipitation (TP) was calculated as the sum of rainfall and snowfall. The fraction of precipitation that falls as snow (F_{snow}) was derived by taking the ratio of snowfall to total precipitation. Similarly, the fraction of precipitation that falls as rain (F_{rain}) was determined as the ratio of rainfall to total precipitation. Total surface runoff ($R_{surface}$) was obtained by summing both the infiltration-excess runoff (when rainfall and snowfall exceed the soil infiltration capacity) and the saturation-excess runoff (when rainfall and snowfall exceed the soil storage capacity). Additionally, subsurface runoff (R_{sub}) was computed as the difference between total runoff (R_{total}) and surface runoff. The snowmelt contribution to runoff was calculated as the ratio between snowmelt and total runoff. Runoff efficiency (R_{eff}), a measure of the effectiveness of total precipitation in generating runoff, was determined as the ratio between total runoff and total precipitation.

3.2.6 Water Balance

When assessing the water balance of the entire USGS HUC 6 watersheds, the inflows into the system are composed of the total precipitation (rainfall + snowfall). Meanwhile, outflows consist of the total runoff (surface + subsurface runoff), evapotranspiration (canopy and soil evaporation

+ vegetation transpiration) and change in total water storage (ΔS). However, in the context of the annual water balance, the storage component approaches near-zero values. The difference between inflows and outflows into the system represents the water balance (Equation 4). For details on hydrological processes modeled in CLM, refer to the Technical Description of CLM5.0 (https://www2.cesm.ucar.edu/models/cesm2/land/).

(4) $$TP = R_{total} + ET + \Delta S$$

When consolidating the findings of the North, South, and Central Sierras into the broader Sierra Nevada region, we aggregated the principal variables by summing their values across the regions (excluding fraction of snow-covered area and temperature which were averaged across the regions). Subsequently, we re-evaluated runoff efficiency, snow and rain contribution to precipitation, and snowmelt contribution to runoff, timing and magnitude of peak SWE were reassessed separately after regional aggregation. For most variables, we quantified the volumes in cubic kilometers (km^3).

3.2.7 Irrigation Water Demand

Based on the results of hydroclimate variability analysis of this study, we produce an estimate of the annual volumes and timing of water that may be available from the Sierra Nevada mountains (from rain and snow) under three different climate warming levels. Additionally, we estimate the amount of primarily rainfall-derived water available in the Central Valley.

We use the novel dataset published by Ruess et al., 2022 to estimate historical (2008-2020) crop irrigation water use by county in the Sacramento Valley, San Joaquin Basin, and Tulare Basin of California (Figure 1b). Ruess et al., 2022 estimated crop-specific irrigation water use from three differentiated water sources (surface water, sustainable groundwater use, and groundwater depletion) for 20 crops and crop groups from 2008 to 2020 at the county-scale (Supplementary Table S3). They accomplished this by using the PCR-GLOBWB 2 global hydrology model (Sutanudjaja et al., 2018) to partition irrigation data from the U.S. Geological Survey Water Use Database to specific crops across the Continental United States and incorporating high-resolution CONUS-specific agricultural production and climate data to obtain crop-specific irrigation estimates (Ruess et al., 2022). PCR-GLOBWB 2 is a "grid-based global hydrology and water resources model" at 5 arc-min spatial resolution. It provides daily hydrologic and water use data, including hydrodynamic river routing and human water use for irrigation, livestock, industry, and households (Sutanudjaja et al., 2018).

Ruess et al., 2022 adapted the PCR-GLOBWB 2 model to the CONUS by updating the model inputs. Crop locations were taken from CropScape (Han et al., 2012). County-specific weighted-average irrigation efficiencies were calculated using the USGS data on water-use and irrigated areas (USGS, 2021) and irrigation efficiency data from (Brouwer et al., 1989). Crop coefficients were calculated using the Crop Calendar Dataset (Sacks et al., 2010) and crop coefficients from FAO (Allen et al., 1998). Precipitation, evapotranspiration, and daily mean temperature data from GridMET (Abatzoglou et al., 2013), was employed to determine the amount of irrigation water demand that could be met by rainfall. Surface water was then applied to the remaining irrigation water demand until the demand was met, or surface water ran out. If rainfall and surface water did not meet total irrigation demand, groundwater withdrawal (sum of sustainable and unsustainable) was applied, where groundwater depletion (unsustainable) is defined as the difference between

groundwater withdrawal and long-term groundwater recharge. Refer to Ruess et al., 2022 for additional details on the development of this dataset.

The irrigation water use data for the 20 crop classes was grouped by watershed, year, and water source to obtain estimates of total irrigation water consumption in each watershed by source from 2008-2020 (Figure 11a-c).

3.3 Results

3.3.1 Snow Water Equivalent

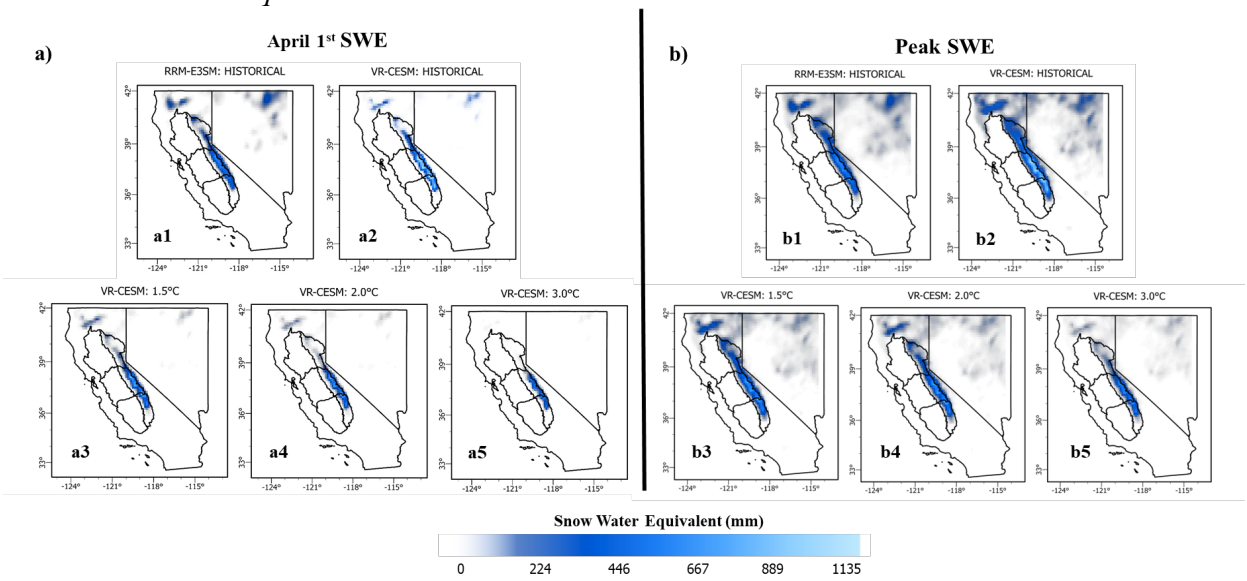

Figure 6. Snow water equivalent under climate change. a) Historical April 1st SWE for both RRM-E3SM and VR-CESM (Panels a1 and a2) and future April 1st SWE under 1.5°C, 2°C, and 3°C warming (Panels a3 – a5). b) historical Peak SWE for both RRM-E3SM and VR-CESM (Panels b1 and b2) and future Peak SWE under 1.5°C, 2°C, and 3°C warming (Panels b3 – b5).

Historically, the peak SWE is 2.8 times greater than April 1st SWE in VR-CESM and 2.5 times greater in RRM-E3SM. Figures 6 (a1, a2, b1, and b2) illustrate that in VR-CESM, higher elevations experience greater SWE volumes compared to RRM-E3SM. The fraction of snow-covered area (F_{SCA}) declines significantly from the day of peak SWE to April 1st, with values decreasing from 0.81 to 0.35 in VR-CESM and from 0.71 to 0.37 in RRM-E3SM (Figure 6, Table 4). Furthermore, SWE peaks before April 1st in both models and VR-CESM peaks on average 11 days earlier than RRM-E3SM in the historical period.

Table 4. Snow water equivalent and precipitation. Key SWE and precipitation metrics across the northern, central, and southern Sierra Nevada regions under historical, 1.5°C, 2°C, and 3°C warming. Historical values are provided for the RRM-E3SM and VR-CESM models for comparison. "All Sierras" refers to results for the three Sierra regions combined.

Region	Total Precip (km^3)	Rain (km^3)	Snow (km^3)	April 1st SWE (km^3)	Peak SWE (km^3)	April 1st F_{SCA}	Peak F_{SCA}	F_{snow}	F_{rain}
RRM-E3SM Historical									
All Sierras	***59.1***	***41.6***	***17.5***	***2.8***	***6.9***	***0.37***	***0.71***	***0.30***	***0.70***
Northern Sierra	28.9	21.1	7.8	0.6	2.4	0.35	0.79	0.27	0.73
Central Sierra	18.7	12.3	6.3	1.8	3.2	0.50	0.74	0.34	0.66
Southern Sierra	11.5	8.2	3.3	0.4	1.3	0.26	0.61	0.29	0.71
VR-CESM Historical									
All Sierras	***53.7***	***22.5***	***31.2***	***4.6***	***12.7***	***0.35***	***0.81***	***0.58***	***0.42***
Northern Sierra	24.1	11.7	12.4	0.9	4.1	0.28	0.85	0.51	0.49
Central Sierra	18.2	6.6	11.6	2.7	5.7	0.48	0.87	0.64	0.36
Southern Sierra	11.4	4.2	7.2	1.0	2.9	0.29	0.70	0.63	0.37
1.5°C									
All Sierras	***56.6***	***31.0***	***24.7***	***2.6***	***7.6***	***0.26***	***0.70***	***0.44***	***0.56***
Northern Sierra	26.1	16.2	9.9	0.3	2.4	0.18	0.78	0.38	0.62
Central Sierra	18.9	9.1	9.7	1.7	3.5	0.39	0.74	0.52	0.48
Southern Sierra	11.7	5.7	5.1	0.6	1.6	0.22	0.59	0.43	0.49
2°C									
All Sierras	***56.2***	***33.0***	***23.2***	***2.0***	***6.5***	***0.23***	***0.67***	***0.41***	***0.59***
Northern Sierra	25.7	17.1	8.6	0.2	2.0	0.13	0.75	0.34	0.66
Central Sierra	18.7	9.7	9.0	1.3	3.0	0.36	0.71	0.48	0.52
Southern Sierra	11.8	6.2	5.6	0.5	1.4	0.20	0.56	0.47	0.53
3°C									
All Sierras	***58.3***	***39.2***	***19.1***	***1.1***	***4.4***	***0.17***	***0.61***	***0.33***	***0.67***
Northern Sierra	26.3	20.0	6.3	0.0	1.2	0.08	0.70	0.24	0.76
Central Sierra	19.6	11.8	7.8	0.8	2.2	0.27	0.65	0.40	0.60
Southern Sierra	12.4	7.5	4.9	0.3	1.0	0.16	0.49	0.40	0.60

April 1st SWE in the Sierra Nevada region exhibits a substantial decline as warming levels increase (Figures 7a and 7d). Historically, mean April 1st SWE volume-equivalent stood at ~4.6 km^3, however, under 1.5°C global temperature rise, it drops to 2.6 km^3. VSWE further diminishes to 2 km^3 under 2°C, and it plummets even further to 1.1 km^3 under a more extreme 3°C of warming scenario (Table 4). In the Northern Sierras, April first VSWE reaches zero as the climate reaches 3°C (Supplementary Figure S1). April 1st VSWE is concentrated in the Central Sierra and is expected to decline from 2.7 km^3 historically 0.8 km^3 under 3°C. In the Southern Sierra, SWE persists on April 1st but only at the highest elevations (Figure 6a3–a5. Looking at peak SWE, historically and under climate change, snow continues to accumulate the most in the Central Sierras, followed by the Northern Sierras with the greatest fraction of snow-covered area. As the climate warms to 3°C, the F_{SCA} and Peak SWE decline in all regions (Figures 7a,c,e,f; Supplementary Figure S1). Peak SWE concentrates in the Central Sierra (VSWE: 2.2 km^3, F_{SCA}: 0.65) with additional SWE spread out across the Northern Sierras with less VSWE (1.2 km^3) over a larger area (F_{SCA}: 0.7), and in high elevation mountains of the Southern Sierras (VSWE: 1 km^3, F_{SCA}: 0.49) (Huning and Margulis, 2018). The Sierra Nevada region undergoes a striking decline in peak SWE due to climate change (Figures 6b3-b5; Figures 7a,c). Peak mean SWE volume-equivalent plummets from 12.7 km^3 during the historical period to 7.6 km^3 under 1.5°C and further

diminishes to 6.5 km^3 and 4.4 km^3 under 2°C and 3°C respectively (Figure 6b3–b5; Table 4). Historically, April 1st has been used as the reference date for the peak or near-peak of snowpack. However, actual peak SWE occurs earlier in the water year with climate change (Figure 7b). According to VR-CESM, on average peak SWE occurs in early March in the central and southern Sierras, and in mid-February in the northern Sierra Nevada for the historical, 1.5°C and 2°C scenarios. Under the more extreme warming of 3°C, SWE peaks even earlier (by one to two weeks) in mid-to-late February for the central and southern Sierras and in early February for northern Sierra Nevada.

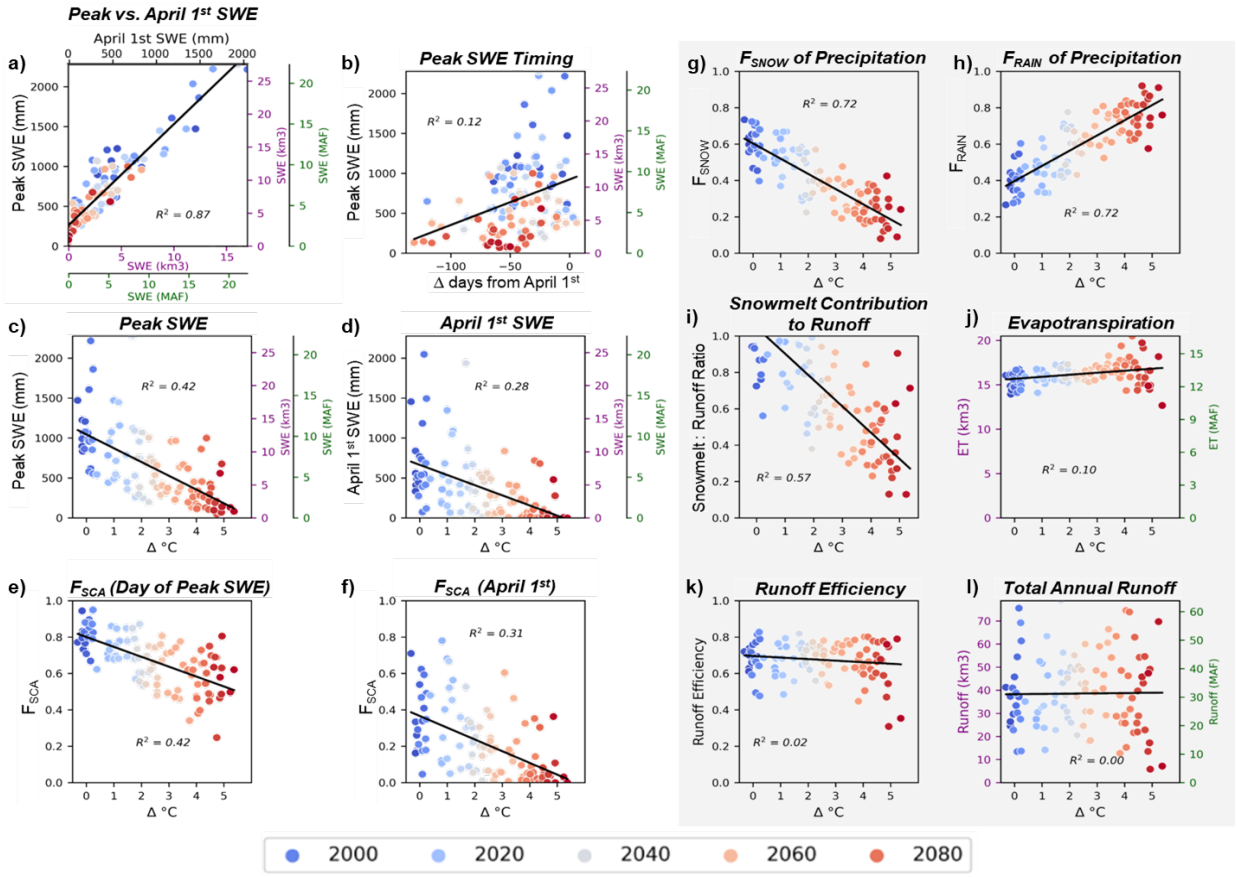

Figure 7. Response of key hydroclimatic factors to increasing climate warming. These factors include snow water equivalent (a-d), fraction of snow-covered area (e and f), precipitation (g-h), runoff characteristics (i, k, l), and evapotranspiration (j). The data spans from the year 1985 to 2099, with each point representing a specific year. The color gradient represents the progression from the darkest blue, indicating 1985, to the darkest shade of red, representing 2099. Panel b displays the x-axis as the number of days earlier than April 1st (represented as 0) when peak snow water equivalent (SWE) occurs. Units of SWE are provided in terms of mm, km^3, and million-acre-feet (MAF). Units of evapotranspiration and runoff are provided in terms of km^3 and MAF. The x-axis represents incremental degrees of warming from the reference temperature in Figures 7c-7l). To assess the fit for each scatterplot, a simple scikit-learn linear regression model was employed, and R^2 values were assigned accordingly. Supplementary Figure S1 provides a breakdown for the three distinct Sierra Nevada regions.

3.3.2 Hydroclimate Variation

From the historical climatological mean to the 3℃ climatology, the fraction of precipitation that falls as snow drops from 58% to 33% (hence, the fraction of precipitation that falls as rain increases from 42% to 67%) across the entire Sierra Nevada region (Table 4; Figures 7g,h). An increase in temperature of 3℃ means that rainfall dominates in the Sierra Nevada. The northern Sierra has the highest fraction of rainfall under all warming levels (Table 4). Understanding the seasonal distribution of precipitation and quantifying the contributions of rainfall and snowfall in the different regions is essential for effective water resource management planning. Hence, it is important to assess both the monthly as well as annual regional climatology.

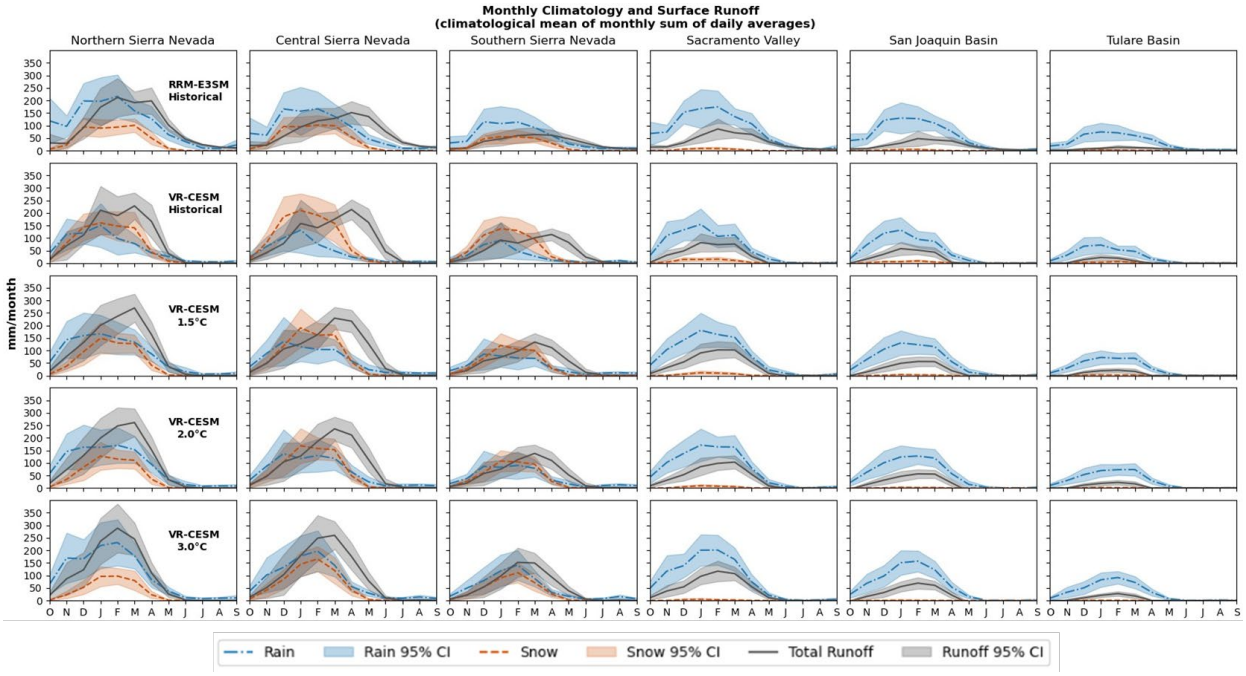

Figure 8. Monthly climatology and surface runoff with 95% confidence intervals. Shaded areas represent the 95% confidence intervals while the lines represent the climatological mean for each variable - rainfall and snowfall, and total runoff in mm/month.

3.3.2.1 RRM-E3SM vs VR-CESM Model Comparison of Hydroclimate Estimates

An annual water balance was assessed for the historical simulations of both models (Table 5). RM-E3SM, simulated 85% more annual rainfall in the Sierra Regions and 31% more in the Valley regions compared to VR-CESM. Conversely, VR-CESM simulates 45% more annual snowfall in the Sierra Nevada than RRM-E3SM (Table 5).

Historical Water Balance - Sierra Nevada						
	Northern Sierra		Central Sierra		Southern Sierra	
	mm / yr	*km³*	*mm / yr*	*km³*	*mm / yr*	*km³*
RRM-E3SM						
Rainfall	1255	21.1	956	12.3	628	8.2
Snowfall	467	7.8	490	6.3	257	3.3
Total Precipitation	***1722***	***28.9***	***1446***	***18.7***	***885***	***11.5***
Total Evapotranspiration	***581***	***9.8***	***558***	***7.2***	***478***	***6.2***
Surface Runoff	368	6.2	315	4.1	198	2.6
Subsurface Runoff	756	12.7	554	7.1	198	2.6
Total Runoff	***1124***	***18.9***	***869***	***11.2***	***396***	***5.1***
Inflows	1722	28.92	1446	18.65	885	11.50
Outflows	1705	28.63	1426	18.4	873	11.35
Water Balance (Inflows - Outflows)	**17**	**0.29**	**19**	**0.25**	**11**	**0.15**
VR-CESM						
Rainfall	696	11.7	511	6.6	325	4.2
Snowfall	737	12.4	902	11.6	555	7.2
Total Precipitation	***1433***	***24.1***	***1413***	***18.2***	***880***	***11.4***
Total Evapotranspiration	***401***	***6.7***	***376***	***4.8***	***308***	***4.0***
Surface Runoff	657	11.0	635	8.2	355	4.6
Subsurface Runoff	370	6.2	399	5.1	217	2.8
Total Runoff	***1027***	***17.2***	***1034***	***13.3***	***572***	***7.4***
Inflows	1433	24.07	1413	18.23	880	11.43
Outflows	1428	23.98	1410	18.19	880	11.43
Water Balance (Inflows - Outflows)	**5**	**0.09**	**3**	**0.04**	**-0.43**	**0.0**

Table 5. Sierra Nevada water balance. See Supplementary Figure S2 for water balance of the Central Valley regions.

Regarding the timing of precipitation peaks, RRM-E3SM exhibits distinct patterns across the different regions (Figure 8). In all Sierra regions and the Sacramento Valley, total precipitation reaches its peak in February, while in the San Joaquin and Tulare Basins, it peaks in January (Figure 9). Specifically, rainfall peaks in February in the N. Sierra, C. Sierra, and Sacramento Valley, in December in the S. Sierra, and in January in the San Joaquin and Tulare basins. In the RRM-E3SM simulations, the Southern Sierra experiences peak snowfall earlier, typically in January. On the other hand, the C. Sierra reaches peak snowfall in February, while the N. Sierra experiences its highest snowfall in March (Table 6). Contrarily, VR-CESM provides more consistent estimates of historical peak precipitation timing. In this model, both snow and rain reach their peaks in January for all six regions.

The timing of peak runoff and evapotranspiration also differs between the models. Under RRM-E3SM, runoff peaks from February to April in the Sierras and in February in the valley regions (Figure 8; Figure 9). Evapotranspiration peaks in May in the mountain regions, but starts peaking in March in the southern Tulare Basin, followed by April in the central San Joaquin basin, and in May in the northern Sacramento Valley (Figure 9). Due to the additional snow modeled by VR-CESM, runoff typically peaks a month later (between March and April) in the mountain

regions compared to RRM-E3SM. In the absence of significant snowfall, runoff in VR-CESM peaks in January, aligning with the peak rainfall month in the Valley regions (Table 6). Furthermore, VR-CESM simulates a later peak in ET compared to RRM-E3SM. In VR-CESM, ET reaches its peak in June in N. Sierra and C. Sierra, and in May in S. Sierra and the valley regions.

Both models agree on the proportional difference in rainfall among the valley regions. They both indicate a 21 - 27% reduction in rainfall between the Sacramento Valley and San Joaquin basin, and a 44 - 47% reduction between the San Joaquin Basin and Tulare Basin (Table 5).

Table 6. Timing and magnitude of hydrological peaks.

Timing and Magnitude of Hydrological Peaks												
	Northern Sierra		Central Sierra		Southern Sierra		Sacramento Valley		San Joaquin Basin		Tulare Basin	
	Month	*Magnitude (mm/yr)*	*Month*	*Magnitude (mm)*	*Month*	*Magnitude (mm)*	*Month*	*Magnitude (mm)*	*Month*	*Magnitude (mm)*	*Month*	*Magnitude (mm)*
RRM-E3SM												
Rainfall	Feb	217 +/- 86	Feb	167 +/- 68	Dec	115 +/- 52	Feb	175 +/- 64	Jan	130 +/- 62	Jan	75 +/- 36
Snowfall	Mar	101 +/- 27	Feb	102 +/- 39	Jan	56 +/- 28	Feb	8 +/- 7	Jan	5 +/- 4	Jan	3 +/- 2
Total Runoff	Feb	212 +/- 76	Apr	152 +/- 45	Mar	64 +/- 27	Feb	86 +/- 41	Feb	48 +/- 30	Feb	14 +/- 8
Total Evapotranspiration	May	84	May	84	May	66	May	84	Apr	76	Mar	54
Historical VR-CESM												
Rainfall	Jan	151 +/- 87	Jan	132 +/- 92	Jan	91 +/- 70	Jan	155 +/- 63	Jan	132 +/- 51	Jan	72 +/- 32
Snowfall	Jan	161 +/- 46	Jan	210 +/- 67	Jan	137 +/- 50	Jan	15 +/- 7	Jan	6 +/- 3	Jan	3 +/- 2
Total Runoff	Mar	228 +/- 53	Apr	214 +/- 40	Apr	114 +/- 24	Jan	82 +/- 36	Jan	58 +/- 26	Jan	23 +/- 13
Total Evapotranspiration	Jun	73 +/- 4	Jun	72 +/- 5	May	59 +/- 3	May	83 +/- 3	May	81 +/- 3	May	71 +/- 3
1.5°C												
Rainfall	Jan	167 +/- 75	Dec	136 +/- 97	Dec	86 +/- 62	Jan	181 +/- 69	Jan	131 +/- 49	Jan	72 +/- 27
Snowfall	Jan	150 +/- 62	Jan	190 +/- 76	Jan	120 +/- 48	Jan	11 +/- 6	Jan	4 +/- 2	Jan	3 +/- 1
Total Runoff	Jan	201 +/- 81	Mar	229 +/- 44	Mar	134 +/- 35	Feb	102 +/- 34	Feb	56 +/- 19	Feb	21 +/- 9
Total Evapotranspiration	Jun	77 +/- 4	Jun	75 +/- 5	May	60 +/- 4	May	85 +/- 3	May	82 +/- 3	May	72 +/- 4
2°C												
Rainfall	Feb	171 +/- 71	Dec	138 +/- 96	Feb	91 +/- 55	Jan	171 +/- 65	Feb	128 +/- 33	Feb	73 +/- 21
Snowfall	Jan	128 +/- 56	Jan	169 +/- 69	Jan	108 +/- 42	Jan	9 +/- 6	Feb	2 +/- 1	Feb	2 +/- 1
Total Runoff	Mar	261 +/- 55	Mar	236 +/- 48	Mar	138 +/- 34	Mar	104 +/- 26	Feb	57 +/- 18	Feb	22 +/- 9
Total Evapotranspiration	Jun	76 +/- 4	Jun	74 +/- 4	May	62 +/- 5	May	87 +/- 3	May	84 +/- 3	May	73 +/- 4
3°C												
Rainfall	Feb	231 +/- 92	Feb	198 +/- 81	Feb	141 +/- 59	Jan	201 +/- 63	Feb	157 +/- 42	Feb	92 +/- 25
Snowfall	Feb	97 +/- 32	Feb	166 +/- 50	Feb	111 +/- 40	Jan	5 +/- 4	Feb	1 +/- 1	Feb	1 +/- 1
Total Runoff	Feb	289 +/- 97	Mar	260 +/- 56	Feb	152 +/- 58	Feb	117 +/- 41	Feb	69 +/- 23	Feb	27 +/- 9
Total Evapotranspiration	Jun	78 +/- 4	Jun	75 +/- 4	May	62 +/- 4	May	86 +/- 3	May	83 +/- 3	May	74 +/- 3

3.3.2.2 Hydroclimate Trends under Climate Change (VR-CESM).

As climate warming intensifies, hydroclimate patterns undergo significant transformations. In particular, the runoff curves deviate from their traditional smooth and more rounded shapes, adopting a more abrupt rise and fall (Figure 9). While total precipitation generally increases, the proportion of precipitation falling as snow diminishes, giving way to a greater contribution from rainfall with critical consequences regarding the timing of downstream water availability as runoff and streamflow. When compared to historical levels (F_{snow} = 0.58), the fraction of precipitation falling as snow is projected to decrease by 22% (to F_{snow} = 0.44) under a 1.5°C scenario, further decline by 29% (to F_{snow} = 0.41) under a 2°C scenario, and experience a further decline of 43% (to F_{snow} = 0.33) under a 3°C warming scenario (Table 4). Notably, the Northern Sierra region is expected to experience a more pronounced decline in snowfall compared to other areas. This study highlights the region-specific impacts of climate change on snowfall patterns.

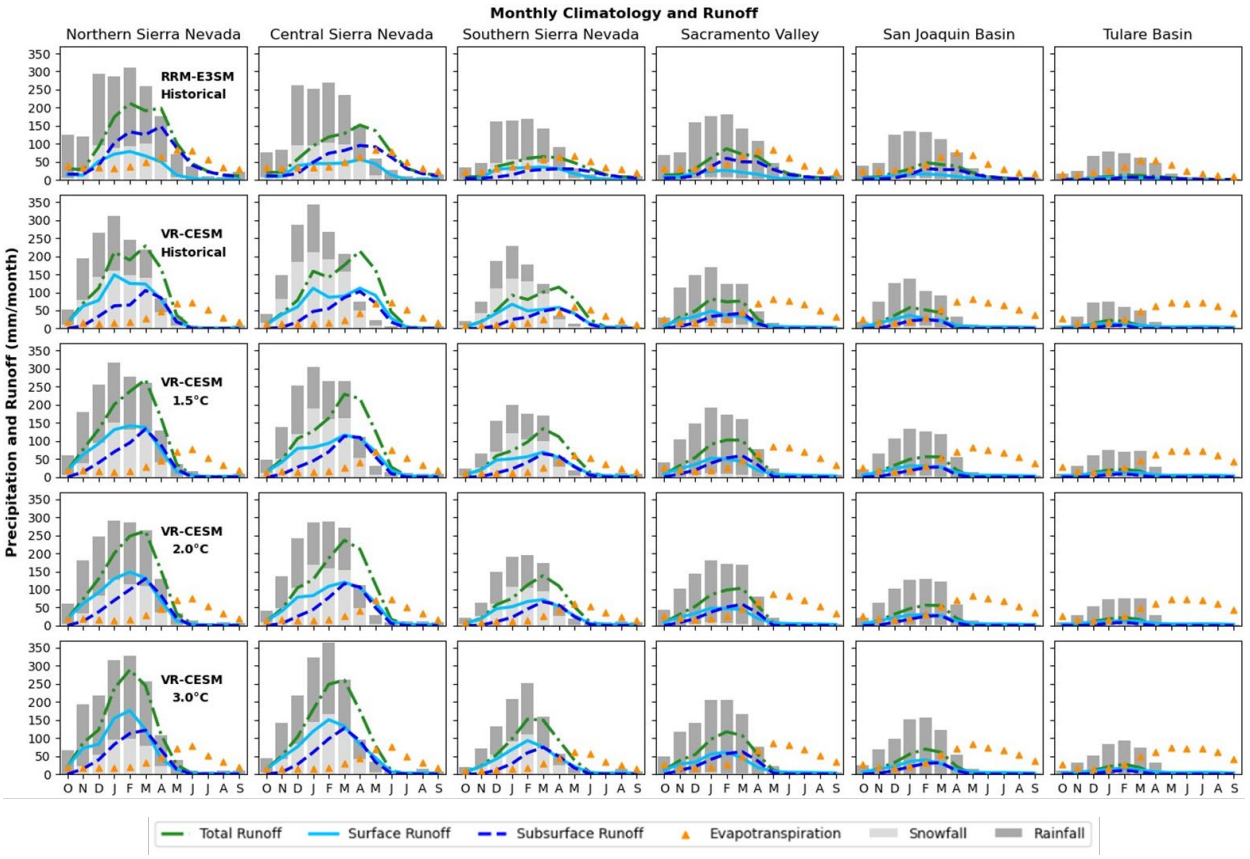

Figure 9. Monthly climatological means of hydroclimate variables.

The differences in precipitation, runoff, and snowmelt trends between the historical RRM-E3SM and VR-CESM simulation and between the historical, 1.5°C, 2°C, and 3°C warming scenarios using VR-CESM are highlighted in Figure 10. In the northern Sierra Nevada region under 3°C warming scenario, there is a slight increase in total precipitation and runoff increase slightly (by ~109-132 mm/month) compared to the historical average. There is also a shift in peak timing of precipitation from January to February and an earlier shift in peak runoff from March to February (Figure 10). Annual snowfall decreases by half while rainfall increases by 70%, resulting in an earlier and lower peak in snowmelt occurring in February (Table 4). In this scenario, the northern Sierra experiences the highest peak in total monthly runoff (289 +/- 97 mm) and rainfall (231 +/- 92 mm), but the least snowfall peak (97 +/- 32 mm) among all other regions (Table 6). Runoff, rain and snow all peak in the month of February and undergo the sharpest decline – halting by late spring (Figure 9).

In the central Sierra Nevada, under a 3°C warmer climate, total precipitation and runoff increase slightly (by ~100 mm/month) compared to the historical average. The peak timing of precipitation shifts from January to February, while peak runoff shifts earlier from April to March (Figure 10). Annual snowfall drops by 32% while rainfall increases by 79%, leading to an earlier and lower peak in snowmelt occurring in March instead of April. Despite the decline in magnitude, as the climate warms to 3°C, the central Sierra Nevada mountains continue to experience the highest peaks in snowfall (166 +/- 50 mm), snow water equivalent (256mm ~ 2.2 km^3)), and fraction of snow-covered area on April 1st (0.27) compared to other regions (Table 4, Table 6,

Figure 8). Historically, precipitation peaked with more snow than rain in January, and peak runoff occurred in April due to ample water storage in the snowpack. However, under 3°C, precipitation is projected to peak in February with more rain than snow, and peak runoff will occur the following month of March, declining until it ends in May (Table 6, Figure 9).

In the southern Sierra Nevada, under 3°C warmer climate, total precipitation and runoff remain constant. Annual snowfall decreases by 32% while rainfall increases by 77%, resulting in an earlier peak in March. Due to the higher fraction of precipitation falling as rain, lower F_{SCA}, and overall decline in snowfall, peak runoff occurs 2 months earlier than historically and coincides with peak rainfall and snowfall, which also occur in February (Figure 10). The southern Sierra Nevada receives less than half of the total precipitation compared to the northern Sierra Nevada and approximately 38% less precipitation than the central Sierra Nevada.

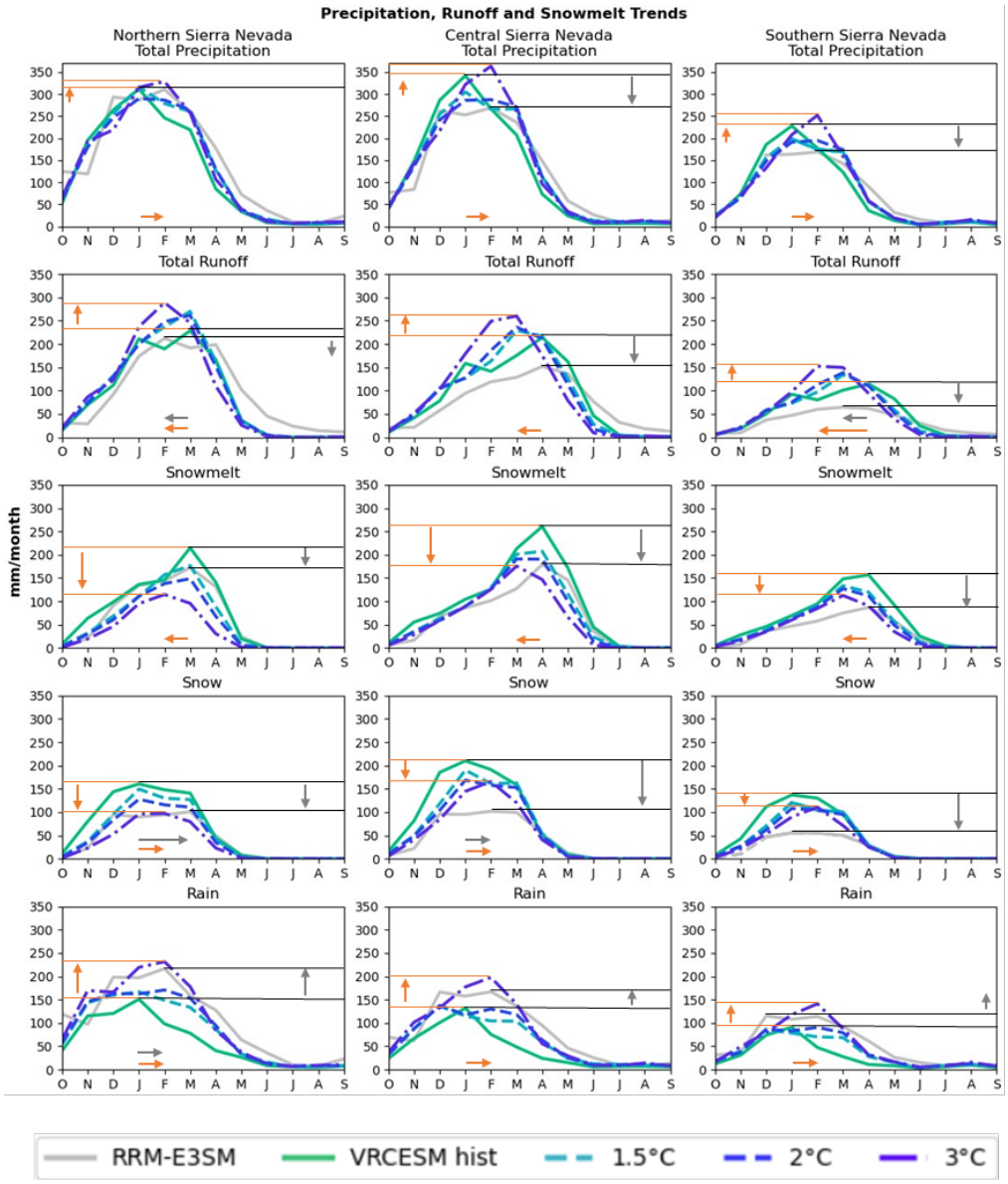

Figure 10. Precipitation, runoff, and snowmelt trends under climate change. The horizontal orange lines and arrows highlight the difference in timing and magnitude of precipitation, runoff, and snowmelt maxima between 3°C (purple) and historical VR-CESM (green) simulations. The vertical orange arrows indicate how the peak for 3°C differs from the peak of VR-CESM. For example, an upward facing arrow indicates that the max for 3°C is greater than that of VRCESM. Likewise, a downward facing arrow indicates that the max for 3°C is less than that of VRCESM. The length of the arrow alludes to the magnitude of the difference. Horizontal arrows represent the difference in timing between the maxima of both simulations. An orange left-pointing arrow indicates that 3°C peaks earlier than VR-CESM, while right-pointing arrows indicate that 3°C peaks later than VR-CESM. The month of VR-CESM peak occurrence serves as the starting point of the arrows and the length indicates the number of months earlier or later. The horizontal black lines and grey arrows point to the maxima of the two historical simulations – RRM-E3SM (grey)

and VR-CESM (green). Supplementary Figure S2 offers a more detailed representation of this figure.

3.4 Discussion

3.4.1 Model Differences and Justification

When comparing both models across the broader Sierra Nevada region for the historical period, the results show strong differences in historic precipitation patterns between the output from the RRM-E3SM model and the VR-CESM model in the various study regions. RRM-E3SM exhibits a 9% higher total precipitation compared to VR-CESM (Table 4). However, the distribution of precipitation differs significantly between the two models during the historical period. In RRM-E3SM, 70% of the historical precipitation is attributed to rainfall, while only 30% is attributed to snowfall. Conversely, in VR-CESM, 58% of the simulated precipitation is attributed to snowfall, with 42% coming from rainfall. As a result, VR-CESM shows a substantial increase on April 1st (4.6 km^3) and peak (12.7 km^3) SWE volumes compared to RRM-E3SM (2.8 km^3 and 6.9 km^3 respectively), representing a 63% and 83% increment by volume. According to comparisons with Margulis and UofASWE datasets in Figure 5, VR-CESM performs better in California over most of the snow accumulation portion of the water year. Notably, both models melt faster and earlier in the snowmelt season portion of the water year compared to historical observations, however, this is consistent with previous studies which utilize other regional or global model simulations (e.g., The North American Coordinated Regional Climate Downscaling Experiment and Framework for Assessing Climate's Energy-Water-Land Nexus using Targeted Simulations Simulations) (Rhoades et al., 2018b).

3.4.2 Agriculture

These findings have important implications for water resource management and planning in the state of California, highlighting changes in hydroclimate variability and the need to adapt to altered precipitation patterns and changes in runoff timing and volumes – particularly for agriculture. Now that we have assessed the projected timing and magnitude of runoff accounting for changes in hydroclimate variability under 1.5°C, 2°C, and 3°C warmer climates in the north, south, and central Sierra Nevada as well as the Sacramento, San Joaquin, and Tulare basins in the Central Valley, we evaluate the ability of these water sources to meet water demand from the agricultural sector.

3.4.2.1 Water Availability under Climate Change

In sum, rainfall in the Sierra Nevada increases from 1530 mm/yr in the historical period to 2680 mm/yr under 3°C of warming. Conversely, snowfall declines from 2190 mm/yr to 1360 mm/yr, and runoff increases from 2640 to 2880 mm/yr under the same warming scenario (Table 7). In a snow and rain-dominated system, only a portion of water is delivered as immediate runoff due to rainfall, while snowfall accumulates forming a snowpack which acts as natural reservoir and gradually contributes to runoff as the snow melts or percolates into the subsurface. In a much more rain-dominated system, almost all the water delivery occurs in days (and may become even more accentuated if extreme rainfall is amplified, as discussed in Ombadi et al., 2023). In the Central Valley, the Sacramento Valley receives the highest amount of rainfall,

followed by the San Joaquin Basin. The Tulare Basin receives approximately 18% less rain than the San Joaquin Valley, and ~30-33% less rain than the Sacramento Valley. Overall, rain in the Central Valley increases from 1590 mm/yr historically, to 1890 mm/yr under 1.5°C and 2°C of warming, and further increases to 2060 mm/yr under a 3°C warming scenario. As the climate warms to 3°C, evapotranspiration is projected to increase by 70 mm/yr in the Sierra Nevada and 50 mm/yr in the Central Valley. This result agrees with previous studies that have assessed increases in evaporative demand under climate warming (Albano et al., 2022; Milly et al., 2020). Total runoff in the entire study area encompassing both Sierra Nevada and the Central Valley increases by 460 mm/yr from the historical period to a 3°C future with runoff efficiency remaining relatively constant.

Table 7. Hydrologic regime by warming level. Precipitation, evapotranspiration, and runoff regimes under historical, 1.5°C, 2°C, and 3°C warming scenarios for the entire Sierra Nevada and Central Valley as well as the whole study area. Total Runoff is highlighted in yellow to emphasize water available for human consumption prior to accounting for environmental flows.

VRCESM (mm / yr)												
Scenario	**Historical**			**1.5C**			**2C**			**3C**		
Region	**SN**	**CV**	**All**	**SN**	**CV**	**All**	**SN**	**CV**	**All**	**SN**	**CV**	**All**
RAIN	1530	1590	3120	2110	1890	4000	2250	1890	4130	2680	2060	4740
SNOW	2190	107	2300	1730	56	1790	1640	44	1683	1360	23	1380
Total_Precip	3720	1700	5420	3840	1950	5790	3890	1930	5810	4040	2080	6120
ET	1080	1600	2680	1120	1630	2750	1130	1640	2770	1150	1650	2790
Surface Runoff	1650	463	2110	1660	508	2170	1660	501	2170	1760	545	2300
Subsurface_Runoff	990	150	1140	1120	238	1360	1110	237	1340	1120	277	1410
Total Runoff	*2640*	*612*	***3250***	*2780*	*746*	***3530***	*2770*	*738*	***3510***	*2880*	*822*	***3710***
Runoff Efficiency	71%	36%	60%	72%	38%	61%	71%	38%	60%	71%	40%	61%
F_{snow}	59%	6%	42%	45%	3%	31%	42%	2%	29%	34%	1%	23%

3.4.2.2 Irrigation Water Demand

According to the California Department of Food and Agriculture, the state accounts for more than 33% of the total vegetable production and a staggering 75% of the fruits and nuts produced in the entire United States. However, sustaining this agricultural output is a challenge due to California's heavy reliance on groundwater sources for irrigation. Unsustainable pumping rates from groundwater aquifers, notably in the southern Tulare Basin, pose significant concerns for the future of California's agriculture (Scanlon et al., 2012).

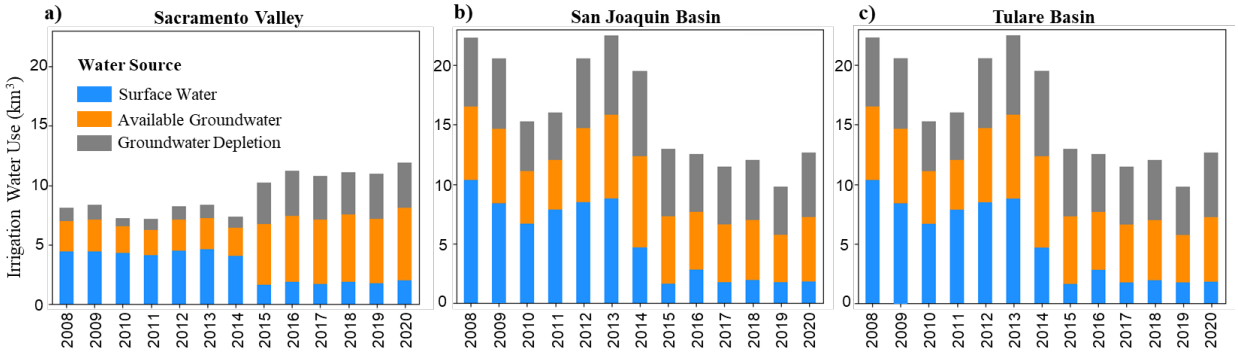

Figure 11. Historical irrigation water use in California's Central Valley from 2008-2020. Irrigation water use categorized by source in the a) Sacramento Valley, b) San Joaquin Basin, and c) Tulare Basin. Surface water consumption is represented by the blue bars, while groundwater withdrawals are split between available groundwater (sustainable) and groundwater depletion (unsustainable) in orange and grey respectively.

In fact, Table 8 shows that historically, the Tulare Basin accounts for the greatest amount of irrigation water consumption (16 km^3) in all categories, with 5.1 km^3, 5.5 km^3, and 5.3 km^3 of water taken from surface water, sustainable (available) groundwater, and groundwater depletion, respectively. Comparatively, the San Joaquin Basin consumed an average of 3.8 km^3, 3.1 km^3, and 2.9 km^3 of surface water, sustainable and unsustainable groundwater- totaling 9.8 km^3. The Sacramento Valley consumed an average of 9.3 km^3 of water per year, with 3.2 km^3 , 3.9 km^3, and 2.2 km^3 attributed to surface water, sustainable and unsustainable groundwater, respectively. On average, over the 2008-2020 period, agriculture accounted for 12.2 km^3 of surface water consumption, 12.5 km^3 of sustainable groundwater extraction, and 10.5 km^3 groundwater depletion annually. Overall, irrigated agriculture utilized a substantial 35.1 km^3 of water from all sources across the Central Valley (Table 8). Irrigation water consumption decreased in the San Joaquin and Tulare Basins from 2015 -2020, coinciding with higher-than-average temperatures and below average precipitation in most years leading to drought conditions (Mount et al., 2018).

Table 8. Historical irrigation water use. Mean irrigation water use in the Central Valley region, categorized by surface water withdrawals, sustainable groundwater withdrawals, and unsustainable groundwater withdrawals (depletion) from 2008 to 2020. The total water consumption for each water source across all Central Valley regions is displayed in light, green-shaded boxes at the bottom of the table. Additionally, the sum of irrigation water consumption from all sources for each region is highlighted in light green on the right. Lastly, the dark green box represents the total mean irrigation water consumption for all Central Valley regions from all sources. The data used in this table are derived from Ruess et al., 2022.

Mean Historical Irrigation Water Use 2008-2020 (km3)				
Region	**Surface Water (sw)**	**Groundwater Available (gwa)**	**Groundwater Depletion (gwd)**	**All water sources**
Sacramento Valley	3.2	3.9	2.2	9.3
San Joaquin Basin	3.8	3.1	2.9	9.8
Tulare Basin	5.1	5.5	5.3	16.0
Central Valley Regions Combined	12.2	12.5	10.5	**35.1**

When comparing the historical mean irrigation water consumption in the Central Valley (outlined in Table 8) to the mean annual runoff from the Sierra Nevada and the Central Valley across different warming levels (historical, 1.5°C, 2°C, and 3°C), it appears that the total water available (runoff) from the Sierras could technically meet the 35.1 km^3 irrigation water demand in the Central Valley if we solely consider water volumes and assume constant water demand in

the future. However, this analysis does not account for water allocations necessary to maintain ecosystem function or the additional water demand from other sectors reliant on the California State Water Project (such as industrial, domestic, and energy sectors). The total runoff from both the Sierra Nevada and the Central Valley ranges from 57.8 km^3 (historically) to 68.5 km^3 (3°C).

Despite the initial impression of sufficient water availability, the study's findings reveal that most precipitation is projected to fall as rain rather than snow due to climate change. Consequently, snowpack storage will decline significantly, resulting in water availability approximately one to two months earlier in the water year and substantial declines in water availability during the hot summer months. Qin et al., 2020 found that water demand in the spring is met by snowmelt-driven runoff in California. However, as we demonstrated here, total runoff declines rapidly in the spring beginning in March and completely disappears in the summer months (by June) when demands for irrigation are highest) and will continue to do so with sharper declines and earlier disappearance as the climate warms. Without sufficient surface and subsurface water storages, meeting water demands for irrigation and other sectors will be a challenge even with increased rainfall runoff which may not fully offset the loss of snowmelt runoff. (Schmitt et al., 2022; Qin et al. 2020; He et al., 2021).

3.4.3 Further Implications

As the Earth's climate continues to warm, not only will the fraction of precipitation falling as snow decline, but extreme rainfall and rain-on snow events will also increase in high elevation regions (Ombadi et al., 2023; Li et al., 2019). The augmentation of rainfall runoff elevates flood risks in the winter and spring months as well as drought and fire risks during the dry season (Davenport et al., 2020; Oakley 2021; Musselman et al., 2018). Additionally, in California, approximately 15% of the state's electricity is derived from snowmelt dependent hydropower (which employs approximately 11,000 workers) and will become increasingly important in meeting the state's base loads in a more renewable energy dominated grid mix (Gleick 2017; Gleick 2015; Szinai et al., 2020; CEC and CPUC 2020). Yates et al., 2022 found that due to the reduction in surface water availability and increased irrigation water demand, water-related electricity water use will increase due to augmenting groundwater pumping. At the same time, total annual hydropower generation will decrease by up to 20% in the Western U.S. by mid-century (Yates et al., 2022). Climate change will continue cause significant economic losses and the population exposure to climate extremes will double in the United States by mid-century (Batibeniz et al., 2020). Unfortunately, climate change will disproportionately impact low-income communities and people of color. These communities will be the most exposed to floods, droughts, extreme heat with a hindered ability to recover (Jay et al., 2018; Sanders et al., 2023). Additionally, these populations will be more vulnerable to economic shocks as agricultural jobs are threatened and cost of produce rises with depleting water sources (Sanders et al., 2023; Hsiang et al., 2017).

3.5 Conclusion

In conclusion, we highlight changing precipitation patterns in the Sierra Nevada as the climate warms with significant decreases in snowfall and consequently snowpack, and an increase in rainfall. The projected shift from a snow to rain dominated region due to significant losses in snowpack, will lead to earlier water availability and substantial declines in runoff during the warm

summer months when irrigation demand is highest. Despite the increased water availability from rainfall and runoff, without sufficient reservoir storage capacity, the excess water will be lost and will not compensate for the loss of snowmelt runoff to meet water demand from the agricultural sector. These changes in California's hydroclimate present significant risks to food, water, energy, and socioeconomic security (Yates et al., 2022; Beltran-Peña et al., 2020; Mankin et al., 2015; Medellín-Azuara et al., 2022). The intersectoral implications of snowpack decline will be further examined in future studies. It is essential to understand and address the implications of these hydrological changes to ensure the sustainable management of water resources in California.

3.6 References

AB 1482, Gordon. Climate adaptation. California, 2015. Retrieved from https://leginfo.legislature.ca.gov/faces/billTextClient.xhtml?bill_id=201520160AB1482

Abatzoglou, J. T. (2013). Development of gridded surface meteorological data for ecological applications and modelling. International Journal of Climatology, 33(1), 121– 131.

Albano, C.M., Abatzoglou, J.T., McEvoy, D.J., Huntington, J.L., Morton, C.G., Dettinger, M.D. and Ott, T.J., 2022. A multidataset assessment of climatic drivers and uncertainties of recent trends in evaporative demand across the continental United States. *Journal of Hydrometeorology*, *23*(4), pp.505-519.

Allen, R. G., Pereira, L. S., Raes, D., & Smith, M. (1998). Crop evapotranspiration-Guidelines for computing crop water requirements-FAO Irrigation and drainage paper 56. Chapter 6: Etc – Single Crop Coefficient (Kc). FAO, Rome, 300(9), D05109. Retrieved from http://www.fao.org/3/x0490e/x0490e00.htm

Bambach, N.E., Rhoades, A.M., Hatchett, B.J., Jones, A.D., Ullrich, P.A. and Zarzycki, C.M., 2022. Projecting climate change in South America using variable-resolution Community Earth System Model: An application to Chile. International Journal of Climatology, 42(4), pp.2514-2542.

Batibeniz, F., Ashfaq, M., Diffenbaugh, N.S., Key, K., Evans, K.J., Turuncoglu, U.U. and Önol, B., 2020. Doubling of US population exposure to climate extremes by 2050. *Earth's Future*, *8*(4), p.e2019EF001421.

Beltran-Peña, A., Rosa, L. and D'Odorico, P., 2020. Global food self-sufficiency in the 21st century under sustainable intensification of agriculture. *Environmental Research Letters*, *15*(9), p.095004.

Brouwer, C., Prins, K., & Heibloem, M. (1989). Irrigation water management: Irrigation scheduling. Annex I: Irrigation efficiencies. FAO. Retrieved from http://www.fao.org/3/t7202e/t7202e08.htm

Brunke, M.A., Welty, J. and Zeng, X., 2021. Attribution of snowpack errors to simulated temperature and precipitation in E3SMv1 over the contiguous United States. *Journal of Advances in Modeling Earth Systems*, *13*(10), p.e2021MS002640.

Caldwell, P. M., Mametjanov, A., Tang, Q., Van Roekel, L. P., Golaz, J.-C., Lin, W., et al. (2019). The DOE E3SM coupled model version 1: Description and results at high resolution. *Journal of Advances in Modeling Earth Systems*, **11**(12), 4095– 4146. https://doi.org/10.1029/2019ms001870

California Department of Food and Agriculture (CDFA) (2021a). California Agricultural Statistics Review 2020-2021. https://www.cdfa.ca.gov/Statistics/PDFs/2021_Ag_Stats_Review.pdf

California Department of Food and Agriculture (CDFA), 2020. County Agricultural Commissioners' Reports Crop Year 2019-2020. https://www.nass.usda.gov/Statistics_by_State/California/Publications/AgComm/index.php

California Department of Water Resources (CDWR) (2022). Water Basics. https://water.ca.gov/Water-Basics

California Department of Water Resources, 2018. California Land and Water Use Data, WY 2011-2015. Accessed August 1, 2022. url: https://water.ca.gov/Programs/Water-Use-And-Efficiency/Land-And-Water-Use/Agricultural-Land-And-Water-Use-Estimates

California Energy Commission and California Public Utilities Commission (CEC and CPUC). (2020). 2020 California Energy and Employment Report. Accessible at: https://www.energy.ca.gov/filebrowser/download/2272

Cooley, H., Donnelly, K., Phurisamban, R. and Subramanian, M., 2015. Impacts of California's ongoing drought: agriculture. Pacific Institute, Oakland, 24.

Cowherd, M., Leung, L.R. and Girotto, M., 2023. Evolution of global snow drought characteristics from 1850 to 2100. Environmental Research Letters, 18(6), p.064043.

Danabasoglu, G., Lamarque, J.-F., Bacmeister, J., Bailey, D.A., DuVivier, A.K., Edwards, J., Emmons, L.K., Fasullo, J., Garcia, R., Gettelman, A., Hannay, C., Holland, M.M., Large, W.G., Lauritzen, P.H., Lawrence, D.M., Lenaerts, J.T.M., Lindsay, K., Lipscomb, W.H., Mills, M.J., Neale, R., Oleson, K.W., Otto-Bliesner, B., Phillips, A.S., Sacks, W., Tilmes, S., van Kampenhout, L., Vertenstein, M., Bertini, A., Dennis, J., Deser, C., Fischer, C., Fox-Kemper, B., Kay, J.E., Kinnison, D., Kushner, P.J., Larson, V.E., Long, M.C., Mickelson, S., Moore, J.K., Nienhouse, E., Polvani, L., Rasch, P.J. and Strand, W.G. (2020) The community earth system model version 2 (CESM2). Journal of Advances in Modeling Earth Systems, 12(2), e2019MS001916. https://doi.org/10.1029/2019MS001916.

Davenport, F.V., Herrera-Estrada, J.E., Burke, M. and Diffenbaugh, N.S., 2020. Flood size increases nonlinearly across the western United States in response to lower snow-precipitation ratios. *Water Resources Research*, *56*(1), p.e2019WR025571.

Diffenbaugh, N.S., Scherer, M. and Ashfaq, M., 2013. Response of snow-dependent hydrologic extremes to continued global warming. *Nature climate change*, *3*(4), pp.379-384.

Fang, Y., Y. Liu. and S. A. Margulis. 2022. Western United States UCLA Daily Snow Reanalysis, Version 1. [Indicate subset used]. Boulder, Colorado USA. NASA National Snow and Ice Data Center Distributed Active Archive Center. https://doi.org/10.5067/PP7T2GBI52I2.

FAO. (2021). FAOSTAT: Food and agriculture association of the United Nations statistical database. Retrieved from https://www.fao.org/faostat/en/%23data/QCL

Gates, W.L., Boyle, J.S., Covey, C., Dease, C.G., Doutriaux, C.M., Drach, R.S., Fiorino, M., Gleckler, P.J., Hnilo, J.J., Marlais, S.M., Phillips, T.J., Potter, G.L., Santer, B.D., Sperber, K.R., Taylor, K.E. and Williams, D.N. (1999) An overview of the results of the atmospheric model Intercomparison project (AMIP I). Bulletin of the American Meteorological Society, 80(1), 29– 56. https://doi.org/10.1175/1520-0477(1999)080<0029:AOOTRO>2.0.CO;2.

Gleick, P. H. *Impacts of California's Five-Year (2012-2016) Drought on Hydroelectricity Generation*. (2017).

Gleick, P.H., 2015. Impacts of California's ongoing drought: hydroelectricity generation. *Oakland, Calif.: Pacific Institute. Retrieved January*, *21*, p.2016.

Gonzales, K.R., Swain, D.L., Nardi, K.M., Barnes, E.A. and Diffenbaugh, N.S., 2019. Recent warming of landfalling atmospheric rivers along the west coast of the United States. *Journal of Geophysical Research: Atmospheres*, *124*(13), pp.6810-6826.

Han, W., Yang, Z., Di, L., & Mueller, R. (2012). CropScape: A web service based application for exploring and disseminating US conterminous geospatial cropland data products for decision support. Computers and Electronics in Agriculture, 84, 111– 123.

He, X., Bryant, B.P., Moran, T., Mach, K.J., Wei, Z. and Freyberg, D.L., 2021. Climate-informed hydrologic modeling and policy typology to guide managed aquifer recharge. Science Advances, 7(17), p.eabe6025.

Hersbach, H., Bell, B., Berrisford, P., Biavati, G., Horányi, A., Muñoz Sabater, J., Nicolas, J., Peubey, C., Radu, R., Rozum, I., Schepers, D., Simmons, A., Soci, C., Dee, D., Thépaut, J-N. (2023): ERA5 monthly averaged data on single levels from 1940 to present. Copernicus Climate Change Service (C3S) Climate Data Store (CDS), DOI: 10.24381/cds.f17050d7 (Accessed on 15-May-2023)

Hsiang, S., Kopp, R., Jina, A., Rising, J., Delgado, M., Mohan, S., Rasmussen, D.J., Muir-Wood, R., Wilson, P., Oppenheimer, M. and Larsen, K., 2017. Estimating economic damage from climate change in the United States. *Science*, *356*(6345), pp.1362-1369.

Hong, C., Mueller, N.D., Burney, J.A., Zhang, Y., AghaKouchak, A., Moore, F.C., Qin, Y., Tong, D. and Davis, S.J., 2020. Impacts of ozone and climate change on yields of perennial crops in California. *Nature Food*, 1(3), pp.166-172.)

Huang, X. and Swain, D.L., 2022. Climate change is increasing the risk of a California megaflood. *Science advances*, *8*(31), p.eabq0995.

Huang, X., Stevenson, S. and Hall, A.D., 2020. Future warming and intensification of precipitation extremes: A "double whammy" leading to increasing flood risk in California. *Geophysical Research Letters*, *47*(16), p.e2020GL088679.

Huning, L.S. and AghaKouchak, A., 2018. Mountain snowpack response to different levels of warming. Proceedings of the National Academy of Sciences, 115(43), pp.10932-10937.

Huning, L. S., & Margulis, S. A. (2018). Investigating the variability of high-elevation seasonal orographic snowfall enhancement and its drivers across Sierra Nevada, California. Journal of Hydrometeorology, 19(1), 47-67.

Huss, M., Bookhagen, B., Huggel, C., Jacobsen, D., Bradley, R.S., Clague, J.J., Vuille, M., Buytaert, W., Cayan, D.R., Greenwood, G. and Mark, B.G., 2017. Toward mountains without permanent snow and ice. *Earth's Future*, *5*(5), pp.418-435.

Immerzeel, W.W., Lutz, A.F., Andrade, M., Bahl, A., Biemans, H., Bolch, T., Hyde, S., Brumby, S., Davies, B.J., Elmore, A.C. and Emmer, A., 2020. Importance and vulnerability of the world's water towers. *Nature*, *577*(7790), pp.364-369.

Jay, A., D.R. Reidmiller, C.W. Avery, D. Barrie, B.J. DeAngelo, A. Dave, M. Dzaugis, M. Kolian, K.L.M. Lewis, K. Reeves, and D. Winner, 2018: Overview. In *Impacts, Risks, and Adaptation in the United States: Fourth National Climate Assessment, Volume II* [Reidmiller, D.R., C.W. Avery, D.R. Easterling, K.E. Kunkel, K.L.M. Lewis, T.K. Maycock, and B.C. Stewart (eds.)]. U.S. Global Change Research Program, Washington, DC, USA, pp. 33–71. doi: 10.7930/NCA4.2018.CH1

Jagannathan, K., A. D. Jones, and I. Ray, 2020. The making of a metric: Co-producing decision-relevant climate science. Bull. Amer. Meteor. Soc., doi: https://doi.org/10.1175/BAMS-D-19-0296.1.

Lehner, F., Deser, C., Maher, N., Marotzke, J., Fischer, E.M., Brunner, L., Knutti, R. and Hawkins, E., 2020. Partitioning climate projection uncertainty with multiple large ensembles and CMIP5/6. Earth System Dynamics, 11(2), pp.491-508.

Li, D., Lettenmaier, D.P., Margulis, S.A. and Andreadis, K., 2019. The role of rain-on-snow in flooding over the conterminous United States. Water Resources Research, 55(11), pp.8492-8513.

Livneh, B. and Badger, A.M., 2020. Drought less predictable under declining future snowpack. *Nature Climate Change*, 10(5), pp.452-458.

Lynn, E., Cuthbertson, A., He, M., Vasquez, J.P., Anderson, M.L., Coombe, P., Abatzoglou, J.T. and Hatchett, B.J., 2020. Technical Note: Precipitation-phase partitioning at landscape scales to regional scales. *Hydrology and Earth System Sciences*, *24*(11), pp.5317-5328.

Maina, F.Z. and Kumar, S.V., 2023. Diverging Trends in Rain-On-Snow Over High Mountain Asia. *Earth's Future*, *11*(3), p.e2022EF003009.

Mankin, J.S., Viviroli, D., Singh, D., Hoekstra, A.Y. and Diffenbaugh, N.S., 2015. The potential for snow to supply human water demand in the present and future. *Environmental Research*

Letters, *10*(11), p.114016.
Margulis, S.A., Cortés, G., Girotto, M. and Durand, M., 2016. A Landsat-era Sierra Nevada snow reanalysis (1985–2015). *Journal of Hydrometeorology*, *17*(4), pp.1203-1221.
Medellín-Azuara, J., Escriva-Bou, A., Abatzoglou, J.A., Viers, J.H., Cole, S.A., Rodríguez-Flores, J.M. and Sumner, D.A., 2022. Economic Impacts of the 2021 Drought on California Agriculture.
Milly, P.C. and Dunne, K.A., 2020. Colorado River flow dwindles as warming-driven loss of reflective snow energizes evaporation. *Science*, *367*(6483), pp.1252-1255.
Mote, P.W., Li, S., Lettenmaier, D.P., Xiao, M. and Engel, R., 2018. Dramatic declines in snowpack in the western US. *Npj Climate and Atmospheric Science*, 1(1), pp.1-6.
Mount, J., Hanak, E., Baerenklau, K., Butsic, V., Chappelle, C., Escriva-Bou, A., Fogg, G., Gartrell, G., Grantham, T. and Gray, B., 2018. Managing drought in a changing climate: four essential reforms. Public Policy Institute of California, San Francisco.
Musselman, K. N., Lehner, F., Ikeda, K., Clark, M. P., Prein, A. F., Liu, C., Barlage, M., & Rasmussen, R. (2018). Projected increases and shifts in rain-on-snow flood risk over western North America. Nature Climate Change, 8(9), 808.
Oakley, N.S., 2021. A Warming Climate Adds Complexity to Post-Fire Hydrologic Hazard Planning. Earth's Future, 9(7), p.e2021EF002149.
Ombadi, M., Risser, M.D., Rhoades, A.M. and Varadharajan, C., 2023. A warming-induced reduction in snow fraction amplifies rainfall extremes. *Nature*, pp.1-6.
Patricola, C.M., O'Brien, J.P., Risser, M.D., Rhoades, A.M., O'Brien, T.A., Ullrich, P.A., Stone, D.A. and Collins, W.D., 2020. Maximizing ENSO as a source of western US hydroclimate predictability. Climate Dynamics, 54, pp.351-372.
Payne, A.E., Demory, M.E., Leung, L.R., Ramos, A.M., Shields, C.A., Rutz, J.J., Siler, N., Villarini, G., Hall, A. and Ralph, F.M., 2020. Responses and impacts of atmospheric rivers to climate change. *Nature Reviews Earth & Environment*, *1*(3), pp.143-157.
Pörtner, H.O., Roberts, D.C., Adams, H., Adler, C., Aldunce, P., Ali, E., Begum, R.A., Betts, R., Kerr, R.B., Biesbroek, R. and Birkmann, J., 2022. Climate change 2022: Impacts, adaptation and vulnerability (p. 3056). Geneva, Switzerland:: IPCC.
Qin, Y., Abatzoglou, J.T., Siebert, S., Huning, L.S., AghaKouchak, A., Mankin, J.S., Hong, C., Tong, D., Davis, S.J. and Mueller, N.D., 2020. Agricultural risks from changing snowmelt. Nature Climate Change, 10(5), pp.459-465.
Qin, Y., Hong, C., Zhao, H. *et al.* Snowmelt risk telecouplings for irrigated agriculture. *Nat. Clim. Chang.* (2022).
Rauscher, S.A., Pal, J.S., Diffenbaugh, N.S. and Benedetti, M.M., 2008. Future changes in snowmelt-driven runoff timing over the western US. *Geophysical Research Letters*, *35*(16).
Rhoades, A.M., Hatchett, B.J., Risser, M.D., Collins, W.D., Bambach, N.E., Huning, L.S., McCrary, R., Siirila-Woodburn, E.R., Ullrich, P.A., Wehner, M.F. and Zarzycki, C.M., 2022. Asymmetric emergence of low-to-no snow in the midlatitudes of the American Cordillera. *Nature Climate Change*, pp.1-9.
Rhoades, A.M., Jones, A.D., O'Brien, T.A., O'Brien, J.P., Ullrich, P.A. and Zarzycki, C.M., 2020. Influences of North Pacific Ocean domain extent on the western US winter hydroclimatology in variable-resolution CESM. Journal of Geophysical Research: Atmospheres, 125(14), p.e2019JD031977.
Rhoades, A.M., Ullrich, P.A. and Zarzycki, C.M., 2018. Projecting 21st century snowpack trends in western USA mountains using variable-resolution CESM. *Climate Dynamics*, *50*(1-2),

pp.261-288.
Rhoades, A.M., Jones, A.D. and Ullrich, P.A., 2018b. Assessing mountains as natural reservoirs with a multimetric framework. Earth's Future, 6(9), pp.1221-1241.
Rosa, L., Chiarelli, D.D., Sangiorgio, M., Beltran-Peña, A.A., Rulli, M.C., D'Odorico, P. and Fung, I., 2020. Potential for sustainable irrigation expansion in a 3C warmer climate. *Proceedings of the National Academy of Sciences*, *117*(47), pp.29526-29534.
Ruess, P.J., Konar, M., Wanders, N. and Bierkens, M., 2023. Irrigation by crop in the Continental United States from 2008 to 2020. Water Resources Research, 59(2), p.e2022WR032804.
Sacks, W. J., Deryng, D., Foley, J. A., & Ramankutty, N. (2010). Crop planting dates: An analysis of global patterns. Global Ecology and Biogeography, 19(5), 607– 620.
Sanders, B.F., Schubert, J.E., Kahl, D.T. et al. Large and inequitable flood risks in Los Angeles, California. Nat Sustain 6, 47–57 (2023). https://doi.org/10.1038/s41893-022-00977-7
Scanlon, B. R., Zhang, Z., Save, H., Sun, A. Y., Schmied, H. M., Van Beek, L. P., et al. (2018). Global models underestimate large decadal declining and rising water storage trends relative to GRACE satellite data. Proceedings of the National Academy of Sciences of the United States of America, 115(6), E1080– E1089.
Schmitt, R.J., Rosa, L. and Daily, G.C., 2022. Global expansion of sustainable irrigation limited by water storage. Proceedings of the National Academy of Sciences, 119(47), p.e2214291119.
Shulgina, T., Gershunov, A., Hatchett, B.J. *et al.* Observed and projected changes in snow accumulation and snowline in California's snowy mountains. *Clim Dyn* (2023). https://doi.org/10.1007/s00382-023-06776-w
Siirila-Woodburn, E.R., Rhoades, A.M., Hatchett, B.J., Huning, L.S., Szinai, J., Tague, C., Nico, P.S., Feldman, D.R., Jones, A.D., Collins, W.D. and Kaatz, L., 2021. A low-to-no snow future and its impacts on water resources in the western United States. *Nature Reviews Earth & Environment*, *2*(11), pp.800-819.
Sutanudjaja, E. H., Van Beek, R., Wanders, N., Wada, Y., Bosmans, J. H., Drost, N., et al. (2018). PCR-GLOBWB 2: A 5 arcmin global hydrological and water resources model. Geoscientific Model Development, 11(6), 2429– 2453.
Szinai, J.K., Deshmukh, R., Kammen, D.M. and Jones, A.D., 2020. Evaluating cross-sectoral impacts of climate change and adaptations on the energy-water nexus: A framework and California case study. *Environmental Research Letters*.
U.S. Department of Labor (USDL). "Findings from the National Agricultural Workers Survey, 2013-14," Research Report No. 12 (published 2016) at iii, 37-38.
USGS. (2021). Water-use data available from USGS. Retrieved from https://water.usgs.gov/watuse/data/index.html
Wehner, M., Castillo, F. and Stone, D., 2017. The impact of moisture and temperature on human health in heat waves. In Oxford Research Encyclopedia of Natural Hazard Science.
Xu, Z., Di Vittorio, A., Zhang, J., Rhoades, A., Xin, X., Xu, H. and Xiao, C., 2021. Evaluating variable-resolution CESM over China and Western United States for use in water-energy nexus and impacts modeling. Journal of Geophysical Research: Atmospheres, 126(15), p.e2020JD034361.
Yates, D., Szinai, J. and Jones, A.D., 2022. Modeling the Water Systems of the Western US to Support Climate-Resilient Electricity System Planning. Authorea Preprints.
Zeng, X., Broxton, P. and Dawson, N., 2018. Snowpack change from 1982 to 2016 over conterminous United States. *Geophysical Research Letters*, *45*(23), pp.12-940.

3.7 Supplementary Tables

Supplementary Table S1. Precipitation and snow water equivalent. This table includes data from Table 4 represented in various units of measurement.

Region	Total Precip (mm/yr)	Total Precip (km^3)	Total Precip (MAF)	Rain (mm/yr)	Rain (km^3)	Rain (MAF)	Snow (mm/yr)	Snow (km^3)	Snow (MAF)	April 1st SWE (mm)	April 1st SWE (km^3)	April 1st SWE (MAF)	Peak SWE (mm)	Peak SWE (km^3)	Peak SWE (MAF)	April 1st F_{SCA}	Peak F_{SCA}	F_{snow}	F_{rain}
RRM-E3SM Historical																			
All Sierras	***4277***	***61.9***	***50.2***	***3095***	***44.8***	***36.3***	***1183***	***17.1***	***13.9***	***455***	***2.8***	***2.3***	***666***	***6.9***	***5.6***	***0.37***	***0.71***	***0.28***	***0.72***
Northern Sierra	1700	28.5	23.1	1237	20.8	16.8	463	7.8	6.3	75	0.6	0.5	174	2.4	1.9	0.35	0.79	0.28	0.72
Central Sierra	1700	21.9	17.8	1237	16.0	12.9	463	6.0	4.8	264	1.8	1.5	330	3.2	2.6	0.50	0.74	0.28	0.72
Southern Sierra	877	11.4	9.2	621	8.1	6.5	256	3.3	2.7	117	0.4	0.4	163	1.3	1.1	0.26	0.61	0.30	0.70
VR-CESM Historical																			
All Sierras	***3694***	***53.3***	***43.2***	***1516***	***22.3***	***18.0***	***2178***	***31.0***	***25.1***	***710***	***4.6***	***3.7***	***1109***	***12.7***	***10.3***	***0.35***	***0.81***	***0.60***	***0.40***
Northern Sierra	1419	23.8	19.3	688	11.6	9.4	731	12.3	10.0	101	0.9	0.7	284	4.1	3.3	0.28	0.85	0.52	0.48
Central Sierra	1402	18.1	14.7	506	6.5	5.3	896	11.6	9.4	385	2.7	2.2	510	5.7	4.6	0.48	0.87	0.65	0.35
Southern Sierra	873	11.3	9.2	322	4.2	3.4	552	7.2	5.8	224	1.0	0.8	316	2.9	2.4	0.29	0.70	0.65	0.35
1.5°C																			
All Sierras	***3890***	***56.3***	***45.6***	***2097***	***30.8***	***25.0***	***1793***	***25.5***	***20.6***	***454***	***2.6***	***2.1***	***738***	***7.6***	***6.1***	***0.26***	***0.70***	***0.46***	***0.54***
Northern Sierra	1548	26.0	21.1	962	16.2	13.1	586	9.8	8.0	48	0.3	0.3	178	2.4	2.0	0.18	0.78	0.38	0.62
Central Sierra	1451	18.7	15.2	700	9.0	7.3	751	9.7	7.9	263	1.7	1.3	352	3.5	2.8	0.39	0.74	0.52	0.48
Southern Sierra	891	11.6	9.4	435	5.6	4.6	456	5.9	4.8	143	0.6	0.5	208	1.6	1.3	0.22	0.59	0.52	0.48
2°C																			
All Sierras	***3896***	***56.3***	***45.7***	***2248***	***33.0***	***26.8***	***1648***	***23.3***	***18.9***	***391***	***2.0***	***1.6***	***655***	***6.5***	***5.2***	***0.23***	***0.67***	***0.42***	***0.58***
Northern Sierra	1537	25.8	20.9	1019	17.1	13.9	518	8.7	7.1	32	0.2	0.2	147	2.0	1.6	0.13	0.75	0.34	0.66
Central Sierra	1452	18.7	15.2	752	9.7	7.9	700	9.0	7.3	231	1.3	1.1	319	3.0	2.5	0.36	0.71	0.48	0.52
Southern Sierra	907	11.8	9.6	477	6.2	5.0	430	5.6	4.5	128	0.5	0.4	190	1.4	1.2	0.20	0.56	0.48	0.52
3°C																			
All Sierras	***4000***	***57.7***	***46.8***	***2637***	***38.6***	***31.3***	***1363***	***19.1***	***15.5***	***258***	***1.1***	***0.9***	***506***	***4.4***	***3.6***	***0.17***	***0.61***	***0.34***	***0.66***
Northern Sierra	1541	25.9	21.0	1164	19.5	15.8	377	6.3	5.1	6	0.0	0.0	92	1.2	1.0	0.08	0.70	0.25	0.75
Central Sierra	1507	19.4	15.8	899	11.6	9.4	608	7.8	6.4	159	0.8	0.7	256	2.2	1.8	0.27	0.65	0.41	0.59
Southern Sierra	953	12.4	10.0	574	7.5	6.1	378	4.9	4.0	93	0.3	0.2	157	1.0	0.8	0.16	0.49	0.40	0.60

Supplementary Table S2. Central Valley water balance for VR-CESM. The CESM2 land model produces negative runoff fluxes in some versions of the model (e.g., CESM2), due to irrigation and lakes (negative P-E). In this study we account for irrigation separately using other data sources, so we assign a value of zero to negative runoff values in CESM. However, this table shows that the CESM model is balanced.

Historical Water Balance - Central Valley									
	Sacramento Valley			San Joaquin Basin			Tulare Basin		
	mm/yr	*km³*	*MAF*	*mm/yr*	*km³*	*MAF*	*mm/yr*	*km³*	*MAF*
RRM-E3SM									
Atmospheric Rain	972	34.3	27.8	711	20.0	16.2	397	11.7	9.5
Atmospheric Snow	32	1.1	0.9	16	0.4	0.4	9	0.3	0.2
Total Precipitation	***1004***	***35.5***	***28.7***	***727***	***20.4***	***16.5***	***406***	***12.0***	***9.7***
Total Evapotranspiration	***560***	***19.8***	***16.0***	***471***	***13.2***	***10.7***	***331***	***9.8***	***7.9***
Surface Runoff	136	4.8	3.9	85	2.4	1.9	33	1.0	0.8
Subsurface Runoff	280	9.9	8.0	149	4.2	3.4	37	1.1	0.9
Total Runoff	***417***	***14.7***	***11.9***	***234***	***6.6***	***5.3***	***71***	***2.1***	***1.7***
Inflows	1004	35	29	727	20	17	406	12	10
Outflows	976	34	28	705	20	16	402	12	10
Water Balance (Inflows - Outflows)	**27**	**1**	**1**	**22**	**1**	**0**	**4**	**0**	**0**
VR-CESM									
Atmospheric Rain	716	25.3	20.5	569	16.0	13.0	304	9.0	7.3
Atmospheric Snow	63	2.2	1.8	27	0.8	0.6	17	0.5	0.4
Total Precipitation	***778***	***27.5***	***22.3***	***596***	***16.7***	***13.6***	***321***	***9.5***	***7.7***
Total Evapotranspiration	***529***	***18.7***	***15.1***	***544***	***15.3***	***12.4***	***525***	***15.5***	***12.6***
Surface Runoff	219	7.7	6.3	161	4.5	3.7	83	2.4	2.0
Subsurface Runoff	28	1.0	0.8	-112	-3.2	-2.6	-283	-8.3	-6.8
Total Runoff	***247***	***8.7***	***7.1***	***49***	***1.4***	***1.1***	***-200***	***-5.9***	***-4.8***
Inflows	778	27.5	22.3	596	16.7	13.6	321	9.5	7.7
Outflows	775	27.4	22.2	593	16.7	13.5	325	9.6	7.8
Water Balance (Inflows - Outflows)	**3**	**0**	**0**	**3**	**0**	**0**	**-4**	**0**	**0**

Supplementary Table S3. Crop category numbers and descriptions. Taken from the California Department of Water Resources- California Land and Water Use Data https://water.ca.gov/Programs/Water-Use-And-Efficiency/Land-And-Water-Use/Agricultural-Water-Use-Models

Crop Category	Crop category description
1	Grain *(wheat, wheat_winter, wheat_spring, barley, oats, misc._grain & hay)*
2	Rice *(rice, rice_wild, rice_flooded, rice-upland)*
3	Cotton
4	Sugar beet *(sugar-beet, sugar_beet_late, sugar_beet_early)*
5	Corn
6	Dry beans
7	Safflower
8	Other field crops *(flax, hops, grain_sorghum, sudan,castor-beans, misc. field, sunflower, sorghum/sudan hybrid, millet, sugarcane)*
9	Alfalfa *(alfalfa, alfalfa_mixtures, alfalfa_cut, alfalfa_annual)*
10	Pasture *(pasture, clover, pasture_mixed, pasture_native, misc._grasses, turf_farm, pasture_bermuda, pasture_rye, klein_grass, pasture_fescue)*
11	Tomato processing *(tomato processing, tomato processing drip, tomato_processing_sfc)*
12	Tomato fresh *(tomato_fresh, tomato_fresh_drip, tomato_fresh_sfc)*
13	Cucurbits *(cucurbits, melons, squash, cucumbers, cucumbers_fresh_market, cucumbers machine-harvest, watermelon)*
14	Onion & garlic *(onion & garlic, onions, onions_dry, onions_green, garlic)*
15	Potatoes *(potatoes, potatoes_sweet)*
16	Truck_Crops_misc *(artichokes, truck_crops, asparagus, beans_green, carrots, celery, lettuce, peas, spinach, bus h berries, strawberries, peppers, broccoli, cabbage, cauliflower)*
17	Almond & pistacios
18	Orchard (deciduous) *(apples, apricots, walnuts, cherries, peaches, nectarines, pears, plums, prunes, figs, kiwis)*
19	Citrus & subtropical *(grapefruit, lemons, oranges, dates, avocados, olives, jojoba)*
20	Vineyards *(grape_table, grape_raizin, grape_wine)*

Supplementary Table S4. Sierra Nevada water balance. See Supplementary Figure S2 for water balance of the Central Valley regions.

Historical Water Balance - Sierra Nevada									
	Northern Sierra			Central Sierra			Southern Sierra		
	mm / yr	*km³*	*MAF*	*mm / yr*	*km³*	*MAF*	*mm / yr*	*km³*	*MAF*
RRM-E3SM									
Atmospheric Rain	1255	21.1	17.1	956	12.3	10.0	628	8.2	6.6
Atmospheric Snow	467	7.8	6.4	490	6.3	5.1	257	3.3	2.7
Total Precipitation	***1722***	***28.9***	***23.4***	***1446***	***18.7***	***15.1***	***885***	***11.5***	***9.3***
Total Evapotranspiration	***581***	***9.8***	***7.9***	***558***	***7.2***	***5.8***	***478***	***6.2***	***5.0***
Surface Runoff	368	6.2	5.0	315	4.1	3.3	198	2.6	2.1
Subsurface Runoff	756	12.7	10.3	554	7.1	5.8	198	2.6	2.1
Total Runoff	***1124***	***18.9***	***15.3***	***869***	***11.2***	***9.1***	***396***	***5.1***	***4.2***
Inflows	1722	29	23	1446	19	15	885	11.5	9.3
Outflows	1705	29	23	1426	18	15	873	11.3	9.2
Water Balance (Inflows - Outflows)	**17**	**0**	**0**	**19**	**0**	**0**	**11**	**0**	**0**
VR-CESM									
Atmospheric Rain	696	11.7	9.5	511	6.6	5.3	325	4.2	3.4
Atmospheric Snow	737	12.4	10.0	902	11.6	9.4	555	7.2	5.8
Total Precipitation	***1433***	***24.1***	***19.5***	***1413***	***18.2***	***14.8***	***880***	***11.4***	***9.3***
Total Evapotranspiration	***401***	***6.7***	***5.5***	***376***	***4.8***	***3.9***	***308***	***4.0***	***3.2***
Surface Runoff	657	11.0	8.9	635	8.2	6.6	355	4.6	3.7
Subsurface Runoff	370	6.2	5.0	399	5.1	4.2	217	2.8	2.3
Total Runoff	***1027***	***17.2***	***14.0***	***1034***	***13.3***	***10.8***	***572***	***7.4***	***6.0***
Inflows	1433	24.1	19.5	1413	18.2	14.8	880	11.4	9.3
Outflows	1428	24.0	19.4	1410	18.2	14.7	880	11.4	9.3
Water Balance (Inflows - Outflows)	**5**	**0**	**0**	**3**	**0**	**0**	**0**	**0**	**0**

3.8 Supplementary Figures

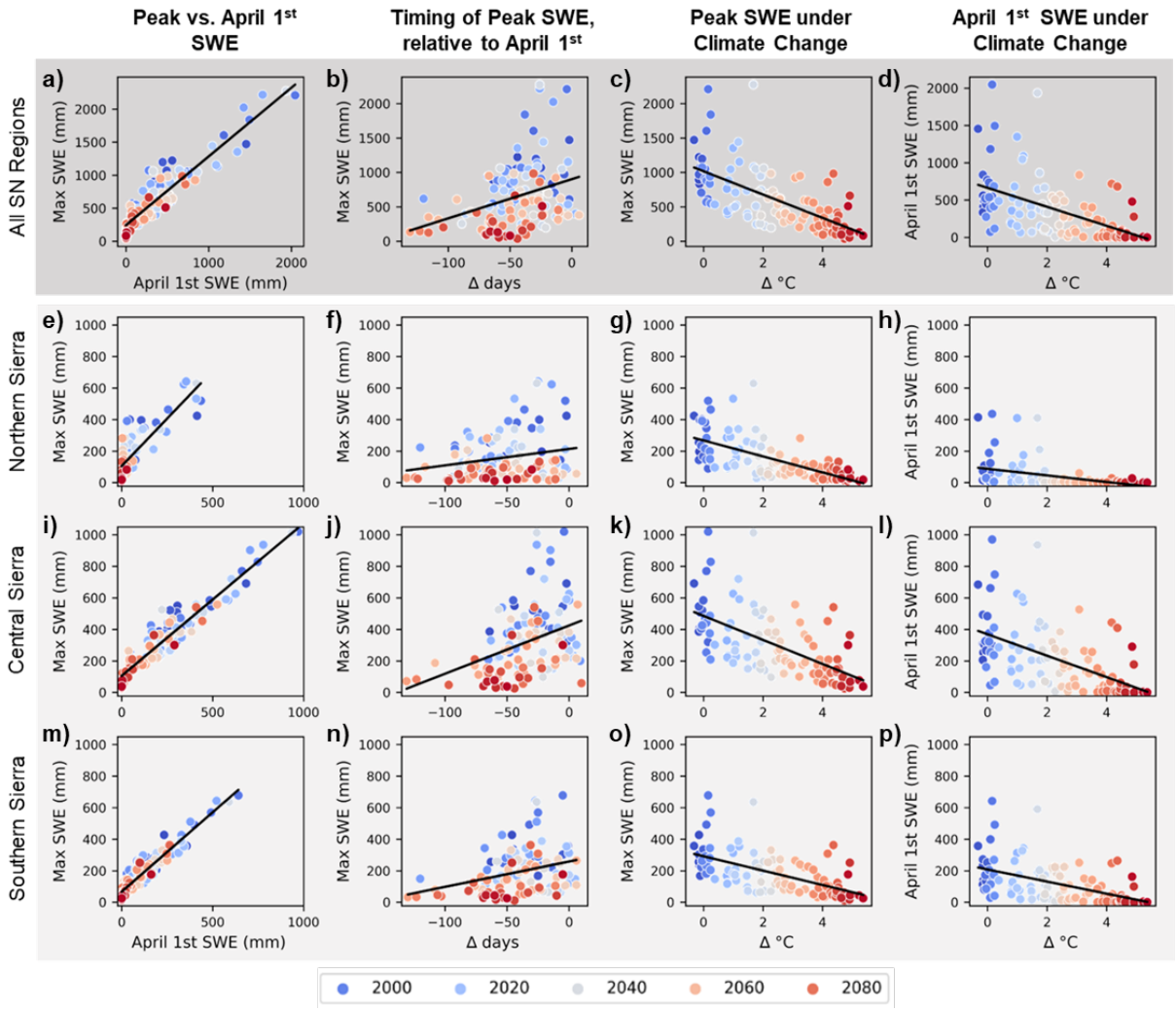

Supplementary Figure S1. Sierra Nevada SWE response to climate change by region.

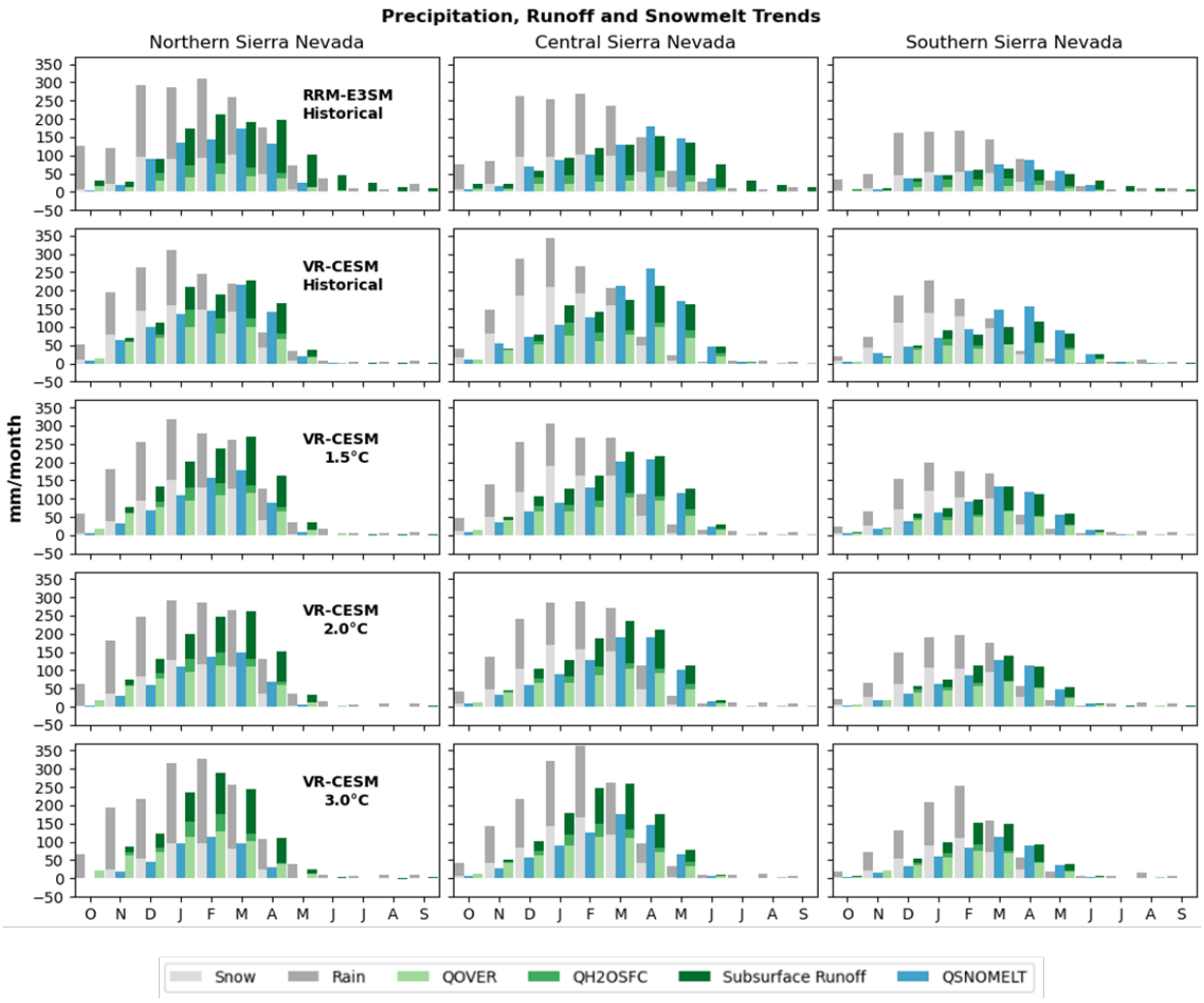

Supplementary Figure S2. Breakdown of precipitation, runoff, and snowmelt trends.

Conclusion of Dissertation

End of hunger, achievement of food security, improvement in nutrition, and environmental sustainability are at the heart of the United Nations' Sustainable Development Goals. We must increase food production while, at the same time, minimizing the environmental footprint of agriculture. Most studies on global food security do not make projections past the year 2050, just as the collision between climate change and population growth is expected to intensify. Moreover, previous studies have accounted for major drivers of global food production and demand independently, without considering the full suite of factors that will affect future food security: climate change, population growth, dietary changes, food waste, and the extent by which crop yield gaps will be narrowed. In this dissertation, I aim to provide an integrated assessment of food security in the 21st century that accounts for the interactions of all these main factors affecting food production and demand while measuring the environmental impacts of population growth and diverse dietary pathways. This assessment is urgently needed to better inform governments of the food security risks each country may face, evaluate changes in trade dependency, and vulnerability.

Mountain regions are important assets as the world's water towers in the Earth system. Many snow-dependent basins are actively threatened by anthropogenic climate change which will reduce freshwater availability from snow and in turn could significantly affect crop yields and crop mixes – aggravating food security at a time when demand is projected to increase. This dissertation highlights the vulnerability of California's agriculture by considering snowmelt runoff availability and whether alternative water sources (i.e. rainfall, groundwater) will suffice to meet the additional irrigation water demand from a changing snowpack. This study emphasizes the need to mitigate anthropogenic climate change to prevent further degradation of the cryosphere and at the same time provide a lens into the vulnerability of agriculture in California to inform adaptation measures (which address both water supply and demand) to ensure water and food security for the people of California and populations dependent on the state's exports.

Future societies' resilience against global challenges such as climate change hinges on successful implementation of policies, actions and development strategies. Hence, mitigating climate change and addressing inefficiencies in the global food system (production and demand), will be essential measures for countries working towards resilience and sustainability in the under societal and climate changes underway. This dissertation aims to shed light on vulnerabilities in the food-water nexus under a changing climate and opportunities for adaptation measures.